UiT The Arctic University of Norway

Faculty of Health Sciences

MRI in musculoskeletal inflammatory disease in children, with a focus on technique, standardisation and findings

Laura Tanturri de Horatio

A dissertation for the degree of Philosophiae Doctor (PhD), August 2024

ISBN 978-82-350-0007-1

Faculty of Health Sciences
Department of Clinical Medicine

MRI in musculoskeletal inflammatory disease in children, with a focus on technique, standardisation and findings.

Laura Tanturri de Horatio
Thesis for the degree of Philosophiae Doctor (PhD), UiT the Arctic University of Norway, 2024

Table of contents

1. Preface

1.1 Acknowledgements

I would like to express my gratitude to a number of people who have had a special impact on this doctoral thesis and on me as a woman and a paediatric radiologist. First of all, I want to thank my great supervisors, Ass. Prof. Derk Frederik Matthäus Avenarius, PhD Dr. Lil Sofie Ording Müller and Prof. Karen Rosendahl for their support during all phases of my PhD. Their professionalism and guidance have been an invaluable source of inspiration and loving support throughout my journey.

Derk has always been a harbinger of good news. I remember as if it was yesterday the joy and excitement of receiving his first phone call in which he told me that our project had received funding from Health North. He always listened to my ideas and proposals and directed me with his practical and essential approach. His undoubted experience and ability to solve any situation and unforeseen circumstances have been of great support to me. We had a lot of fun scoring MR-images together. His passion for Italy makes him even closer to me. I am truly grateful for his invaluable guidance and support as my main supervisor.

Heartfelt thanks to Lil Sofie, a brilliant paediatric radiologist with innate communication skills and a genuine passion for her work (as well as for Italian cantuccini!), with whom I also share a passion for beautiful clothes. She always gave me timely and fruitful suggestions when needed. I greatly appreciate not only her expertise but also her friendship and her belief in my potential, which fills me with deep affection and gratitude.

I express all my gratitude to Karen, a strong and charismatic woman, a true leader from whom everyone should learn something. Always ready to listen to me and to give me the best possible advice. Since our first meeting in 2008 for the Health-e-Child Project I share with her a passion for paediatric musculoskeletal imaging and most especially for the "search for truth." She made me passionate about research, actively involved me in numerous works, always fostering contacts with stimulating international groups and made me grow by always being one step ahead of me. Really none of this would have been possible without Karen.

To Pia Zadig and Elisabeth von Brandis, who started this adventure before me with the same passion and enthusiasm, I wish them the best in their professional and private lives, with the hope of continuing to collaborate with both of them in the future.

To Prof. Paolo Tomà for believing in me from the first day he met me, for everything he taught me, for never backing down when I asked him to see a case together, it's a good thing

I didn't accept his invitation to work at the Gaslini Institute otherwise none of this would have happened.

To Dr. Massimiliano Raponi for granting me leave from the hospital, for believing in this project and for his words of appreciation for me over the years that motivated me to do my utmost.

To my real "old" friends, Laura C, Edda, Laura V, Simona, with whom distance has not driven us apart, indeed when we see each other it seems like a day has passed since the previous time.

To Valentina R, Valentina S, Fabrizia, Francesca, Chiara, there is not a day when they are not ready to listen and advise me, I am really lucky to have you as friends.

To Mimmo Barbuti, who always has an answer to my questions, for his endless availability, for everything he has taught me and for the good he has loved me from the first day I arrived at Bambino Gesù Children's Hospital, I will never cease to be grateful.

To Enzo Pacciani, Mauro Colajacomo and Fausto Fassari, undoubtedly more friends than colleagues, endowed with professionalism and experience that are more unique than rare, with whom a laugh was never missed.

To Pier Luigi Di Paolo and Paola d'Angelo, for your sincere friendship, for your precious help with the paper 2, I know it has not been easy to balance research and clinical work, I'm sure we will continue to work together in the future.

Thank you from the bottom of my heart to my mother Stefania, an extremely intelligent and strong-willed woman, for never backing down when I asked her for help, who followed me through all the stages of this PhD as if it were her own, without whom I would not have come this far.

To my father Paolo, I am happy that life has brought us closer together in these last years. As Friedrich Nietzsche said: "What doesn't kill me, strengthens me." And life has fortified him so much.

To my sister Cecilia, whom I love so much even though when I say white, she always says black.

To my beloved grandfather Sandro, who followed me through my medical studies proud that his dearest granddaughter had entered his profession and yet never concealing his concern for what would have been certainly a demanding job. To him who looks down on me today from a little cloud, for all his teachings in the medical field and in life, for his poise and infinite goodness that I will never forget, I wish he was still here with me.

To my loving grandmothers Emma and Olga who played a key role in my childhood, always ready to welcome and cuddle me, who will live forever in my heart.

To my in-laws Franco and Simonetta, for welcoming me into their family, and for the way they raised and educated their son. They could not have done a better job.
To Alberto, I could say a second dad, kind and caring, for his sincere affection and deep esteem and trust in me, thank you from the bottom of my heart.
To my wonderful husband Luca for his sincere love, for always encouraging and supporting me in research as well as in life, believing in my dreams even before me.
To my daughters Lavinia and Vittoria, the greatest joy of my life, for being so proud of their mom and her work, with the hope that they will believe in themselves and, once they will grow up, they will realise all the dreams they have in their drawer.

My sincere thanks to Health North (Helse Nord) for funding this research from 2021.

1.2 Scientific environment and work leading up to this thesis

The research work presented in this thesis was funded by Health North, Tromsø/NO, and was carried out from 2019 to 2023 at the Department of Radiology, University Hospital of North Norway (UNN), in collaboration with the Department of Radiology at Bambino Gesù Children's Hospital (BGCH) in Rome and the Division of Radiology and Nuclear Medicine at Oslo University Hospital (OUS).

The thesis is in part based on previous experiences in, and data from two multicentre projects. The first, named the Health-e-Child (HeC) Project, was founded on the collaboration of four large European paediatric centres (Great Ormond Street Hospital, London/United Kingdom, Hôpital Necker-Enfants malades, Paris/France, Gaslini Hospital, Genoa/Italy and Bambino Gesù Children's Hospital (BGCH), Rome/Italy) from 2006 onwards. One of the aims of the HeC Project was to devise accurate imaging tools for both active and chronic changes in children with juvenile idiopathic arthritis (JIA) with the final goal to improve the patients' long-term outcome. For this purpose, a child-specific Magnetic Resonance Imaging (MRI) scoring system for all pathological MRI features (synovitis, tenosynovitis, BMO, bone erosions) for wrist, and a radiographic scoring system for hips involvement in patients with JIA was established and validated by the HeC Radiology group, in which I have been involved since 2008 (1-5).

The second multicentre project included 196 healthy, asymptomatic children and adolescents, examined at UNN/Tromsø or at OUS/Oslo during 2018-2020, aiming at characterising bone marrow changes during growth as seen on whole-body MRI (WBMRI). Hitherto, a scoring system for bone marrow appearances during childhood has been established and validated (6), followed by two papers describing bone marrow appearances of the normal axial and appendicular system (7, 8) and a study comparing T2 Dixon water-only and STIR sequences for the assessment of high signal bone marrow change (9). In short, significant bone marrow changes were found in healthy children and adolescents, which, in a clinical setting, might have been mistaken for pathology.

The current thesis further elaborates on the findings from the abovementioned multicentre projects. In addition, it adds data from a large study collecting data from BGCH and Haukeland University Hospital (HUS), Bergen Norway, to expand our knowledge on the use of MRI in children with musculoskeletal disorders in general, and with rheumatological diseases in particular.

1.3 List of publications

Paper 1

Paola d'Angelo, **Laura Tanturri de Horatio,** Paolo Toma, Lil-Sofie Ording Müller, Derk Avenarius, Elisabeth von Brandis, Pia Zadig, Ines Casazza, Manuela Pardeo, Denise Pires-Marafon, Martina Capponi, Antonella Insalaco, De Benedetti Fabrizio, Karen Rosendahl. Chronic nonbacterial osteomyelitis — clinical and magnetic resonance imaging features. *Pediatric Radiology (2021) 51:282–288.*

Paper 2

Laura Tanturri de Horatio, Susan C. Shelmerdine, Paola d'Angelo, Pier Luigi Di Paolo, Silvia Magni-Manzoni, Clara Malattia, Maria Beatrice Damasio, Paolo Tomà, Derk Avenarius, Karen Rosendahl. A novel magnetic resonance imaging scoring system for active and chronic changes in children and adolescents with juvenile idiopathic arthritis of the hip. *Pediatric Radiology (2023) 53:426–437.*

Paper 3

Laura Tanturri de Horatio, Pia K. Zadig, Elisabeth von Brandis, Lil-Sofie Ording Müller, Karen Rosendahl, Derk F.M. Avenarius. Whole-body MRI in children and adolescents: can T2-weighted Dixon fat-only images replace standard T1-weighted images in the assessment of bone marrow? *European Journal of Radiology 166 (2023) 110968.*

Related papers

1. Zadig P, von Brandis E, d'Angelo P, **Tanturri de Horatio L**, Ording-Müller LS, Rosendahl K, Avenarius D.Whole-body MRI in children aged 6-18 years. Reliability of identifying and grading high signal intensity changes within bone marrow. *Pediatr Radiol 2022 Jun;52(7):1272-1282.*

2. Zadig PK, von Brandis E, Flatø B, Ording Müller LS, Nordal EB, **Tanturri de Horatio L**, Rosendahl K, Avenarius DFM. Whole body magnetic resonance imaging in healthy children

and adolescents: Bone marrow appearances of the appendicular skeleton. *Eur J Radiol 2022 Aug;153:110365.*

3. von Brandis E, Zadig PK, Avenarius DFM, Flatø B, Knudsen PK, Lilleby V, Nguyen B, Rosendahl K, Ording Müller LS. Whole body magnetic resonance imaging in healthy children and adolescents. Bone marrow appearances of the axial skeleton. *Eur J Radiol 2022 Sep;154:110425.*

4. Zadig P, von Brandis E, Ording Müller LS, **Tanturri de Horatio L,** Rosendahl K, Avenarius DFM. Pediatric whole-body magnetic resonance imaging: comparison of STIR and T2 Dixon sequences in the detection and grading of high signal bone marrow changes. *Eur Radiol 2023 Jul;33(7):5045-5053.*

5. Capponi M, Pires Marafon D, Rivosecchi F, Zhao Y, Pardeo M, Messia V, **Tanturri de Horatio L**, Tomà P, De Benedetti F, Insalaco A. Assessment of disease activity using a whole-body MRI derived radiological activity index in chronic nonbacterial osteomyelitis. *Pediatr Rheumatol Online J. 2021 Aug 14;19(1):123.*

1.4 Abbreviations

BGCH	Bambino Gesù Children's Hospital
BMO	Bone marrow oedema
CCD	Caput-collum-diaphyseal angle
CNO	Chronic nonbacterial osteomyelitis
CRMO	Chronic recurrent multifocal osteomyelitis
CRP	C-reactive protein
DWI	Diffusion-Weighted Images
ERA	Enthesitis-related arthritis
ESR	Erythrocyte Sedimentation Rate
FOV	Field-of-view
FS	Fat saturated
GOSH	Great Omond Street Hospital
GRE	Gradient Echo
HeC	Health-e-Child
HUS	Haukeland University Hospital
IBD	Inflammatory Bowel Disease
ICC	Intraclass Correlation Coefficient
IGG	Istituto Giannina Gaslini
IR	Inversion Recovery
ILAR	International League of Associations for Rheumatology
JIA	Juvenile Idiopathic Arthritis
LCH	Langerhans Cell Histiocytosis

ms	Millisecond
MSK	Musculoskeletal
OM	Osteomyelitis
OMERACT	Outcome Measures in Rheumatology Clinical Trials
OUS	Oslo University Hospital
MRI	Magnetic Resonance Imaging
PACS	Picture Archiving and Communication Systems
RIS	Radiology Information System
SAPHO	Synovitis, Acne, Pustulosis, Hyperostosis, and Osteomyelitis
SD	Standard deviation
SpA	Spondyloarthropathy
STIR	Short Time Inversion Recovery
T	Tesla (field strength)
T1	Longitudinal Relaxation Time
T2	Transverse Relaxation Time
T2-fs	T2-weighted Fat suppressed
TE	Time to Echo
TR	Repetition Time
TSE	Turbo Spin Echo
UNN	University Hospital of North Norway
US	Ultrasound
WBMRI	Whole-body MRI

1.5 Abstract

Background

Inflammatory diseases of the musculoskeletal (MSK) system are relatively prevalent in children and adolescents. Early diagnosis and instigation of treatment play an important role for long-term outcome. As clinical assessment of disease activity is challenging, magnetic resonance imaging (MRI) has become increasingly used to guide treatment. However, validated, child specific MRI tools for monitoring disease are sparse.

Aims

The overall aim of the work presented in this thesis was to provide knowledge for better diagnostics and management of children and adolescents with inflammatory MSK-disorders, with a focus on juvenile idiopathic arthritis (JIA) and chronic nonbacterial osteomyelitis (CNO), by addressing different aspects of MR-imaging. More specifically, we aimed to examine clinical, laboratory and WBMRI findings in patients with chronic non-bacterial osteomyelitis, to establish and validate a MR-scoring system for the assessment of active and chronic hip-changes in patients with juvenile idiopathic arthritis and to explore whether or not

a T2 Dixon fat-only sequence might replace a T1 TSE sequence as part of a WBMRI, and thus reduce scan time.

Material and methods

The work in this thesis is based on three different cohorts; one cohort including 75 children and adolescents with a known diagnosis of CNO, of whom most had a whole-body MRI as part of the diagnostic work-up; one cohort including 60 children, adolescents and young adults with a known diagnosis of JIA of whom all had a targeted MRI-examination of the hips and one cohort of 196 healthy children and adolescents who underwent a whole-body MRI for research purposes only.

Results

Results showed that nearly 80% of the children with CNO presented with pain, with or without swelling or fever, amongst whom nearly one fourth (22.6%) presented with isolated low back pain or pain around the sacroiliac joints. On whole-body MRI, a median number of 6 involved sites (range 1–27) was found. The long bones of the lower limbs were affected in nearly 80%, whereof the femur was the most common. Of lesions located in the long tubular bones, the proximal and distal metaphysis were involved in at least one bone in around half of the patients. Spinal involvement was often multifocal. Inflammatory markers, which were raised in 46/75 (61.3%) children, significantly predicted the number of sites (β=0.250, P=0.045). Neither age (β=0.186, P=0.132) nor gender (β=0.103, P=0.387) nor disease duration (β=0.025, P=0.841) predicted the number of involved bone sites at a statistically significant level.

Moreover, we have devised and validated a set of MRI markers for hip involvement in children and adolescents with JIA. Among active changes, there was good intra- and interobserver agreement for grading overall inflammation (kappa values 0.6–0.7). Synovial enhancement showed a good intraobserver agreement (kappa values 0.7–0.8), while the interobserver agreement was moderate (kappa values 0.4–0.5). Regarding acetabular erosions on a 0–3 scale, both intra– and interobserver agreement was good, with kappa values of 0.6-0.7 for intra- and 0.6 for interobserver agreement). Direct measurements were imprecise.

In a large cohort of healthy children and adolescents, nearly 93% of the bone marrow areas with high signal identified on T2 Dixon water-only images returned low-signal on both T2

Dixon fat-only and T1-w images. <2% did not return low signal on either of the two sequences, with an absolute agreement of 94.6%. The agreement between the two sequences was fair to good, with an average kappa value of 0.4, but higher in older children and for "major findings", i.e. areas which in a clinical setting might have been mistaken for pathology. Conversely, the majority of the discordant findings were classified as "minor". These are important observations that support the use of T2 Dixon fat-only images as an alternative to an additional T1-w sequence for assessment of bone marrow lesions on whole-body MRI in children.

Conclusions

This study demonstrates the distribution of clinical, laboratory and MRI-findings in a large cohort of children and adolescents with CNO. Interestingly, elevation of inflammatory markers significantly predicted the number of skeletal sites involved as identified on MRI. Moreover, MRI is a reliable method for the assessment and grading of active and chronic hip-change in patients with JIA. Finally, T2 Dixon fat-only might replace a T1-w sequence on whole-body MRI for bone marrow assessment in children, thus reducing scan time.

2. Background

2.1 General introduction

Juvenile idiopathic arthritis (JIA) and chronic nonbacterial osteomyelitis (CNO) are relatively common musculoskeletal (MSK) diseases in children characterized by chronic inflammation. JIA is the most prevalent rheumatological disease in children (10) and represents the major cause of acquired disability in the paediatric population. There is increasing evidence that many, if not most children with JIA will have chronic disease with ongoing activity into adulthood (11, 12). Moreover, recent research suggests that an early diagnosis with a prompt instigation of therapy may be associated with slower progression of joint damage and higher rates of remission (13, 14). As for CNO, the diagnosis is probably more prevalent than previously thought, and its treatment depends on disease severity and which bones it affects (15-17). The abovementioned highlights the need for sensitive and accurate disease markers, both for JIA and CNO, as many of the existing, based on clinical, laboratory and conventional imaging are imprecise and inaccurate.

Of the different imaging techniques, ultrasound (US) and MRI have become the most frequently applied modalities for diagnosing and monitoring inflammatory MSK-disorders in children. None of the methods use ionising radiation, with US emerging as a useful technique used bedside, as a supplement to the clinical examination, and MRI being used as a problem-solver when clinical examination and US are equivocal. Interpreting MR examinations of the skeletal system can be challenging, though, due to changes in the appearances of shape, structure and bone marrow during skeletal maturation. Establishing imaging references across age in order to confidently differentiate particularly imaging findings in early disease from normal findings, constitutes one of four key aims of the European Society of Paediatric Radiology (ESPR) research strategy, the others being facilitation of multicentre studies and data sharing, development of robust, image-based classification systems and last, but not least, the development of evidence-based clinical guidelines (18).

This thesis will focus on two of the above-mentioned issues, namely the use of multicentre design to enhance robustness of the results and development of a MRI-based classification system for hip-involvement in children with JIA. In addition, technical aspects and findings of whole-body MRI will be addressed. As for technical aspects, it is well known that MRI examinations can be intimidating and distressing for children, particularly those who suffer from anxiety. Longer scan duration increases the likelihood of children feeling apprehensive, claustrophobic, or restless during the procedure. Furthermore, rheumatological diseases often

require frequent follow-ups to monitor disease activity and progression. Therefore, optimization of MRI protocols and particularly reduction of scan time are important to minimise children's discomfort.

2.2 Magnetic resonance imaging (MRI)

MRI is an imaging modality allowing for accurate, three-dimensional visualisation of anatomical structures involved in bone and joint inflammation, with imaging appearances basically depending on the inherent molecular structure of the tissues. The patient is placed in a large, static magnetic field, often 1.5 or 3 Tesla (T), and radiofrequency waves are used to induce signals from different body tissues, such as bone marrow, cartilage, fluid and tendons. These signals are then registered by coils that are placed around the patients. By adjusting timing and length of the different radiofrequency waves, images with different weighting of the inherent tissue contrasts are produced. Based on the timing properties of the acquisition, the produced image can be grouped into T1-weighted (T1-w), T2-weighted (T2-w) or proton-density-weighted (PD) images. MRI sequences can also be grouped according to the type of sequence, such as spin echo (SE), inversion recovery (IR) or gradient echo (GRE), for instance. For most standard sequences used in children, sufficient signal is acquired in around 3-4 minutes, thus, if the child cooperates, a typical MR scan, which is composed of 4-6 sequences, can take up to 25-30 minutes, including the time for patient positioning. Children under the age of five or subjects that cannot lie still need sedation, because movement during scanning gives artefacts in the images. Contraindications for an MRI-scan include some, but not all metal implants, leads, and electrical devices due to the strong magnetic field and radiofrequency pulses, as well as known claustrophobia. Moreover, MRI is relatively costly, and is unavailable for routine use in some countries.

In the following, I will describe in more detail some concepts behind MRI pulse sequences used in this thesis.

T1 weighted (T1-w) imaging sequences

A T1-w imaging sequence is one of the basic sequences on MRI, and can be obtained using spin echo (SE), fast/turbo-SE or gradient echo (GRE). It shows the differences in the T1 relaxation times of tissues. A tissue's T1-time reflects the time for the protons' spins to realign with the main magnetic field (B_0). T1 weighted sequences tend to have short TE and TR time. While fat rapidly reorients its longitudinal magnetization with B0, resulting in bright pixels on a T1-w image, water undergoes a significantly slower longitudinal magnetization

realignment following an RF pulse, leading to diminished transverse magnetization after an RF pulse, therefore water generates low signal pixels and appears dark.

Among the main advantages of T1-w sequences are the anatomical detail and the contrast between fat and other types of tissues, while the main disadvantages are the lower sensitivity to pathology and the limited soft tissue contrast. Most pathological conditions such as oedema and inflammation may not be as conspicuous on T1-w images as compared to other sequences such as T2-w. As for the soft tissue contrast, while T1-w images are excellent in distinguishing between some types of tissues, they may not provide as much contrast between soft tissues as T2-w images.

T2 weighted (T2-w) imaging sequences

T2-w sequences are widely used in diagnostic radiology, and play an important role in most examination protocols. One of the advantages of a T2-w sequence is its ability to provide high contrast between different soft tissues. In these images, fluid and oedematous tissues appear bright, making them particularly useful to identify pathologies like tumours, infections and inflammatory conditions. T2-w sequences are also valuable for assessing the integrity of ligaments and tendons. The drawback is that the sequence requires relatively long TE and TR times, resulting in longer scan times as compared to T1-w sequences. Therefore, T2-w images are more susceptible to motion artefacts, which can degrade image quality. Prolonged scan times can also be a challenge for patients, especially those who struggle to remain still during the procedure. Together with Short-T1 inversion recovery (STIR) images, fat-suppressed T2-w images are the most commonly used water-sensitive sequences. When this sequence is used with shorter echo times (TE) and therefore less T2 weighting, it is called proton density PD-w. In PD-w sequence the image contrast is caused by differences in proton density more than the magnetic characteristics of the tissue as in T1 and T2 weighting: tissues with few protons have low signal intensity, while tissues with many protons have high signal intensity.

Short-TI Inversion Recovery (STIR)

A STIR sequence is an inversion recovery (IR) sequence designed to suppress the signal from fat, allowing for good visualisation of abnormalities in soft tissues and fluid-filled structures. STIR nullifies the signal from fat by using a very short inversion time, and is useful in MSK imaging to highlight areas of oedema, tumours or inflammation.

STIR images are characterised by the bright signal from fluids, such as cerebrospinal fluid or joint effusion, and their dark signal from fat, which makes them useful to diagnose conditions

like bone marrow disorders, nerve root compression and joint diseases. Radiologists often use a STIR sequence when a high degree of contrast between pathology and tissue, without the interference of fat signal is required. The sequence is relatively immune to variations in field homogeneity and can be applied in proximity to metallic objects and over a large field-of-view. This allows for improved detection and characterization of abnormalities especially when imaging extremities. The signal suppression is not specific to fat; any material with a short T1 (e.g. melanin, methemoglobin, mucus) will be nullified. Therefore, STIR cannot be used after gadolinium administration to show contrast enhancement, which represents a limitation for T1-w STIR.

Gradient Echo (GRE)

GRE sequences represent an alternative approach to obtain different MR-weightings. It differs from spin echo (SE) sequences in two key aspects. First, GRE is produced by a single radiofrequency (RF) pulse while SE is produced by pairs of RF pulses. Second, GRE can use flip angles below 90°, commonly varying over a range of 10 to 80 degrees. In contrast to SE and IR SE sequences, GRE sequences exhibit greater versatility. The basic sequence can be modified by adding dephasing or rephasing gradients at the end of the sequence. In a basic GRE sequence, the choice of flip angle plays a crucial role in determining the type of contrast weighting in the resulting images. Larger flip angles give more T1 weighting of the image, while smaller flip angles are often used for more T2, or in gradient echo imaging T2* weighting, to the images. T2 and T2* weighting focus on highlighting differences in the transverse relaxation times (T2 and T2*) of tissues. These weightings are useful to accentuate differences in tissue properties, such as water content and mobility, and can be valuable to detect abnormalities like lesions or oedema. T2* is a parameter that helps characterise the decay of the MRI signal due to various factors, including magnetic susceptibility differences in tissues and the presence of paramagnetic materials.

In MRI, when a strong magnetic field is applied to the body, the hydrogen protons in different tissues align with this magnetic field. When a radiofrequency pulse is applied, these protons temporarily flip their spins and create a detectable signal. However, after the pulse is turned off, the protons gradually lose coherence and return to their original alignment with the magnetic field. The time it takes to this loss of coherence is described with the T2* curve and T2* time.

T2* can vary more than T2 between different tissues and substances in the body. For example, tissues with iron deposits or other magnetic materials may have a shorter T2* because these

materials cause faster signal decay. By measuring T2* and how it changes in different regions of the body, MRI can provide valuable information about tissue composition and properties. GRE sequences have several advantages, of which the following are the two most important. First, due to the low flip angle excitation and the consequent faster recovery of longitudinal magnetization which allows shorter TR/TE, GRE sequences are typically faster than some other MRI sequences like SE-sequences; this makes them well suited to image dynamic processes or to reduce scan time in patients who may struggle lying still for a long time. Second, GRE are sensitive to T1 relaxation, which means they are good at highlighting differences in tissue relaxation times; this makes GRE sequences useful for creating images with good anatomical contrast and contrast between fat and other tissues. GRE sequences may also have some limitations, such as susceptibility artefacts in the presence of metal or air, which can degrade image quality.

Dixon technique

The Dixon, or chemical shift-based water-fat separation technique exploits the chemical shift between protons of water and fat to decompose the signal from these two tissues in the same voxel and generates a set of four images per acquisition: in-phase (similar to standard T2-w images), out-of-phase, water-only (WO) (equivalent to fat- suppressed images) and fat-only (FO) (Figure 1) (19-21).

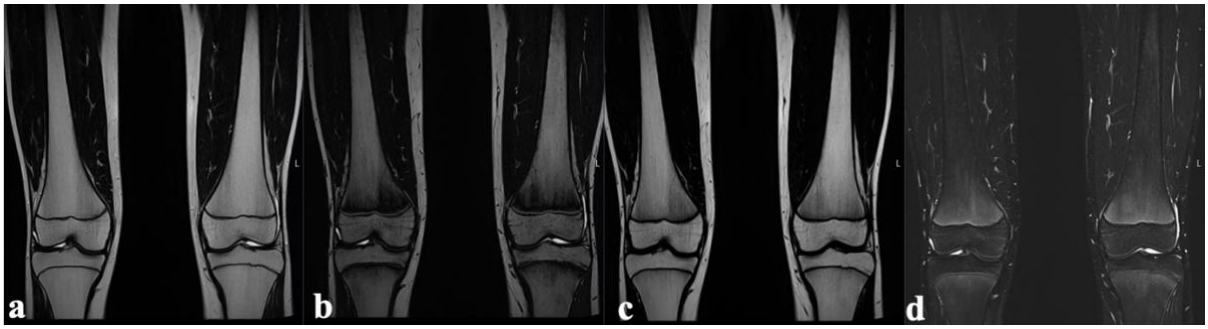

Figure 1. Knee MRI of a healthy 14-year-old boy. T2 Dixon sequence with all four image reconstructions (a. in phase, b. out of phase, c. fat-only, d. water-only).

Advantages of Dixon sequences are the uniform and robust fat suppression compared to other fat suppression techniques such as chemical shift-selective fat saturation (CHESS), and relatively higher SNR than STIR. On the other hand, the main disadvantage of Dixon sequence is represented by fat-water swapping artefact which is due to the presence of

chemical shift misregistration of water and fat, and results in images were fat signal in certain areas is depicted as water and vice versa.

Dixon T2-w images are increasingly being used for the evaluation of the MSK system in adults (22-24). Conversely, the use of the Dixon sequence in the study of MSK diseases in children is still relatively uncommon. A recent study from our group showed a high concordance between STIR and T2 Dixon water-only in the detection of high signal intensity areas in bone marrow on whole-body MRI in healthy subjects (9).

Regarding the fat-only images, several studies on adults have been carried out to demonstrate its potential to replace the T1-w Turbo Spin Echo (TSE) sequences in patients with suspected vertebral bone metastases (25) or low back pain and/or lumbar radiculopathy (26, 27). On the other hand, comparative studies between T2-Dixon fat-only and T1-w Turbo Spin Echo sequences aimed at replacing this latter for bone marrow pathology are lacking in children.

2.3 MRI in inflammatory MSK disease in children

MRI has a high sensitivity for the detection of early manifestations of inflammatory MSK disease that are not clinically or radiographically evident, before irreversible cartilage destruction and bony erosions occur (28). Furthermore, MRI is the most suitable technique for the detection of bone marrow oedema (BMO) (29) and for the assessment of bone erosions and progression of joint damage (30). In the following I will address the main imaging characteristics of different tissues involved in the two inflammatory MSK diseases addressed in this thesis, namely JIA and CNO.

2.3.1 Soft tissues on MRI

With MRI, soft tissues such as the synovium, joint capsule, tendons and surrounding musculature can be depicted. The synovium is composed of a thin inner cell layer, the intima, and a subintima containing a network of vessels (31). In the early phase of inflammation, the increased perfusion and vascular permeability, with subsequent aggregating inflammatory cells, can be visualised with MRI and is especially conspicuous on gadolinium enhanced, T1-w fat saturated images (32). Another marker of arthritis is joint effusion. Normally, all joints hold a small amount of fluid, however, in arthritis, the amount increases. On MRI, a joint effusion is depicted as homogenous high signal on T2-w sequences, and corresponding low signal on T1-w images. Notably, timing of the post-contrast sequence is important for synovial detection since gadolinium leaks into the joint fluid in 5-10 minutes; therefore, after

this short period of time, it becomes difficult to distinguish between synovium and joint effusion, especially in cases of severe inflammation (33, 34).

Tendons, consisting of collagen (mostly type I collagen) and elastin embedded in a proteoglycan-water matrix, appear dark on both T1- and T2-w images. The tendon sheath is thin and barely visible unless there is a pathological swelling. Tenosynovitis is identified as increased fluid inside the tendon sheath, synovial sheath thickening with or without increased vascularity potentially extending into the tendon sheath and subcutaneous oedema around the tendon.

2.3.2 Osteochondral tissues on MRI

On MRI, cortical bone appears dark on all sequences due to lack of hydrogen protons. Traditionally, T1-w SE sequences were used to detect bone erosions. As suggested by the Outcome Measures in Rheumatology Clinical Trials (OMERACT) group in adults (35-37), erosions can be seen as sharply marginated bone lesions with correct juxta-articular localization and low signal intensity on T1-w images in at least 2 planes, with a cortical break seen in at least 1 plane. Recently, a so-called black bone sequence, using short TEs and TRs as well as an optimal flip angle to minimise soft-tissue contrast and enhance the bone–soft-tissue boundary has been developed (38-40). We have little experience with this particular sequence, and have previously used, and validated T1-w SE sequence to identify bone erosions and depressions in children with JIA and wrists involvement (4).

The joint surface is covered by a thin rim of articular cartilage, best visualised on PD-w images (41, 42). The addition of a cartilage sequence to the MRI protocol has been previously recommended by the OMERACT MRI in JIA working group and the Health-e-Child Group as a way to differentiate true erosions from bony depressions, assuming that the latter are covered with cartilage while the erosions are not (43).

Bone marrow is made of hematopoietic, active “red” marrow, which is composed by 40% of water content, 40% of fat content and approximately 20% of proteins, and inactive, fatty “yellow” marrow, which is characterised by a higher proportion of fat (80%) and a lower percentage of water and protein (15% and 5% respectively) (44). The distribution of red and yellow marrow changes over time in response to normal development. At birth, the marrow is completely hematopoietic. During maturation, cellular red bone marrow is replaced by fatty marrow, and the remaining red marrow undergoes changes. Conversion from red to yellow marrow begins in the first year of life, and continues until around 25 years of age when the adult configuration is reached (45) following a predictable sequence within the body and

individual bones. In the long bones, the conversion first occurs in the epiphyses and then proceeds from diaphysis to metaphysis. At approximately 25 years of age, the red marrow is present only in the axial skeleton and in the proximal metaphysis of femora and humeri. In addition, during growth there is a continuous ossification process at the zones of provisional calcification, where cartilage is transformed into bone. Moreover, the skeleton in children is softer and more vascular than in adults (46).

The bone marrow response to inflammation consists in bone oedema which merely represents increased water content compared to the surrounding tissue. BMO is bright on T2-w images and is even more conspicuous on fat saturated and IR sequences (STIR, TIRM). On T1-w images, it appears as hypointense areas, which enhance after contrast administration.

Due to the exclusive fat composition of bone marrow, in adults the interpretation of bone oedema is rather straightforward on MR-images, as fat appears bright on T1-w images and is dark on T2-w fat saturated images. Conversely, in children the presence of hematopoietic marrow introduces diagnostic challenges, as it in large appears bright on T2-w sequences, similar to BMO. In addition, bright areas in the bone marrow suggestive of bone oedema in patients with musculoskeletal inflammatory disease have been found in the skeleton of healthy children too. In this regard, we have previously shown that more than half of healthy children aged 5-16 years have focal bone-marrow-oedema-like changes in the hand skeleton (47) and in the appendicular and in the axial skeleton (7, 8). Other authors have shown similar findings to the feet (48) and pelvis (49).

2.3.3 Whole body MRI

Whole-body MRI (WBMRI) has emerged over the last 20 years as a new promising imaging tool that allows a wide coverage assessment of both the skeleton and soft tissues with high spatial resolution in a single scanning session. The technique consists of a combination of high-spatial-resolution images obtained in limited body parts by bringing each segment of the body to the magnet isocenter by successive or continuous table motion. Consecutive stacks of sections with high-spatial-resolution are achieved on 20–50-cm fields of view and then merged using reconstruction software (50, 51).

Over the last decades the technique has gained importance in the field of oncology, and particularly in cancer predisposition syndromes, Langerhans cell histiocytosis (LCH), lymphoma, sarcomas, and neuroblastoma (52-54). The addition of diffusion-w sequences (DWI) allows for functional evaluation of neoplastic lesions, which is helpful in the assessment of viable tumour and response to treatment after neoadjuvant or adjuvant therapy.

In recent years, thanks to the combination of fast sequences, rapid table movement and the exquisite sensitivity of WBMRI to bone marrow changes, the indications for WBMRI have been progressively extended to the assessment of severity and extent of rheumatological and multifocal disorders affecting the musculoskeletal system, the latter being more frequently encountered in children and adolescents as compared to adults, such as CNO, dermatomyositis, and more recently JIA (55, 56). The main advantage of whole-body MRI is the simultaneous evaluation of the entire body as compared to conventional MRI, most often assessing one joint at the time. The technique is particularly useful to monitor treatment effect during follow-up (57).

WBMRI can be performed on both 1.5 T and 3 T scanners, but 1.5 T may be preferred when patients have non-removable metallic prostheses. An advantage of 3T scanners is seen in higher signal-to-noise (SNR), but the lower homogeneity of the static field can increase the water fat misregistration, leading to an increased risk of 'phase-wrapping' in Dixon scans (58).

A WBMRI protocol may vary according to the clinical question and the specific information needed by the healthcare provider, however protocols in adults generally consist of morphological T1- and T2-w sequences along with DWI (59). For children, a recent systematic review showed that no consensus has been reached on whole-body MRI-sequences, scan plans or parameters although most used coronal Short Time Inversion Recovery (STIR) with or without T1-w images (60).

2.3.4 Need for MRI scan time reduction

The increasing use of MRI and WBMRI has revolutionised the assessment of musculoskeletal inflammatory diseases in children, providing a comprehensive and non-invasive approach to diagnosis and follow-up of these conditions.

WBMRI, which allows for an MRI of the entire body in a single imaging session (61), ideally should include few sequences (at best only one) and few planes (at best only one) to shorten the examination time. However, at present, due to lack of validation and standardisation, most radiologists prefer to use a set of different sequences in fear of missing out important information.

The optimisation of paediatric protocols in general, and the reduction of scan time in particular are important issues for a set of reasons. Despite using different distraction techniques such as movie watching, an MR-examination can be intimidating and uncomfortable for children, especially for the younger ones. Moreover, longer scan times increase the chances of children

becoming anxious, claustrophobic or restless during the procedure. The chronic nature of both JIA and CNO warrants numerous follow-ups throughout childhood. A short and efficient MR-examination can reduce anxiety and may help the child to better tolerate both MRI scans and other medical procedures, contributing to a better overall patient experience.

MRI scans require patients to remain still for an extended period to obtain clear and detailed images. Children may find it challenging to lay still for a long period, which may cause motion artefacts. Examination time shortening reduces the likelihood of motion artefacts leading radiologists to obtain high-quality images and to improve diagnostic accuracy.

Moreover, prolonged MRI scans often necessitate sedation for paediatric patients to ensure they remain still throughout the procedure. Sedation carries inherent risks (62, 63) and can be avoided or minimised by optimising MRI protocols and reducing the acquisition times; therefore, reducing the need for sedation can improve patient safety and reduce healthcare costs. Last but not least, faster MRI exams can help reduce waiting times for paediatric patients by enabling more scans to be performed in a day, thereby decreasing the backlog and shortening the wait for diagnosis or treatment planning. This can ultimately increase the efficiency of the radiology department, benefiting both patients and healthcare providers. Paper 3 was carried out with the aim of achieving a reduction in scan time without losing diagnostic accuracy.

2.4 Common inflammatory MSK diseases in children

2.4.1 Chronic nonbacterial osteomyelitis (CNO)

CNO is an autoinflammatory non-infectious musculoskeletal disorder occurring primarily in childhood and adolescence, and more often in girls, first described by Giedion in 1972 (64). The disease covers a wide clinical spectrum, with mild and self-limited monofocal lesions at one end, and recurrent episodes of multifocal, sterile osteomyelitis known as chronic recurrent multifocal osteomyelitis (CRMO) at the other end (65).

CNO is characterised by unifocal or multifocal pain, more frequent at night, and swelling. It primarily affects the metaphysis of long bones with symmetrical involvement, although lesions can occur in almost every bone (66-68). Affection of tissues other than bone, such as skin, eyes, gastrointestinal tract and lungs, has been described (69). CNO often has a protracted course with numerous exacerbations and relapses at new and old sites (70-72). It mainly occurs in children and adolescents, with a peak of onset at 7–12 years.

The term SAPHO (Synovitis, Acne, Pustulosis, Hyperostosis, and Osteomyelitis) is frequently used by adult rheumatologists when discussing CNO (73). However, SAPHO should only be used for patients presenting with cutaneous features, including acne and pustulosis (65).

The annual incidence of CNO is estimated at 0.4 per 100,000 children. However, awareness of the disease has been raised. Recent studies have shown that CNO is more frequent than previously reported (15, 74, 75) and may represent one of the most prevalent autoinflammatory diseases in childhood. In a previous study (15) CNO was almost as common as bacterial osteomyelitis (OM). Particularly, children with acute or subacute nonrecurrent CNO are frequently misclassified as bacterial OM, without identification of causative pathogens. This is of special interest, since a correct and timely diagnosis is essential for long-term outcomes in both disorders.

Despite intensive scientific efforts, the exact physiopathology of CNO remains unclear. However, in the past few years it has been shown that altered cytokine and chemokine expression in innate immune cells have been involved in CNO/CRMO pathophysiology. It has been demonstrated that monocytes from patients with CRMO fail to express IL-10, resulting in an imbalance between pro- (IL-6, TNF-α) and anti-inflammatory cytokines (IL-10) (76, 77).

Treatment strategies for children with CNO vary widely. Nonsteroidal anti-inflammatory drugs (NSAIDs) are commonly used as a first-line treatment, while second-line therapies include glucocorticoids, methotrexate, sulfasalazine, tumour necrosis factor (TNF)-α inhibitors and bisphosphonates (78).

There is no confirmatory diagnostic test for CNO. Currently, the diagnosis of CNO may be given after the exclusion of other diseases such as blood diseases, histiocytosis, acute bacterial osteomyelitis, bone tumours or fibrous dysplasia, and in some cases is challenging (17). Histological examination of bone biopsies reveals acute and chronic inflammatory and reparative bone features like hyperostosis, without the recognition of any infectious agent. The diagnosis of CNO may be delayed, frequently up to years, due to the nonspecific and sometimes discrete clinical findings, slow symptom onset and relatively normal laboratory tests. This might lead to overtreatment, especially with antibiotics, bone biopsies sometimes repeated, and excessive exposure to ionising radiation.

Imaging is key for the diagnosis of CNO. In the presence of nonspecific bone pain, the first imaging modality is radiography. A focal lesion, lytic, sclerotic or mixed can be observed depending on the age and evolution of the lesion; hyperostosis and periosteal reaction can be present, although less frequently found (17). However, in the early stages of the disease, bony

changes can be very discrete and difficult to detect radiographically. Often the patient undergoes several x-ray examinations over time before the diagnosis of CNO is suggested. Computed tomography (CT) can visualise small bone lesions, however its role in the diagnosis of CNO is limited. Novel developments such as photon counting CT-techniques have not yet been validated in children, but have the potential for high resolution bone imaging at a considerably lower radiation dose. 99 m-technetium bone scintigraphy has no place in imaging CNO.

MRI, on the other hand, has proven helpful in the assessment of CNO, both with respect to lesion detection and pattern of involvement (17, 79). On T2-w sequences, the typical CNO lesion appears as a hyperintense geographic area in the metaphysis of the long bones or in the spine, pelvis, clavicle and/or sternum. On T1-w images, the lesion most often has a mixed signal intensity, depending on the amount of sclerosis. On diffusion weighted images (DWI) the apparent diffusion coefficient (ADC) values are significantly higher in CNO lesions as compared to reference locations (80). In sum, none of the MR-changes are pathognomonic for CNO, and the findings must be interpreted together with the history, clinical and laboratory findings.

As targeted MRI underestimates the number and characteristic distribution patterns (81), a WBMRI is now widely used to assess the rest of the skeleton for additional lesions (16, 82-84). WBMRI can also be performed as a screening test during the initial clinical assessment, whenever CNO is a likely differential diagnosis.

Performing WBMRI in the early stages of the disease is helpful, not only for a prompt detection of bone marrow involvement suggesting the diagnosis, but also because the presence of multiple bone lesions at typical sites on imaging might reduce the need for a biopsy. Some authors suggest that a bone biopsy should be reserved for cases where clinical or radiological findings are inconclusive or multifocality cannot be detected (79).

To date, there is a paucity of studies exploring a potential association between clinical and/or laboratory findings and MRI-features in patients with CNO. In a study on 178 patients with CNO (85) the authors reported that patients who presented with a multifocal form at baseline clinical assessment had higher CPR values as compared to those presenting with a mono-focal form. Subgrouping the patients into three phenotypes, including a “severe form” with raised inflammatory markers and a high prevalence of clinical multifocality/rare involvement of the clavicle, the authors found that the severe form had a poorer prognosis. This indicates that the number of symptomatic sites at baseline represents a prognostic marker, emphasising the

importance of identifying multifocality on WBMRI at an early stage for prompt instigation of treatment. Paper 1 was performed to make a contribution to fill this knowledge gap.

2.4.2 Juvenile idiopathic arthritis (JIA)

JIA is a broad term that describes a clinically heterogeneous group of arthritides of unknown cause with an onset before 16 years of age typically lasting for more than six months (86). For several years the classification system proposed by the International League Against Rheumatism (ILAR) has been accepted worldwide (87), however it has been recently shown that some JIA categories still include heterogeneous conditions (88, 89). Therefore, a new evidence-based classification system has been proposed (90).

The primary abnormality of JIA is the presence of persistent synovial inflammation of joints and tendon sheaths. Disease remission is actually the treatment goal for all children with JIA (91). Hence, early diagnosis is essential as it enables prompt initiation of pharmacological treatment which has the potential to reduce chronic long-term disability and consequently a poor and undesirable quality of life for the patient (92). Although the majority of children with JIA have ongoing disease into adulthood, it has been suggested that there is a "window of opportunity" during the early, subclinical stage, where prompt instigation of treatment might delay progression and induce remission (13, 14). It has been demonstrated that a rapid onset of treatment with anti-TNFα drugs significantly reduces inflammation, and may even lead to complete remission of cervical spine arthritis, thus preventing serious chronic/late changes (93). However, despite therapeutically advancements having reduced the morbidity, the observed long term side effects are concerning (94). Both over and under pharmacological treatment should be avoided, thus therapy should be adjusted according to treatment response. Unfortunately, clinical assessment of deep-lying joints such as the hips, even when performed by experienced rheumatologists, is difficult. According to the literature, hip-involvement in children with JIA is seen in up to 50% of the patients (95) and is considered a predictor of severe course disease. The majority of children with active hip disease develop irreversible changes within 5 years of diagnosis (96) and approximately 26–44% require a total hip replacement within the first 10 years of disease onset (11).Thus, imaging plays an essential role in assessment of hip-pathology.

Conventional radiography, in addition to exposure to ionising radiation, has a lower sensitivity and specificity as compared to ultrasound or MRI for the detection of disease activity and early destructive changes. However, radiography is still useful, particularly for the exclusion of differential diagnosis and for assessment of secondary growth disturbances.

Ultrasound (US) is often the initial imaging technique for the evaluation of joint inflammation, in particular for the detection of synovitis, tenosynovitis and enthesitis but also to guide intra-articular injections. However, US is less helpful for the examination of deep-lying joints and for the assessment of inflammatory osteitis and BMO.

MRI is the gold standard imaging modality for diagnosing JIA thanks to the multiplanar capabilities, excellent detail and soft tissue contrast and the absence of ionising radiation. It is able to depict features of the active inflammatory as well as the chronic changes. As for the active changes, it may detect synovial enhancement/thickening, joint effusion, tenosynovitis and BMO. Particularly, it is the most effective tool available for the detection of active synovial inflammation. Contrast-enhanced MRI can reliably differentiate the active destructive hypervascular pannus from the inactive fibrotic pannus and joint effusion (97) (Figure 2).

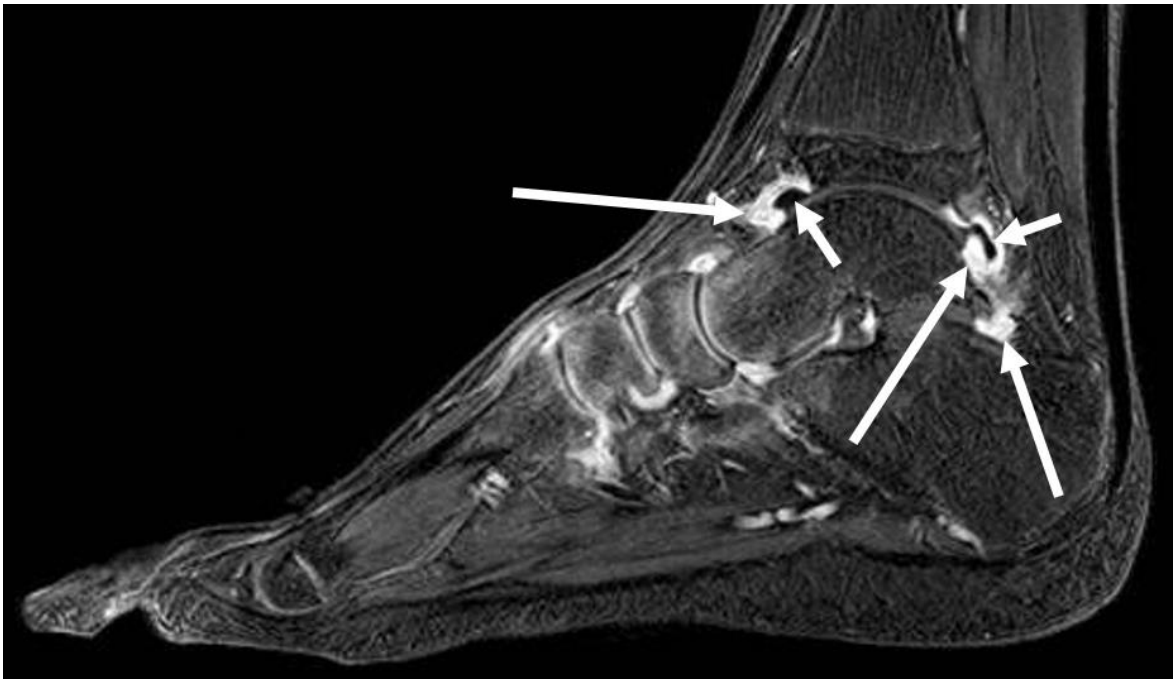

Figure 2. MRI of the ankle in a 13-year-old girl with a known diagnosis of JIA. A post-contrast fat saturated T1-w GRE sequence shows synovial thickening with increased enhancement (long arrows) which can be can easily differentiated from effusion (short arrows).

As for chronic changes, MRI can identify damage to cartilage, erosions and bone deformity. All joints can be assessed, including the complex or deep-seated joints that cannot easily be

evaluated on clinical examination or on US, such as the cervical spine, sacro-iliac and temporomandibular joints (TMJ) and hips.

In 2015 the European Society of Musculoskeletal Radiology (ESSR) Arthritis Subcommittee published their own set of recommendations on the standards of the use of MRI in the diagnosis of musculoskeletal rheumatic diseases, including JIA (98). These recommendations have been updated in 2020 by the ESSR and the European Society of Paediatric Radiology (ESPR) musculoskeletal imaging taskforce (99). The role of MRI is even more essential during follow-up for the assessment of disease progression.

Another key point in the management of patients with JIA is the definition of clinical remission and inactive disease, both of which currently are based on subjective symptoms and clinical assessment alone. Particularly, it is of utmost importance to understand whether clinical remission truly reflects the absence of synovial inflammation and whether the presence of focal contrast enhancement is a predictor of relapse and consequently of future chronic damage. In a recent study on 90 patients with clinically inactive JIA, it was demonstrated that subclinical synovitis detected on MRI is present in a large proportion of patients, being the best predictor of disease relapse and joint deterioration, with potential implications for patients' management of the disease (100). As for bone marrow changes, in adults it has been shown that BMO seen on MRI is predictive of erosive damage and poor outcome. Conversely, the prognostic value of bone marrow changes in children is still under investigation.

For all the above-mentioned issues it is of utmost importance to have repeatable and accurate child-specific imaging tools to monitor both active and chronic JIA-related joint changes to aid in clinical decision-making (99) and to prevent chronic damage (92, 101).

Many international efforts have been made during the past years to establish valid, MRI-based imaging protocols and child-specific semiquantitative scoring systems for the assessment of the JIA pathological features for different joints. However, methodological difficulties, and particularly lack of references for normal findings and imprecise scoring systems have led to both over- and underreporting of signs of pathology. A child-specific MRI scoring system for the knee named Juvenile Arthritis MRI Scoring (JAMRIS) was published in 2013 (102). As for the wrist, the development of a scoring system was initially based on the OMERACT Rheumatoid Arthritis MRI scoring system (RAMRIS) for adults (103). Malattia and colleagues developed the first paediatric targeted MRI scoring system in 2011 (104), comprising synovitis, BMO and bone erosions derived from RAMRIS. In the following years, the Radiology Health-e-Child group published a revised version of the three individual items

and added a fourth item: tenosynovitis (1-4). Very recently, a scoring system for the assessment of TMJ involvement in children with JIA including four variables in the inflammatory domain and seven variables in the osteochondral domain has been proposed (105).

As for hips, in adults with rheumatoid arthritis several validated scoring systems exist, including the Hip Inflammation Magnetic Resonance Imaging Scoring System (HIMRISS) and Hip Osteoarthritis MRI Scoring System (HOAMS) (106, 107). For children, however, although several scoring systems have been proposed (28, 108-111), no child- and hip-specific scoring systems including both inflammatory and chronic changes have been validated (99). In one study including 79 children with hip involvement, of whom 22 had confirmed JIA, the inter- and intra-observer agreement of several selected parameters were addressed using a simplified MR-based scoring system on a 0–1 scale (109). The most reliable features were the presence of joint effusion, BMO and the subjective assessment of synovium. The study reported significant differences across parameters in the intra-observer reliability and a poor to moderate interobserver reliability for most parameters, however, it was limited to the active inflammatory domain. Moreover, as underlined by the authors, most children with JIA did not have a confirmed inflammatory disease, further weakening the robustness of the study. Other authors have compared MRI and clinical or laboratory findings in small datasets, thus without testing the precision of the MRI markers applied (28, 108, 110, 111). More recently, two papers addressing non-enhanced MRI in the diagnosis of hip changes in JIA were published - one retrospective observational study including 97 children with clinically suspected hip JIA (29) and one study on whole-body MRI for the quantification of a total inflammatory joint score (112). However, again, repeatability studies of the suggested scores were not performed. From these premises comes the need to establish a specific and robust MRI-based scoring system for active and chronic JIA changes of the hip in children to be used for monitoring treatment effect in daily practice as well as measuring outcomes in clinical trials. Paper 2 was designed to accomplish this purpose.

3. Aims and hypothesis

The overall aim of the work presented in this thesis was to provide knowledge for better diagnostics and management of children and adolescents with inflammatory MSK-disorders, with a focus on JIA and CNO, by addressing different aspects of MR-imaging.

The specific study aims and hypotheses are as follows:

1. To examine patient characteristics, clinical presentation and pattern of involvement in children with a known diagnosis of CNO, with a special focus on MRI findings, combining clinical, laboratory and imaging data *(paper 1).*

   Hypothesis: Pain is a common presenting symptom in children with CNO; most have multifocal disease; the metaphysis of the long bones are most often affected and there is no correlation between the number of high-intensity-signal areas within the bone marrow on MRI and laboratory findings.

2. To devise and validate a child-specific MRI scoring system for changes of the hip joint in patients with a known diagnosis of JIA, in order to define the most precise MRI-markers for active and permanent change *(paper 2).*

   Hypothesis: MRI is a reliable method for assessment of active and permanent change of the hip joint in patients with JIA.

3. To compare T2 Dixon fat-only and TSE T1-weighted sequences in the assessment of bone marrow high signal areas seen on T2 Dixon water-only in healthy children and adolescents *(paper 3).*

   Hypothesis: There are no significant differences in the appearances of bone marrow between the two sequences under investigation, thus, T1 TSE can be replaced by T2 Dixon fat-only as part of a WBMRI examination in children and adolescents.

4. Materials and methods

4.1 Populations and data collection

The work in this thesis is based on three different cohorts; one cohort of children suffering from CNO, one with JIA, and a healthy cohort of children and adolescents examined for research purposes only.

4.1.1 CNO cohort

For paper 1, which is a retrospective bicentric study, we included 75 consecutive children and adolescents with a diagnosis of CNO seen at Ospedale Pediatrico Bambino Gesù (OPBG), Rome, or Haukeland University Hospital (HUS), Bergen, during 2012-2018. The criteria for CNO were mono- or multifocal inflammatory bone lesions, duration of symptoms >6 weeks, and exclusion of infections and malignancy (68, 113). We used the established normal ranges for laboratory data as follows: C-reactive protein (CRP) <0.5 mg/dL and erythrocyte sedimentation rate (ESR) <15 mm/h. In addition, we categorised inflammation severity (based on blood markers, ESR and CRP) as mild when at least one marker was raised but not >100, or moderate when at least one marker was >100. To secure the diagnosis in equivocal cases, a biopsy was performed. Data on age, sex, age of symptom onset, age at diagnosis, duration, clinical symptoms, laboratory and radiologic findings at diagnosis and follow-up was obtained from the clinical journal systems and the radiology information system (RIS) and picture archiving and communication systems (PACS) at the two institutions, while demographic, clinical and laboratory data along with histological findings, when available, were retrieved from the medical records.

4.1.2 JIA cohort

For paper 2 we included 60 children and adolescents aged 6-18 years with a known diagnosis of JIA according to the International League of Associations for Rheumatology (ILAR) classification criteria (87), of whom 37 were examined at OPBG and 23 at Istituto Giannina Gaslini (IGG). All patients had confirmed or suspected JIA-related hip involvement, and were included regardless of the severity and activity level of their condition and of current or previous medical treatments. All patients underwent MRI without the need for sedation.

4.1.3 Healthy cohort

For paper 3, 196 healthy children and adolescents aged 6–19 years during 2018–2020 were examined (78 at the Department of Radiology of Oslo University Hospital and 118 at the University Hospital North-Norway in Tromsø) as part of a larger national multicentre study (6-9). The participants were divided into 4 groups according to age (n = 47 for group 1, n = 52 for group 2, n = 47 for group 3, n = 50 for group 4). The subjects were recruited via mail, announcements on social media or direct invitation. None of the participants had contraindications to MRI, a history of cancer, current infection, chronic or systemic disease, metabolic or musculoskeletal disorder, or a symptomatic trauma within the past four weeks. No musculoskeletal symptoms were reported within 18 months after the first examination. All children and adolescents underwent a whole-body 1.5 T MRI performed for research purposes only. In no case was sedation needed.

4.2 Image protocols

Paper 1

All MRIs were performed on a 1.5 Tesla (T) Siemens MRI system. At OPBG an Aera and at HUS an Avanto machine was used (Siemens, Erlangen, Germany). The whole-body MRI included a STIR sequence (repetition time/echo time/inversion time [TR/TE/TI] 5,000/58/160 milliseconds (ms) and flip angle 147°; and a sagittal STIR sequence of the spine and feet, with additional T1-w images (TR/TE 400/7 ms) turbo spin-echo (TSE) in equivocal cases. Typical scan time for the whole-body MRI was 35–45 minutes.

Paper 2

All MRI examinations were performed on a 1.5-tesla (T) MRI system (Achieva Intera; Philips Medical Systems, Best, The Netherlands), using a body coil. The field-of-view (FOV) included the whole pelvis to allow visualisation of both hips. The children were imaged supine with the legs straight and the feet in a neutral position.

The following sequences were acquired:

- Three-dimensional (3-D) T1-w TSE sequence with repetition time/echo time (TR/TE) 600/10 ms, acquired and reconstructed voxel size of 1 × 1 × 1 mm, number of signal averages 2, acquisition time about 5 min;

- T2-w TSE fat-saturated (FS) sequence with TR/ TE 4,400/70 ms, voxel size 0.55 × 0.69 × 3 mm, base resolution 218, section thickness/gap 3/0.3 mm, number of signal averages 1, acquisition time about 4 min;
- 3-D spoiled gradient echo (GRE) FS sequence with TR/ TE 40/7 ms, flip angle (FA) 25°, voxel size 1×1×1 mm, acquisition time about 4 min, acquired immediately ("early") and approximately 5 min ("late") after manual injection of 0.2 mL/kg of gadoteric acid 0.5 mmol/m (Dotarem; Guerbet, Roissy, France) through a 21-gauge (G) cannula inserted into an arm vein, followed by a flush of 10 mL saline.

All sequences were acquired in the coronal plane. The mean scan time, including the time for positioning and injection, was approximately 25 min.

Paper 3

The whole-body MRIs were performed during free breathing, using phased array surface coils and a 1.5 T MRI scanner (Philips medical systems, Best the Netherlands, Intera model release 2.3 (n = 118) or Magnetom Siemens Aera, software e11c (n = 78)). Coronal T2-w Dixon and T1-w sequences were acquired from the skull-base to toes in 3–5 steps. The scan parameters including scan time are shown in table 1.

Sequence	TR (ms)	TE (ms)	NSA	Slice thickness (mm)	Readout band width (Hz per pixel)	Acquired voxel size (mm)	Scan time (min)
Coronal T1-w TSE	450	5.1	1	3.5	391	0.9x0.9x3.5	1:48
Coronal T2-w Dixon fat-only	5156	100	1	3.5	293	0.9x0.9x3.5	3:16
STIR	3500	80	1	3.5	312	0.9x0.9x3.5	3:16
Sequence	**TR (ms)**	**TE (ms)**	**NSA**	**Slice thickness (mm)**	**Readout band width (Hz per pixel)**	**Acquired voxel size (mm)**	**Scan time (min)**
Coronal T1-w TSE	467	7.6	1	3.5	303	0.9x0.9x3.5	1:30-2:00
Coronal T2-w Dixon fat-only	5640	109	1	3.5	521	0.9x0.9x3.5	2:30-3:00

Table 1. Basic MRI parameters for the whole-body 1.5 T MRI. T2-w Dixon, T1-w TSE and STIR sequences (for Philips scanner in the upper table, for Siemens in the lower). TSE = Turbo Spin Echo, TR = Repetition Time, TE = Time to Echo, NSA = Number of Signal Averages.

During the examination the child could either listen to music or watch a movie, and total scan time was approximately 30–45 minutes.

4.3 Image reading

Paper 1

All MRIs performed at the time of diagnosis were retrieved, and analysed by one of three radiologists with 3, 12 and 30 years of experience in paediatric radiology, respectively. Prior to the analysis, several calibration sessions were performed. The following features were registered: the bone(s) involved and the segment affected (epiphysis, metaphysis or diaphysis); and whether or not there was a periosteal reaction, growth plate involvement, vertebral compression or soft-tissue inflammation. BMO and soft-tissue inflammation were defined as increased signal intensity (as compared to the remainder of the bone, or to the contralateral side) on fluid-sensitive sequences, and scored on a 0-1 scale.

Paper 2

All hip MRIs were scored independently for active and chronic changes, growth abnormalities and secondary post-inflammatory changes by two sets of radiologists (Appendix 1). The first set scored the same MR images twice at an interval of 3 weeks. In this set, the scoring was performed in consensus by one paediatric radiologist (L.T.d H., with 14 years of experience) and one of two additional paediatric radiologists (P.L.D.P., with 9 years of experience, or P.d A., with 5 years of experience) at BGCH. The second set included one paediatric radiologist (S.C.S., with 7 years of experience) at Great Ormond Street Hospital (GOSH), London, who scored all the MRI images once, independently. All radiologists were blinded to disease duration, clinical symptoms and findings, JIA subtype and prior imaging.

Prior to scoring, we conducted three calibration sessions lasting 2 days each, using 30 MRI cases not included for analysis in this study to ensure standard terminologies and definitions could be agreed upon. We devised an imaging atlas with relevant examples of each variable and grade as a reference to help maintain a consistent standard of scoring across all readers (Appendix 2).

Inflammatory changes

Based on the pre- and late post-contrast 3D GRE and the coronal T2-w FS images, we scored:

1. Synovial enhancement intensity (using different scoring scales) and synovial thickening (measured both subjectively and objectively);
2. Presence of effusion;
3. Degree of overall synovial inflammation including thickening and enhancement intensity;
4. Degree of overall inflammation (Figure 3), adding effusion to the degree of overall synovial inflammation;

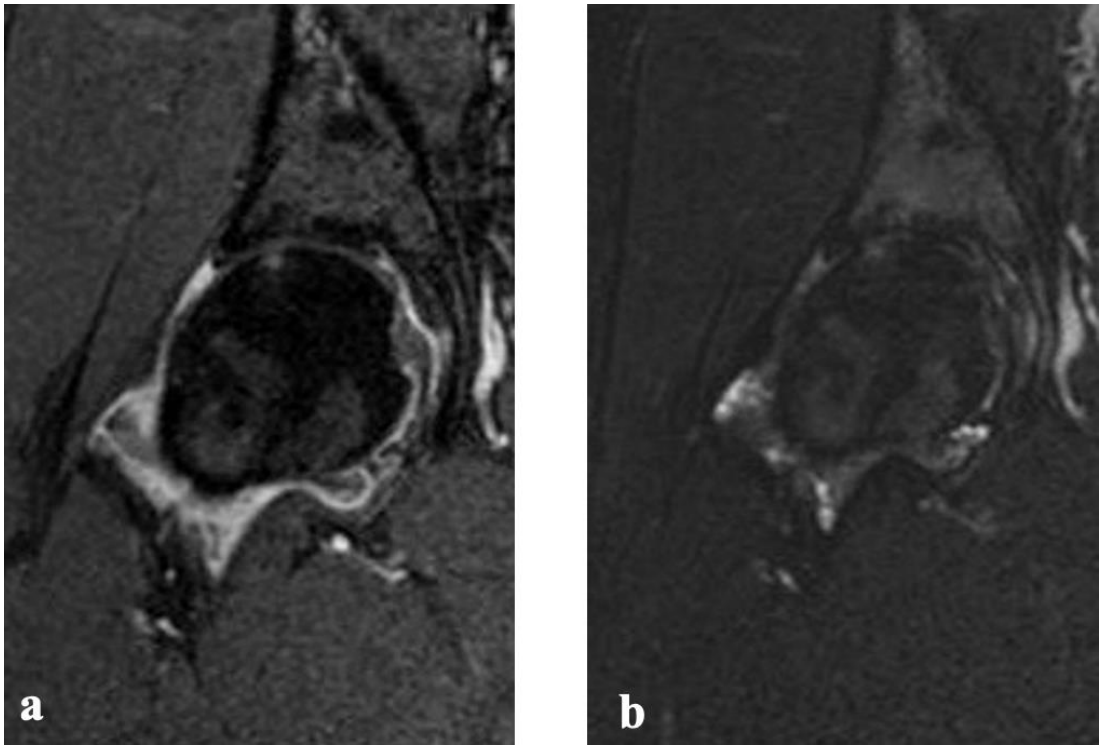

Figure 3. Coronal three-dimensional (3D) fat-saturated T1-w GRE sequence (a) and coronal T2-w FS MRI image (b) in a 15- year-old boy with JIA, showing a moderate (grade 2) overall degree of inflammation.

5. BMO, which was defined as an area of high signal intensity on T2-W FS images with corresponding low signal intensity on T1-W images and was assessed in the femoral head based on the proportion of bone involved (volume), in the acetabulum (measured subjectively) and in the femoral neck as absent or present (0/1).

Structural joint damage

Structural joint damage was evaluated on the 3-D TSE T1-W images, using fluid-sensitive and post-contrast images when appropriate. The following features were evaluated and scored:

1. Erosion (defined as a bony depression seen on at least two planes) in the femoral head based on the proportion of head volume involved, in the femoral neck and in the acetabulum as absent or present (0/1). Active erosions (defined as an erosion filled with enhancing pannus) were scored in the femoral head (Figure 4).

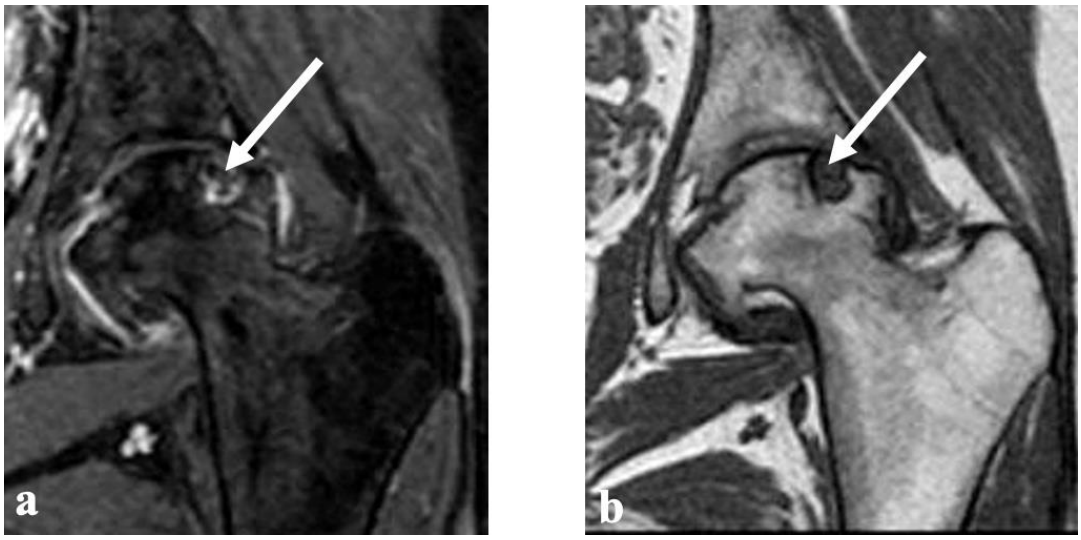

Figure 4. Coronal MR-images in an 18-year-old female with JIA. a) post-contrast 3-D gradient echo with fat saturation showing an erosion filled with enhancing pannus (arrow) and b) T1-W TSE image showing a large erosion in the lateral aspect of the femoral head (arrow).

2. Flattening of the femoral head was assessed in the coronal plane (mid-section) compared to what is expected for age, first subjectively and thereafter using a Mose circle. Bone cysts were described as sharply delineated, enhancing lesions with high signal on fluid-sensitive sequences and were scored as absent/present in three locations (femoral head, neck and acetabulum).

Cartilage damage

Based on 3-D GRE T1-W sequences, we assessed the joint cartilage width superiorly (mid-weight-bearing area), first judging it subjectively to be normal, mildly, moderately or severely narrowed and then taking measurements in millimetres. We also evaluated and scored cartilage in terms of signal abnormalities and morphological changes, as well as symmetry (right versus left joint space width). Based on the coronal T1-W sequences, we measured femoral neck width (in mm), femoral head/neck length (in mm), caput–collum–diaphyseal (CCD) angle and trochanteric femoral head distance (in mm). We also evaluated whether the physis was patent; the presence of coxa magna, coxa brevis or protrusio acetabuli; and the presence of fovea enlargement. Finally, we evaluated the presence of osteophytes and sclerosis on both coronal T1-W and fluid-sensitive FS sequences.

Paper 3

We employed a whole-body MRI child-specific scoring system for bone marrow assessment recently devised and validated using coronal T2 Dixon water-only images (6). According to this scoring system, signal intensity was graded on a 0–2 scale, where 0 = absent, 1 = mildly increased, and 2 = moderate increased up to fluid-like signal and extension on a 1–4 scale, where most bones were divided into predefined anatomical areas, 1 = very small lesion (<5%), 2 = involvement of up to 1/3 of the anatomical area, 3 = involvement of up to 2/3 of the anatomical area, 4 = involvement of up to the entire anatomical area. Based on intensity and extension, all the focal high signal intensity areas were scored and classified as “major” or “minor” findings, except for the hands, where only intensity was recorded (table 2). High signal intensity areas with a speckled appearance (defined as two or more roundish/punctuated high signals, size 2–5 mm) in the epi-, meta-, or diaphysis of the long tubular bones were excluded from the analysis.

For the present study the whole body was arbitrarily divided into 117 anatomical areas.

All the bone marrow high signal areas on T2 Dixon water-only were identified and scored in consensus by two radiologists with 20 and 6 years of experience in paediatric musculoskeletal imaging respectively, according to the abovementioned scoring system. The presence or absence of corresponding low signal was then evaluated initially on fat-only T2 Dixon images and, to avoid recall bias, on T1-w TSE images after at least 3 weeks in a blinded fashion by the same radiologists.

	Signal intensity on a 0–2 scale / extension on a 0–4 scale
Major MRI findings	-Signal intensity 1 and extension 3–4 or -Signal intensity 2 and extension 2–4
Minor MRI findings	-Signal intensity 1 and extension < 3, or -Signal intensity 2 and extension < 2

Table 2. Subclassification of MRI-findings into minor or major on water-only Dixon T2W images, based on signal intensity on a 0–2 scale and signal extension on a 0–4 scale.

When high signal areas on T2-Dixon water-only images were not visible as low signal areas on either T1-w or T2 Dixon fat-only sequences, the images were also evaluated on T2 Dixon out-of-phase as visible or not for confirmation of T2-Dixon water-only signal as a true finding. Areas flawed by image artefacts or by too low SNR for image analysis were registered and excluded from further analysis. In the event of discrepancies, the consensus was achieved by discussion. All evaluations were performed under identical conditions (on a high-resolution Sectra viewing system - IDS7 PACS - and optimised light settings).

For this study no children under the age of 6 years were included hence the results cannot necessarily be extrapolated to children under this age.

4.4 Statistical analysis

Paper 1

Differences between genders were examined using t- tests or Fisher exact/Chi-squared tests as appropriate. Multiple linear regression analysis was used to test whether rise in inflammatory markers (ESR/CRP), time to diagnosis, age or gender significantly predicted the total number of bony sites involved at diagnosis.

Paper 2

Intra- and interobserver agreement were analysed using a simple or a weighted (linear) Cohen's kappa coefficient with 95% confidence interval. A kappa value of < 0 was considered poor, 0-0.20 slight, 0.21–0.40 fair, 0.41–0.60 moderate, 0.61–0.80

substantial (good) and 0.81–1.00 almost perfect (very good) (114). Differences in measurements were analysed using 95% limits of agreement (termed repeatability coefficient, when used for repeat measurements) as per Bland–Altman. Bland–Altman plots are generally interpreted informally and a clinically acceptable agreement was set at 15% (115).

Paper 3

To examine for differences according to age using Chi-Squared tests, subjects were divided into four age groups (1 = < 9 years, 2 = 9–11 years, 3 = 12–14 years, 4 = 15–19). The agreement between T2 Dixon fat-only and T1 in the detection of low-signal areas was analysed using kappa statistics (with 95% CI) and percentage absolute agreement. Kappa values were interpreted as for paper 2 (114).

For all three papers, statistical analyses were performed using Predictive Analytics Software (SPSS) version 25-28 (IBM, Armonk, NY). All tests were two-sided and statistical significance was set at $p<0.05$.

4.5 Ethical approvals

When including children and adolescents in research, particular ethical concerns arise. The Helsinki Declaration emphasises the importance of voluntary participation in research ("World Medical Association Declaration of Helsinki: ethical principles for medical research involving human subjects," 2013). For inclusion of patients/ subjects to paper 1 addressing CNO, the Institutional Research Ethics Committee at OPBG approved the study. For patients residing in Bergen, the study was approved by the Norwegian Regional Ethics Committee (REK; no 28756). For paper 2, ethical approval was given by the Institutional Research Ethics Committees at OPBG or IGG, respectively.

As for the healthy Norwegian children and adolescents (paper 3), the study was approved by the Regional Ethics Committee, REK; no 2016/1696. Written informed consent was obtained from each participant (when > 16 years of age) or a caregiver (when < 16 years of age) according to national guidelines.

5. Main results

5.1 Paper 1

Chronic nonbacterial osteomyelitis — clinical and magnetic resonance imaging features

In paper 1, we studied patient characteristics, clinical presentation and MRI pattern of involvement in 75 children and adolescents (26 boys) with a known diagnosis of CNO. Mean age was 10.5 years (range 1-17 years) at time of diagnosis, while the median time from disease onset to diagnosis was 4 months (range 1.5–72.0 months).

We found that 59/75 (78.7%) of the children presented with pain, with or without swelling or fever; amongst whom 17 presented with isolated low back pain or pain around the sacroiliac joints (table 3).

	Boys (*n*=26)	Girls (*n*=49)	*P*-value[a]	Total (*n*=75)[b]
Age at diagnosis, year, mean (SD)	10.4 (3.3)	10.5 (3.1)	0.832	10.5 (3.2)
Age at onset, years, mean (SD)	9.5 (3.4)	10.0 (3.0)	0.534	9.8 (3.1)
Symptoms at presentation, number (%)				
Body pain	19	40	0.393	59 (78.7)
Localized pain[c]	9	10		19 (25.3)
Low back pain	3	14		17 (22.7)
Multifocal pain	5	5		10 (13.3)
Localized pain and swelling	1	11		12 (16.0)
Localized pain and fever (>38°C)	1	0		1 (1.3)
Fever only	2	2		4 (5.3)
Swelling only	1	2		3 (4.0)
Limp	3	5		8 (10.7)
Elevated inflammatory blood makers[d], number (%)	13	33	0.209	46 (61.3)
Mild	10	20		30 (40.0)
Moderate	3	13		16 (21.3)
Increased white blood count (WBC)	0	1		1 (1.3)

[a] Differences between genders were examined using *t*-tests or chi-square tests as appropriate; 2-sided *P*-values are given; $P<0.05$ is significant

[b] One boy age 4 months presented with agitation, crying

[c] Other than low back pain

[d] Erythrocyte sedimentation rate and C-reactive protein

SD standard deviation

Table 3. Age and symptoms for 75 children (26 boys) diagnosed to have chronic nonbacterial osteomyelitis (CNO) based on history and clinical, laboratory and imaging findings, with an additional biopsy in 54 children (72%).

A biopsy of the most prominent bone lesion on imaging, performed in 54/75 children (72.0%), showed features consistent with subacute/chronic osteomyelitis in 27, nonspecific changes in 17 and were inconclusive in the remaining 10.

Of the 75 MRIs performed at baseline, 68 were whole-body MRIs while 7 were targeted MRIs. On whole-body MRI, a median number of 6 involved sites (range 1–27) was found, whilst only five children (6.7%) had unifocal disease. The long bones of the lower limbs were affected in 58/75 (77.3%), of which the most common were femur in 46 (61.3%) children and tibia in 48 (64.0%) (figure 5). The pelvis was involved in 29 (38.7%), the long bones of the upper limbs in 20 (26.7%) and the spine in 20 (26.7%). Spinal involvement was often multifocal (61%) and thoracic spine was the most frequently affected (70% of cases) (figure 6). Sacro-iliac involvement was found in eight children (10.7%), of which seven were females.

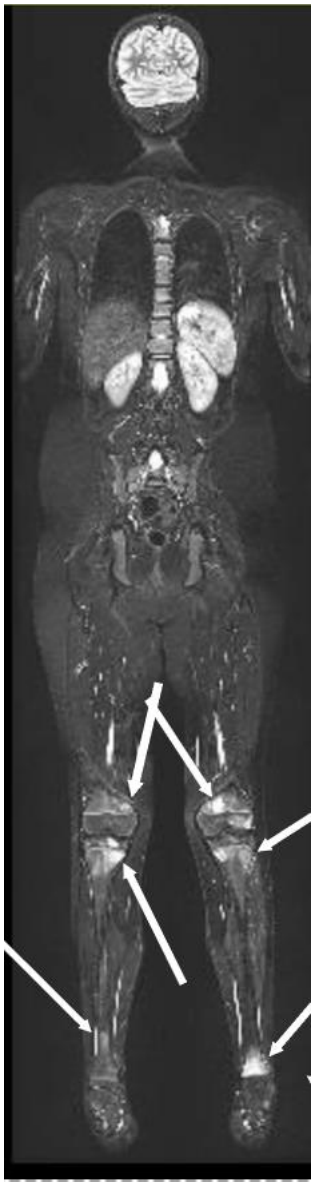

Figure 5. Whole-body MRI in a 10 old female with CNO (confirmed on histology). Coronal T2-W STIR sequence showing high signal intensity areas around the knee and ankle joints (arrows), consistent with CNO lesions.

Figure 6. A sagittal T2-w STIR of the spine in a 8-year-old girl with CNO showing diffuse high signal and height reduction of the 6th thoracic vertebral body (long arrow) and more limited high signal with endplate irregularity of the 9th thoracic vertebral body (short arrow).

Of lesions located in the long tubular bones, the proximal and distal metaphysis were involved in at least one bone in 43 and 37 children, respectively, while corresponding figures for the proximal and distal epiphysis were 19 and 26 children, respectively. At least one diaphyseal lesion was found in 27 children, in all cases located in the long bones of the lower limbs. A periosteal reaction was seen in four patients.

Inflammatory markers, which were raised in 46/75 (61.3%) children, significantly predicted the number of involved sites (β=0.250, P=0.045). Neither age (β=0.186, P=0.132) nor gender (β=0.103, P=0.387) nor disease duration (β=0.025, P=0.841) predicted the number of involved bone sites significantly. No statistically significant differences according to gender were seen in the number of bone alterations except for the fibula, prevalent in males, and for the spine, prevalent in females ($p = 0.01$ and $p = 0.03$ respectively).

5.2 Paper 2

A novel magnetic resonance imaging scoring system for active and chronic changes in children and adolescents with juvenile idiopathic arthritis of the hip

This study was undertaken to test the intra- and interobserver agreement of several MRI markers for active and chronic hip changes in children and young adults with JIA and to examine the precision of measurements commonly used for the assessment of growth abnormalities. 60 consecutive JIA patients (35 female) with confirmed or suspected hip involvement were included in the study. Of these, 23 had oligoarticular JIA (18 oligoarticular-extended and 5 oligoarticular-persistent), 17 had the polyarticular JIA subtype, 8 had enthesitis-related arthritis, 10 systemic JIA, 1 psoriatic JIA and 1 undifferentiated JIA. The mean disease duration at the time of the MRI was 8.6 years (range 0.2–18 years).

For active change, there was good intra- and interobserver agreement (with a kappa value of 0.7 and 0.6, respectively) for grading overall impression of inflammation on a 0-3 scale (effusion included). Grading overall impression of inflammation, omitting effusion, performed well for the intraobserver kappa of 0.7–0.8 while the interobserver kappa was 0.4. Synovial enhancement on a 0-2 scale showed a good intraobserver agreement (kappa 0.7–0.8), while the interobserver agreement was moderate (kappa 0.4–0.5). The intraobserver agreement for subjective evaluation of synovial thickening was good to very good (kappa of 0.8–0.9) while the interobserver agreement was moderate (0.4–0.5).

There was a good intra- and interobserver agreement for grading erosions in the acetabulum on a 0–3 scale, with kappa values of 0.6–0.7 and 0.6, respectively.

Regarding the grading of femoral head erosions, the intraobserver agreement was substantial (kappa values of 0.7–0.8), while the interobserver agreement was moderate (kappa 0.4–0.5). There was an excellent intraobserver agreement for grading active erosions of the femoral head, with kappa values of 0.9 and the interobserver agreement was good with a kappa of 0.6. Measurements of joint space width, caput–collum–diaphyseal angle, femoral neck–head length, femoral width and trochanteric distance were imprecise.

5.3 Paper 3

Whole-body MRI in children and adolescents: can T2-weighted Dixon fat-only images replace standard T1-weighted images in the assessment of bone marrow?

This study was performed to compare T2 Dixon fat-only and T1-w images for the assessment of high signal areas seen on T2 Dixon water-only images in order to shorten scan time of the whole-body MRI examination.

Areas with increased bone marrow signal on T2 Dixon water-only images were scored using a novel, validated whole-body MRI scoring system and classified into “major” or “minor” findings according to size and intensity. The areas were assessed for corresponding low signal on T2 Dixon fat-only images and on a T1-w sequence.

196 whole-body MRI from healthy children and adolescents (95 males) aged 6 to 19 years were included. Among 22.932 body-regions evaluated on T2-Dixon water-only images, 1290 high signal areas were identified of which 20 were excluded due to suboptimal T2 Dixon fat-only images and 20 due to suboptimal T1-w images, leaving a total of 1250 high signal areas to be examined.

730/1250 high signal areas were of mildly increased signal intensity while 520/1250 were moderately increased. The majority of high signal areas were seen in the lower limbs (n=564), pelvis (n=269) or in the upper limbs (n=287). 48 areas were found in the mandibles/spine and 82 in the thoracic cage.

1159/1250 (92.7%) high signal areas had corresponding low signal on both the T2 Dixon fat-only and T1 images while 24/1250 (12 major) (1.9%) showed no low-signal on either of the sequences (kappa value 0.39 (0.28-0.51), absolute agreement 94.6%). All 24 high signal areas with no corresponding low signal on either of the sequences were visible on the out-of-phase images. The agreement between the two sequences differed between age groups ($p<0.001$), with a kappa value of 0.10 (-0.12-0.3) for those under 9 years, 0.31 (0.06-0.56) for those 9-11 years, 0.51 (0.34-0.69) for those 12-14 years and 0.42 (0.18-0.66) for those 15-19 years.

67 high signal areas (5.4%) showed no concordance between T1-w and T2 Dixon fat-only images. Of these, 49 returned low signal on T2 Dixon fat-only images alone, and 18 on T1-w images alone (3.9% and 1.5% of the total, respectively).

The agreement between T2 Dixon fat-only and T1-w images was better for “major” findings as compared to “minor” findings, with kappa values of 0.69 and 0.29 respectively. When evaluating intensity alone, the agreement between T2 Dixon fat-only and T1 was similar for both mildly and moderately increased signal intensity.

As for locations, the agreement ranged between 0.51 for lower limbs and -0.01 for the pelvis. Discordance between the two sequences was frequently found in the humeri and in the ischiopubic/para-acetabular region.

6. Discussion

6.1 Study design

Paper 1

The first study was a retrospective, bicentric, cross-sectional study, well suited to describe the distribution of bone marrow findings on MRI in a large cohort of children with CNO. The retrospective nature of the study implies that the data were collected from the PACS-systems and clinical notes at the respective departments; bicentric in that patients were recruited from two different centres (BGCH in Rome and HUS in Bergen) and cross-sectional in that we collected data for all patients at time of diagnosis/baseline.

The retrospective and bicentric nature of this study have the following advantages: 1) the cost-effectiveness, being less expensive and quicker to conduct compared to prospective studies since it used existing data; 2) the inclusion of a large number of participants, which can enhance statistical robustness and 3) less ethical concerns since it did not require additional collection of data. On the other hand, the retrospective design have some challenges, being 1) limited data control as researchers must rely on existing data, which may lack important information or be subject to inaccuracies and missing data; 2) temporal ambiguity as it can be challenging to establish causality and the temporal sequence of events in retrospective studies as data were collected after the fact and 3) selection bias, in this particular study implying that patients not having CNO could have been included. As for the latter, although 21 of the 75 (28%) patients included had no biopsy performed, all met the diagnostic criteria for CNO.

Although seven patients, all with a confirmatory biopsy, did not have a whole-body MRI at baseline, they were included in the analysis of distribution of MR-findings. This might have led to an underestimation, although small, of MR-based lesions. The correlation between laboratory markers and sites of involvement on imaging was performed on the 68 cases with whole-body MRI. Another methodological issue is whether or not our cohort can be considered population-based. True population-based studies should include all cases within a pre-defined geographical area, and the number of cases should then be analysed in light of the total, age-matched population in the same area. In our study the cohort of children and adolescents with CNO comes from one of two paediatric centres, Rome and Bergen. Both centres are the only units within a particular geographical area that deal with this patient group, thus, we believe the results to be representative also for other areas, although it does not fulfil the strict criteria for a population-based study.

Paper 2

Paper 2 is a prospective study, including a group of children and adolescents with a known diagnosis of JIA and hip involvement from two different centres (BGCH and IGG). The prospective design has the main advantage of control with data collection which ensures that data are collected consistently and accurately, enhancing the reliability and validity of the findings.

Prospective studies have some disadvantages, the main being: 1) attrition, when participants drop out, making it difficult to maintain a representative sample, affecting the generalizability of the findings; 2) follow-up, requiring extended periods, which may not be always feasible; 3) ethical considerations as in some cases participants are exposed to risks or interventions.

However, in this study we analysed a single hip MRI from each patient and follow-up was not planned, thus drop-out was not a problem. Moreover, no participant was exposed to risks or interventions as the MRI was part of each patient's diagnostic procedure. Prior to the assessment, a scoring system was established and piloted. An imaging atlas was devised, showing typical examples of each variable and grades as a reference to facilitate a consistent standard of scoring across readers.

In this study, addressing an objective assessment of hip-changes, both in the inflammatory and the destructive domain, methodological issues included the nature of the dataset and the scoring method. As for the dataset, we included consecutive children, adolescents and young adults with a diagnosis of JIA and confirmed or suspected hip involvement, of any disease severity and activity level, over a 2-years period, irrespective of current or previous medical treatments in order to achieve a balanced dataset, allowing for all grades of the scoring system to be tested.

Regarding the evaluation of MRI-based scoring systems' precision, our research group has extensive experience (1-4). Experiences from these repeatability exercises were shared and discussed, and criteria for different grades and scores employed in the current study were agreed on and tested prior to the actual scoring process.

Paper 3

The third cohort included 196 healthy children and adolescents between 6 and 19 years of age who underwent a whole-body MRI for research purposes only during 2018-2020, as detailed in the paper. The participants can be considered "healthy" since none of them reported any

musculoskeletal symptoms during the enrolment and within 18 months after the first examination.

Methodological issues include the nature of the dataset used. To obtain a balanced dataset with respect to sex and age, stratified sampling was performed. Stratification is the process of dividing members of the population into homogeneous subgroups before sampling.

The initial dataset included 1290 high signal areas, however 40 of these were excluded due to suboptimal T2 Dixon fat-only images or T1-w images, resulting in 1250 high signal areas for analysis. These 40 excluded areas were predominantly found in the upper limbs, which are more susceptible to motion artefacts. Nonetheless, we believe that omitting these areas introduced only a minor bias which did not notably affect the study outcomes.

6.2 Technical aspects of MRI

Setting up an MRI protocol includes choosing MR-machine, sequences and coil. In addition, technical parameters for each of the sequences, beyond field strength, TR, TE, fat saturation and slice thickness, have to be determined and standardised between centres to obtain comparable images, particularly for research purposes; amongst these, for instance are echo-train length, number of averages, phase-encoding direction, receiver bandwidth, acceleration techniques, interslice gap, and sampling percentage. These are all factors with a direct impact on the acquisition, and can affect both the possibilities of post-processing and the quality of the images presented to the radiologist.

In paper 1, although all the examinations were performed on a 1.5 T magnet (Siemens) using similar sequences, the retrospective nature of the study did not allow for a detailed standardisation of the sequences. Moreover, in equivocal cases, additional TSE T1-w sequences were performed which may have led to a higher detection rate in children with a higher number of MR-series.

In paper 2 all patients were examined with a Philips 1.5 T MRI system using the same protocol, coil (body coil), position (supine with straight legs and feet in neutral position) and field of view (which included the entire pelvis to allow visualisation of both hips). These data were prospectively sampled and a uniform protocol was agreed upon between the participating centres to ensure the homogeneity of the MRI images.

The protocol was standardised for the sequences employed as well as for the timing of post-contrast images. Despite the increasing use of MRI in arthritis, there is no consensus on the exact timing for post-gadolinium images. The suggested interval between contrast

administration and image acquisition is within 5 minutes (116), which is approximately what we did employ. The rationale behind early post-contrast images is that, if acquisition is delayed too long, contrast washout from the synovium into the joint fluid obscures the borders between the synovium and an effusion, as was demonstrated in two studies of patients with rheumatoid arthritis (117, 118). For paper 2, however, timing of the post-contrast images was not an issue, as the aim of this study was to device a scoring system rather than describing MRI findings in a cohort of JIA patients.

In paper 3 we compared two different MRI sequences that were part of the same examination. Examinations were performed on two different sites with two 1.5T machines from different vendors. The scan protocols used were carefully adjusted to be as similar as possible, although small differences, such as differences in artefacts and SNR remained.

6.3 Statistical considerations

The statistical analysis used in this thesis are as described in the different papers. In the following I will elaborate on some important issues.

Precision and reproducibility

Precision of diagnostic methods can be measured in several ways and along different scales. For instance, along a scale of intraobserver agreement when the same observer measures twice at a certain interval to avoid recall bias (repeatability), or when two observers in a blinded fashion measure the same measurement (reproducibility). The variability of the measurements reflects the degree of precision. In other words, intraobserver variability refers to the consistency of measurements or observations made by the same person or observer at different times. It assesses how reliable an individual's measurements or judgments are when they perform the same task repeatedly. Interobserver variability pertains to the consistency of measurements or observations when different individuals or observers perform the same task or make judgments on the same subjects or samples. It assesses how well different observers agree on their findings, indicating the degree of objectivity and consistency in the observations or measurements. In both cases, low variability indicates a high level of precision, meaning that the results or observations can be trusted to be consistent and reliable when the study is repeated or when different observers are involved. High variability, on the other hand, suggests that there may be inconsistencies or uncertainties in the data, which can impact the reliability and validity of the study's results. Consistent training and standardisation of observers can reduce both intra and inter-observer variability.

In general, different statistical methods are used to analyse precision or agreement of continuous and categorical variables, respectively. For qualitative (categorical) data we used a simple or a weighted (linear) Cohen's kappa coefficient, with 95% confidence intervals (CIs) to evaluate the degree of intra- and interobserver agreement (papers 2 and 3). A simple kappa coefficient was used for dichotomous categorical variables, while weighting, taking the degree of disagreement into account, was used for three or more categories, as detailed in papers 2 and 3. The kappa coefficient is a commonly used method to assess agreement beyond chance (119) with values ranging between -1 (perfect disagreement) and +1 (perfect agreement). If there is a skewed distribution of the number of observations in each category, a situation with high observed absolute agreement but low kappa value can occur; the so-called "kappa paradox". Opposite, asymmetrically, unbalanced marginal totals might lead to a high kappa (120). This problem was addressed by Gwet (121) who developed a model for assessing agreement regardless of prevalence. The method might have some strengths as compared to Cohen's kappa, but it is not as thoroughly tested and known as its predecessors and was not used in this thesis. Given the above-mentioned caveats, we presented the distribution of MRI scores for the various features assessed in paper 2, and added contingency tables and the percentage of absolute agreement in paper 3.

As for the evaluation of the concordance of continuous variables, agreement within and between observers was assessed using 95% limits of agreement (termed repeatability coefficient, when used for repeat measurements) as per Bland-Altman. Bland-Altman plots are generally interpreted informally and a clinically acceptable agreement was set at 15% (115).

In the literature, intraclass correlation coefficient (ICC) is often used to assess the agreement between or within observers. However, ICC only measures the strength of an association without giving information on agreement (122). Correlation does not take into account, for instance, systematic bias between two observers, and consequently, even a high correlation between two observers does not guarantee a clinically acceptable agreement (115).

Calibration of measurements and scores

Detailed definitions and appropriate calibration and standardisation of scores are crucial when assessing agreement between observers. In paper 1, the MRIs were analysed by at least one of three experienced paediatric radiologists. Prior to the MRI assessment, two of these researchers had standardised their scoring techniques through several studies (1-5) and were

thus sufficiently calibrated. The third researcher was trained by LTdH through assessment and discussion of 20 cases, not included in the present study.

For paper 2, three two-days calibration sessions were performed to ensure standard terminology and definitions, using 30 hip MRIs not included in the present study. Moreover, an imaging atlas showing examples of each grade of the MRI features assessed was devised and used during the scoring process (Appendix 2).

As for paper 3, scoring of the images was done by two radiologists in consensus. Although this method has been criticised for introducing potential bias of semi consensus and neglecting the individual variability within scoring systems, it is widely used (123). Notably, it has been demonstrated that an additional reader can improve the reproducibility of MRI interpretation compared to one expert alone, even when the second is moderately experienced (124).

6.4 Ethical considerations

Research involving children requires careful ethical considerations (125, 126). Children, as a vulnerable population, warrant special protection and respect in research to ensure their wellbeing and rights are upheld. There are some issues in research on children, in particular concerning informed consent, the protection of privacy and confidentiality, the assessment of risks and benefits, the psychosocial impact and the use of age-appropriate communication.

Regarding informed consent, it must be taken into account that children may lack the capacity to fully understand the research purpose, risks and benefits and are not legally capable of providing consent on their own. Therefore, parental or guardian consent is mandatory while also considering the child's assent, depending on their age and maturity level.

It is also essential to protect the privacy and confidentiality of children who participate in research. Therefore, researchers must establish robust measures to safeguard sensitive information and ensure that data cannot be traced back to individual participants. In our studies, data security was handled according to the existing regulations.

Moreover, researchers must carefully assess the potential risks and benefits associated with children's participation. Balancing the pursuit of knowledge with the well-being of children is crucial to avoid exposing them to unnecessary harm. Participation in research can have psychosocial effects on children, including stress, anxiety, or feelings of vulnerability. Researchers must be sensitive to these potential impacts and take steps to mitigate them.

Furthermore, communication with children must be age-adequate, including appropriate information sheets according to age, ensuring that research information is presented in a way they can understand. A clear and simple language to convey complex concepts should be used. Additional considerations should be taken into account when healthy children are involved in scientific research. Particularly, it is essential to justify the necessity of recruiting this specific population. Researchers must demonstrate that the research question cannot be adequately addressed including children already within the medical care system due to different diagnosis, adult participants or other methods, and that the potential benefits of the research are significant.

Furthermore, it is important to ensure that participation of healthy children does not interfere with their education, social development or overall well-being. Researchers should closely monitor the children's well-being throughout the study. Any adverse effects or unanticipated consequences should be promptly addressed and the study may need to be modified or stopped if children's safety or well-being is at risk.

Last but not least, independent ethics review boards or committees play an important role in assessing and approving research involving children. These boards evaluate the ethical aspects of the research ensuring that it adheres to established guidelines and principles. In our studies, none of the above ethical issues violated the Norwegian law 'Helseforskningsloven' §18 that regulates medical research stating that in all medical research the disadvantage or risk from participation in a research project must be insignificant.

Moreover, our research, when applicable, also took into account §18b, which requires that the participation of all subjects must be voluntary and that informed consent must be obtained, and §18c, which states that the research should be beneficial for the research 'object' itself or for other individuals with similar age-specific illness or disease. Special attention was given as not to cause any distress to the young volunteer subjects included in paper 3. Written information was given to all participants (Appendix 3). The MRI unit was shown to children and adolescents before undergoing the examination and all were informed about the possibility of leaving the study at any time. One of the responsible researchers was always present during the scan to ensure the well-being of all participants. Of note is that a few incidental MRI findings were seen in some of the children, who were subsequently referred to the appropriate Specialist outpatient Clinic, according to the a priori protocol.

6.5 Discussion of results

Results presented in this thesis show that nearly one fourth of children with CNO presented with isolated back pain, that the most commonly affected sites were the femur, tibia and pelvis and that increased inflammatory markers seem to predict the number of MRI sites involved. Moreover, MRI is a reliable method for grading of active and chronic change in children and adolescents with JIA-related hip involvement. Finally, the study showed that T2 Dixon fat only can replace a TSE T1-w sequence in the assessment of bone marrow findings.

Paper 1

Paper 1 describes the clinical and laboratory, as well as the MRI findings, in a large cohort of children and adolescents with a diagnosis of CNO. Most had multifocal disease, with up to 27 involved sites on MRI, with a median of six.

It is well known that there is a discrepancy between the number of painful sites at clinical examination and the number of bone marrow changes seen on MRI/whole-body MRI (81, 85). Particularly, in the study from Wipff et al including 178 patients with CNO, mean age at diagnosis 10.9 years (85), the authors found that nearly 70% of the patients presented with multifocal disease based on clinical examination, rising to 93% when based on MRI findings, suggesting that the clinical evaluation underestimates the "true" bone involvement. We found a similar discrepancy in our study, as only ten (13.5%) patients reported on multifocal bone pain, while a whole total of 69 (93.3%) had multifocal bone marrow signal alterations on MRI, the number of sites varying between two and 27 with a median number of six (figure 7).

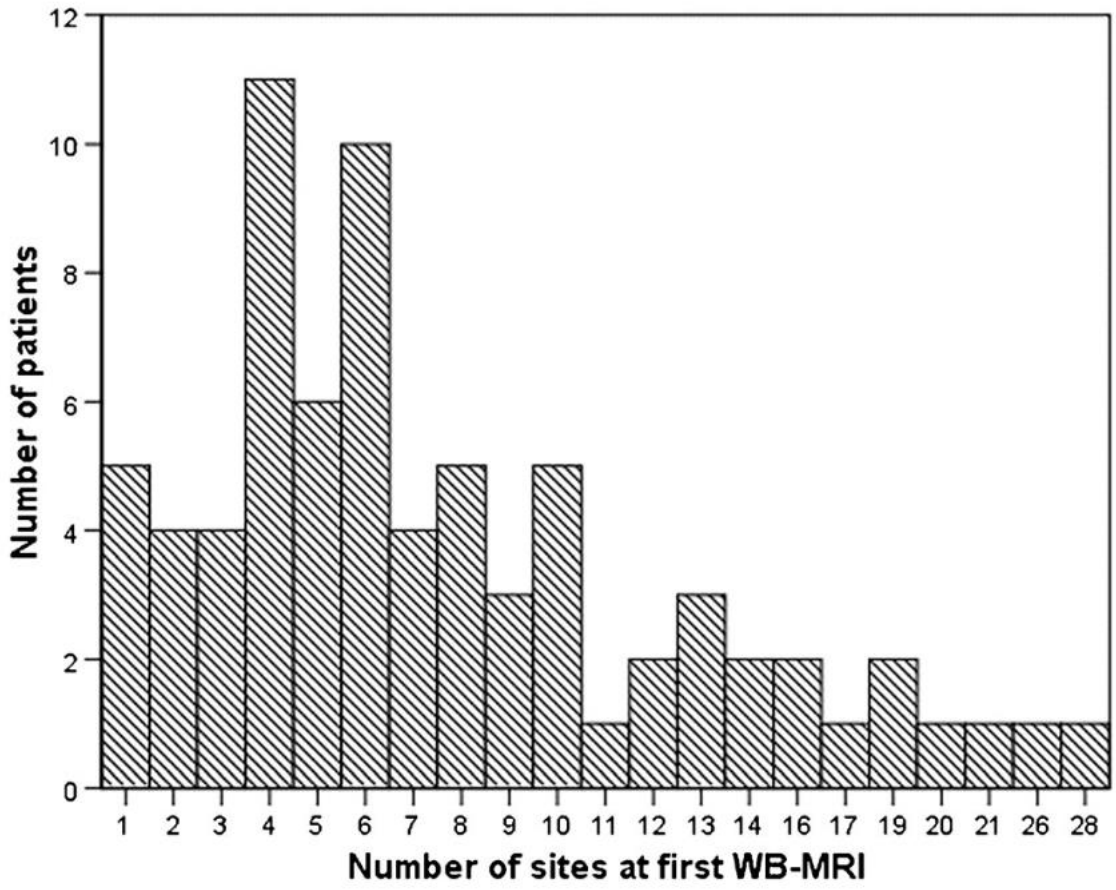

Figure 7. Graph shows number of sites based on the initial whole-body MRI examination in 67 of the 75 children with chronic CNO.

In a retrospective study by Andronikou et al on 37 children with CNO diagnosed on whole-body MRI, 8.6 lesions per patient were reported, with 89% of the patients having multifocal disease (81). The authors noticed two patterns, namely a tibio-appendicular multifocal pattern, i.e. a multifocal appendicular lesion with predominantly tibial involvement, and a clavicular-spinal pauci-focal pattern, i.e. a primarily clavicular group with a paucity of other lesions predominating in the spine.

In our study, we were not able to identify specific patterns in distribution except for the fact that 57% of patients with involvement of the clavicle had concomitant involvement of the tibia. Statistical pattern recognition analysis might have added to the results; however, the sample size was too small. Interestingly, we found that elevation of inflammatory markers significantly predicted the number of sites (β=0.250, P=0.045) as identified on MRI; this result indicates that the number of MR-positive sites might mirror the severity of

inflammation. Given future studies confirm these findings, this finding might support an early WBMRI to guide treatment. However, the cross-sectional design of the current study did not allow for association analysis between the number of MRI-sites at presentation and long-term outcomes.

In our study, the observed female/male ratio of 2:1 was in line with that reported by others, both for CNO and for other autoimmune diseases such as juvenile dermatomyositis and juvenile idiopathic arthritis reflecting that sex hormones might play a role in autoimmunity (127).

The lower limb was the most commonly involved site, a finding that compares well with that of others (17, 128). Particularly, Falip et al reported that in 90% of cases the lesions in long bones were centred at the metaphysis, of which 55% had an associated oedematous epiphyseal reaction. In a study of 53 WBMRIs of children and adolescents, von Kalle et al found, in 75% of patients, the combinations of at least one metaphyseal lesion in a lower limb and an additional lesion in the clavicle, sternum, pelvis or spine. The reason for this particular predilection site is still unknown, however. Similar to previous studies (17, 79, 129) we found periosteal reaction, non-aggressive type, in four patients only, all of whom reported focal pain.

In our study, bone pain, although nonspecific, was the most common presenting symptom, reported by nearly 80% of the patients. Nearly one fourth of the children suffered low back pain. In contrast to others, the time from onset of symptoms to diagnosis was relatively short, with a median of four months, reflecting an increased awareness of the disease amongst paediatricians. The proximal metaphysis was involved in at least one bone in 43/75 (57.3%) and the distal metaphysis in 37/75 (49.3%), an observation also reported by others (17, 65, 68, 130).

In our study, the diaphysis was involved in more than a third of the patients, all within the lower limbs. This figure is somewhat higher than reported by others (68). This discrepancy may reflect a true difference, or it may be caused by methodological differences. Future studies might clarify.

Spinal involvement has been reported in 2-43% of cases, depending on study design, method of ascertainment and definition of changes (82, 131). In their study of 31 patients, Falip et al speculate that the wide variation might reflect underdiagnosis of spinal involvement (17). Others have obviously already taken this possibility into account, by adding a sagittal STIR sequence to the WBMRI protocol in cases where vertebral and/or sacral involvement is suspected (17, 128).

In spine involvement, the thoracic part is most frequently affected (Hospach 60%; Falip et al. 75%) (17, 132) often involving non-contiguous vertebrae without crossing the disc. The latter finding allows for differentiation between CNO and infectious spondylodiscitis. Typical MRI findings are abnormal bone marrow signal intensity and endplate irregularity (82), however vertebral compression fractures with consequent kyphosis are not uncommon (133). Thus, early detection of spinal involvement is crucial since vertebral fractures have important implications on patient outcome (134). In particular, vertebra plana is of utmost importance for optimising treatment and further management, as the vertebral deformity most unlikely responds to current medication (130, 135).

In our cohort, 27% of patients had spine involvement as shown on MRI (134, 136). We can consider this incidence reliable as the readings were taken by 3 experienced radiologists and sagittal scans were performed in all patients. The involvement was often multifocal, the thoracic spine being the most frequently affected. Three patients presented with vertebral compression with mild kyphosis. No cases of scoliosis, a seldom reported finding (137) was found. We found that more than 10% of the patients had involvement of the sacroiliac joint on MRI. This finding, in line with previous studies (138, 139) supports the hypothesis that CNO might represent an unusual form of spondyloarthropathy (SpA). Particularly, in a multicentre study on 41 children with CNO and SAPHO syndrome the authors reported that osteomyelitis in the pelvic region was significantly associated with other features of juvenile spondylarthritis, such as inflammatory bowel disease (IBD) and an increased prevalence of the HLA-B27. The authors indicated that CNO can be considered an atypical SpA since the sacroiliac involvement tended to be unilateral, there was no familiar background and the anterior thoracic spine was often involved. An overlap between imaging findings of enthesitis-related arthritis (ERA) subtype of JIA and CNO has also been reported (140).

In sum, our findings in CNO patients shed some light over this intriguing, autoimmune disease, although important imaging-related questions remain. In particular, this study is not able to answer if clinically “silent” MRI-lesions represent true CNO-related pathology as suggested by some authors (70, 75) or if they merely reflect normal, growth-related changes. This second hypothesis is supported by recent work from our research group showing that a high proportion of healthy children and adolescents have one or more high signal changes within bone marrow (7, 8). However, based on the fact that elevation of inflammatory markers significantly predicted the number of sites as identified on MRI, we speculate that the majority of high signal, asymptomatic areas in this particular patient group might represent true disease. Future studies might help clarify this issue, though.

Paper 2

Paper 2 represents a first step toward establishing a valid MRI scoring system for JIA- related hip changes. The precision of different measurements and scoring systems used in radiology is essential for their clinical validity, thus for their usefulness in a clinical setting. Unlike previous studies (table 4) (28, 29, 108-112) we included a relatively large number of patients, and assessed multiple parameters (isolated and in combination) for both acute and chronic pathologies in children with hip-JIA. In addition, we examined the precision of MRI-based measurements for secondary growth abnormalities.

Previous studies	N of patients	Study characteristics
Argyropoulou MI et al 2002	28 JIA	Symplified scoring (six-point scoring system) No intra and inter-reader agreement
Nistala K et al (2007)	34 JIA	Retrospective Only inter-observer agreement
Porter-Young FM et al (2018)	79 suspected JIA (22 with JIA)	Retrospective Only active features Moderate agreement between observers
Kirkhus E et al (2011)	59 with non-specific arthritis (27 with JIA)	No hip-specific scoring Different MRI sequences used
Abd El-Azeem MI et al (2012)	30 JIA	Symplified scoring (seven-point scoring system) No intra and inter-reader agreement
Ostrowska M et al (2021)	97 (suspected JIA)	No contrast Severe chronic damage only in 3 patients
Panwar et al (2021)	Initial consensus-driven phase towards developing a scoring system	No contrast WBMRI scoring system Only synovial and entheseal inflammation
Tanturri de Horatio et al (2022)	60 JIA	Prospective Bicentric study Intra and inter-reader agreement Both active and chronic features Balanced dataset

Table 4. MRI scoring systems proposed for hips in children with JIA.

Amongst the examined parameters for active disease, the overall degree of inflammation on a 0-3 scale performed best, with good intra- as well as interobserver agreement. Less favourable was the agreement for synovial enhancement on a 0-2 scale and synovial thickening with subjective assessment on a 0-3 scale, separately scored, where, despite a very good intraobserver agreement, the agreement between observers was only moderate.

As for structural bone damage, we found an excellent agreement for assessing active erosions on a 0-1 scale, both within and between observers. The high reliability of this parameter is particularly important since it reflects disease activity within chronic change, which is important information for further therapeutic steps. The assessment of acetabular erosions was also precise, as was the assessment of femoral head and neck erosions for the same reader.

Interestingly, grading of synovial enhancement on a 0–1 scale performed poorer than grading on a 0–2 or 0–3 scale. Indeed, the discrimination between normal and discrete pathology is a key issue. This is particularly true for the evaluation of patients with JIA in clinical remission where the presence of mild synovial thickening might be suggestive of relapse with important clinical implications, requiring prompt intervention. In fact, the lack of a precise cut-off between physiological and pathological features is still a diagnostic challenge that might lead to both overdiagnosis with unnecessary treatment, and underdiagnosis with an increased risk of structural damage and poorer long-term outcome. This underscores the need for more prospective studies establishing reference standards across ages.

As already stated, another challenge is timing of post-contrast images which has proven to strongly influence the degree of synovial enhancement in studies on wrists and knees (figure 8) (33, 141).

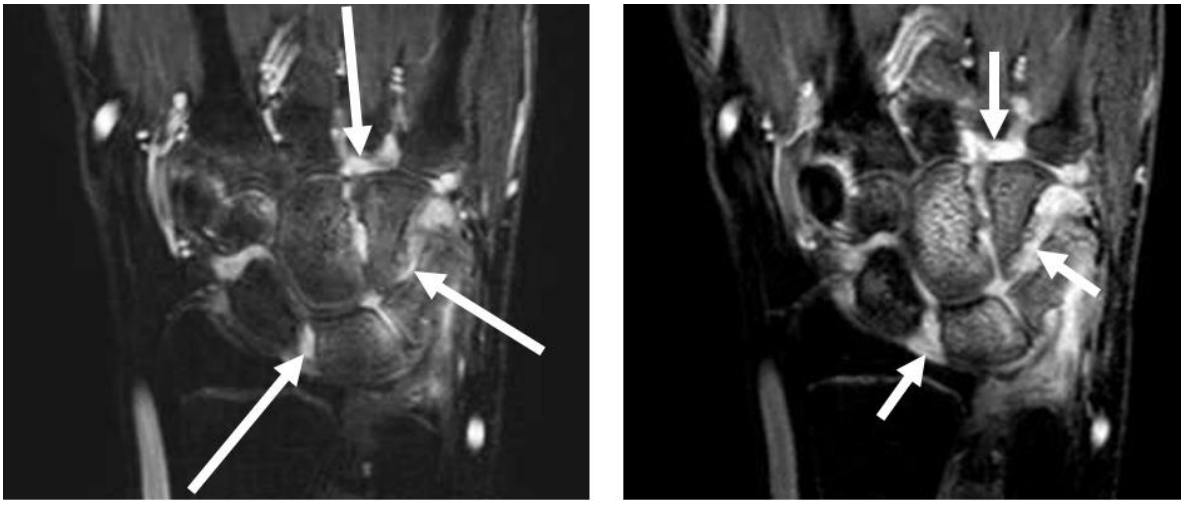

Figure 8. Coronal post-contrast fat-saturated 3D gradient echo MR images of the wrist in a 14-year-old girl with JIA. a) Mildly abnormal synovial enhancement of the mid-carpal joints

and of the 4th carpo-metacarpal joint (arrows) is seen in the early post-contrast image. b) Image taken 10 min after contrast administration shows moderate to severely abnormal enhancement in the same joints (short arrows).

The suggested interval is within 5 min after the contrast injection (116) which is the approximate interval we have used in our study. Thus, a standardised protocol with a fixed interval between the administration of intravenous contrast medium and image acquisition is crucial for follow-up of known pathology, and also for clinical trials across institutions.

Regarding BMO, despite the good intraobserver agreement, the interobserver agreement was fair and not in line with a previous study on wrist MRI (1). We speculate that the size and shape of the scored volumes may have played a role since carpal bones are significantly smaller than hips, thus fewer slices are included for assessment.

Among the markers for structural damage, the agreement for assessing lesions to the cartilage was poor. This may in part be due to the fact that the articular cartilage covering the acetabular and femoral head is very thin, thus hampering the differentiation between partial- and full-thickness lesions. The poor results for direct measurements such as the CCD, femoral neck–head length, femoral width and trochanteric distance were expected and in line with a previous study (5).

Paper 3

In recent years, there has been a growing interest to examine the potential of T2-Dixon fat-only images to replace a separate T1-w sequence in adult musculoskeletal imaging (25-27). For children, this is the first study comparing these sequences for bone marrow assessment on WBMRI.

The high absolute agreement between T2 Dixon fat-only and T1-w (94.6%) found in our study, varying from 93.3% in 12-14-year-olds to 95.4% in 15-19-year-olds, indicates that these two sequences might be used interchangeably between patients, although the same sequence should be preferred for follow-ups. The fair to moderate agreement, with kappa values ranging from 0.10 in children under 9 years of age to 0.51 in 12-14-year-olds, reflects limitations to the kappa statistics itself, rather than poor agreement. As previously mentioned, this statistical phenomenon termed the kappa paradox is caused by an imbalance in case distribution, as was the case in our analysis.

Interestingly, the two sequences under investigation showed discordant findings in 67 out of 1250 high signal areas (5.4%), of which 49 (3.9%) returned low signal on T2 Dixon fat-only

images alone versus 18 (1.5%) on T1-w images alone. This implies that low-intensity areas are more conspicuous on T2 Dixon fat-only images as compared to T1-w images, thus favouring T2 Dixon fat-only over T1.

Moreover, omitting the T1-w coronal sequence might reduce examination time by approximately 7-9 minutes, depending on the number of stacks required, and this is also in favour of T2 Dixon fat-only. This time improvement is particularly significant in children where the last few minutes are less tolerated and consequently the final sequences are most prone to motion artefacts.

Further, we experienced that T2 Dixon allowed for better definition of some low-signal areas as compared to T1 (figure 9), probably due to subtle movements of the child between the two scans, whilst water-only and fat-only images are acquired in the same sequence.

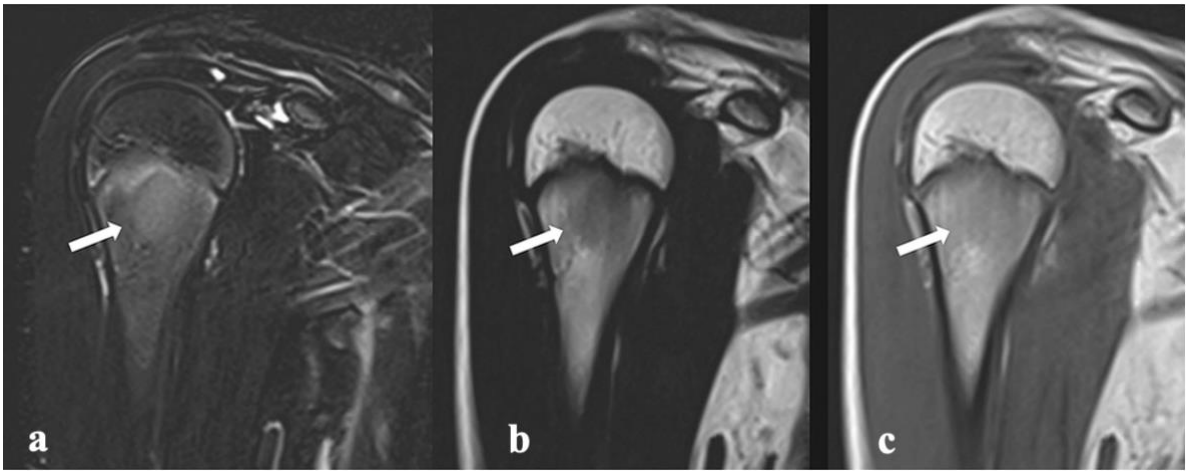

Figure 9. Right proximal humerus in a 14-year-old, healthy boy. a) Area of increased signal on T2 Dixon water-only (arrow). b) On T2 Dixon fat-only reconstruction a well delineated corresponding low signal area is seen (arrow). c) On the T1-w image there is a lower signal as well, but less demarcated than that seen on the fat-only Dixon image (arrow).

Finally, the Dixon sequence also includes out-of-phase images, which have proven helpful for the assessment of several musculoskeletal diseases, including oncological (142) and rheumatological conditions (143, 144). Also in our study, the out-of-phase images were able to confirm the true presence of high signal changes in a few cases where these areas were not detectable on either the fat-only or the T1-w sequence.

Given the statistical limitations as outlined above, the agreement for assessment of low-signal changes between Dixon fat-only images and T1-w images was high for "major findings" while the agreement for minor findings was fair. When evaluating intensity alone, the agreement between the two sequences was quite similar between areas with mild and moderately increased signal intensity, indicating that the extension of a lesion plays a role for the perception of findings.

As for location, the best agreement between T2-Dixon fat-only and T1-w images was found in the lower extremities which are frequently affected in CNO. Conversely, as for the pelvic locations, we found a number of discordances. However, independently of the sequence used, areas close to the triradiate cartilage were challenging, as they are known to contain a higher content of red bone marrow in the immature skeleton resulting in lower signal on both T2-Dixon fat-only and T1; therefore, it can be difficult to decide if the signal originates from the bone marrow or from the physiological cartilage.

Notably, agreement between the two sequences was higher for the older children as compared to the younger**.** Again, the abovementioned limitations to the kappa statistics might play a role. On the other hand, the immature skeleton contains a higher amount of red marrow which appears lower in intensity than yellow marrow on both T2 Dixon fat-only and T1 images. We noticed that bone marrow areas with low signal on both sequences tended to have a lower "background" signal intensity on T2 Dixon fat-only images as compared to T1 in several of the youngest children, predominantly in the axial skeleton. It is well known that the process of marrow conversion in the appendicular skeleton progresses more rapidly and to a greater extent than in the axial skeleton, thus challenging the interpretation of the T2 Dixon fat-only images in the younger age group.

One might argue that focal "major" T2-w bone marrow hyperintensities on WBMRI with corresponding low signal on T2 Dixon fat-only and T1-w images are non-specific. However, the clinical significance of the T2-w Dixon water-only high signal areas was beyond the scope of our study, which was only to test the concordance between the Dixon fat-only and the T1. Furthermore, one might say that our study was limited since it was carried out on healthy children and adolescents. On the other hand, high signal areas on water-only images and particularly major findings found in healthy children can be quite similar to clinically silent lesions in subjects with multifocal MSK pathology such as CNO (7, 8); therefore, we are led to infer that our results are valid in subjects with true bone marrow pathology.

A previous study carried out by our group on the same healthy population showed a substantial concordance between STIR and T2 Dixon water-only sequences in assessment of high signal bone marrow changes (9). In sum, and based on previous and present results, we might infer that both STIR and T1-w sequences, commonly employed in a WBMRI, could be reliably replaced by a single T2 Dixon sequence, thereby shortening the overall examination time. An additional sagittal STIR sequence might be beneficial in cases with suspected vertebral involvement, though.

6.6 Clinical implications

In children with CNO, elevation of inflammatory markers significantly predicted the number of skeletal sites involved as identified on MRI, supporting an early WBMRI to guide treatment.

For the assessment of JIA-related hip-changes, a standardised MRI and a thorough disease score can help monitor treatment. In particular, the total inflammation score at a 0 to 3 scale, provides a quick, precise marker for disease activity, which represents important information for the clinicians in their daily practice. Further, the MR-based score might be used in future clinical trials across institutions.

Last but not least, a WBMRI protocol in children may safely be shortened as compared to today's practice. This is essential for children, with a potential to reduce patient stress and improve image quality.

6.7 Future perspectives

One of the main challenges of imaging musculoskeletal inflammatory diseases in children still remains, namely to distinguish between bone marrow signal changes due to normal growth and changes due to pathological processes. For this purpose, a worldwide database, holding information on laboratory, clinical and imaging data on patients with CNO as well as on healthy children and adolescents might prove helpful. Collaborative research with rheumatologists will ensure the relevance and applicability of the findings, facilitating the

development of guidelines for the management of CNO based on real-world models of disease involvement.

Moreover, advanced imaging techniques, such as DWI and ADC values, might help distinguish between different causes of restricted diffusion in the skeleton, and in this way increase the specificity of MRI findings.

Regarding JIA, the identification of a few biomarkers that can predict outcomes will help personalization of treatment plans based on the likelihood of disease progression or remission.

Artificial intelligence and machine learning algorithms will be developed to analyse and classify bone marrow pathology, simplifying the diagnostic process and reducing the subjectivity of interpretations. Training AI models with large sets of bone marrow images, annotated with expert assessments, might improve the accuracy of the model in detecting and classifying pathology. AI tools might support clinicians by providing rapid and objective assessments of bone marrow findings, potentially reducing the need for invasive biopsies in ambiguous cases.

By increasing diagnostic specificity, identifying disease patterns in CNO, finding prognostic markers in JIA and developing AI tools, both undertreatment and overtreatment might be minimised, substantially improving patient care and outcomes in inflammatory bone disease.

6.8 Strengths and limitations

Paper 1

Strengths

The main strengths of study 1 are the large number of children who underwent WBMRI and the combination of imaging, clinical and laboratory data (including histology when available) to investigate clinical-radiological associations.

Limitation

Currently, there is no agreement on a standardised evaluation tool on the scoring of lesions in CNO. We did not score the extent and intensity of BMO. Being a key finding in CNO, it is reasonable to believe that the extent/degree of BMO might be of value, assuming that we will be able to distinguish between true inflammatory change and changes caused by normal growth.

Paper 2

Strengths

Study 2 boasts several notable strengths. Firstly, it includes a large sample size covering a wide spectrum of pathological changes within both the inflammatory and the bone damage domain. Second, the rigorous calibration sessions prior to the scoring preceded with a pilot study and establishment of an MRI-atlas enhance the study's reliability and accuracy. Furthermore, the study employs a state-of-the-art protocol.

Limitations

Subjective nature of any scoring system with differences in measurements and inherent biases caused by different radiologists' experience and understanding of the factors required to score.

Paper 3

Strengths

The main strengths of study 3 are the high number of volunteers included, stratified by age and sex; the high number of examined areas, the use of a validated scoring system for high signal areas, the wide range of signal intensity in the high signal lesions and the blinded design. The inclusion of two different centres using different vendors but similar MRI protocols and scan resolution strengthens the applicability of the results.

Limitations

First, the whole-body MRIs were performed on 1.5 T machines. One might speculate that a 3 T magnet would provide higher agreement between the two sequences due to better image resolution and/or higher SNR. However, previous studies (26, 27) have shown that the sequences perform equally well at 1.5 T and 3 T. Second, the results of this study are valid for the sequences used and could change if different resolutions or imaging parameters were applied. Finally, the study was performed on healthy children and adolescents only. However, we believe that including children with for instance CNO-related lesions, which tend to be larger and more conspicuous than high signal areas seen in healthy children, might have increased the overall agreement between the two sequences.

7. Conclusions

This thesis demonstrates the distribution of clinical, laboratory and MRI-findings in a large cohort of children and adolescents with CNO. Interestingly, elevation of inflammatory markers significantly predicted the number of skeletal sites involved as identified on MRI, indicating that this number represents a marker for disease activity.

MRI is a reliable method for the assessment of active inflammation of the hip in children with JIA. Several markers isolated and in combination are robust enough to be included in a future simplified MRI scoring system, of which the most precise is the overall degree of inflammation, including effusion. As for permanent changes, the most reliable markers are the acetabular erosions and the active erosions of the femoral head.

T2 Dixon fat-only images can replace the T1-w TSE sequence in the assessment of bone marrow high signal areas on WBMRI in children and adolescents, with an advantageous reduction in scan time.

8. References

1. Tanturri de Horatio L, Damasio MB, Barbuti D, Bracaglia C, Lambot-Juhan K, Boavida P, Ording Müller LS, Malattia C, Ravà L, Rosendahl K, Tomà P. MRI assessment of bone marrow in children with juvenile idiopathic arthritis: intra- and inter-observer variability. Pediatr Radiol 2012;42(6):714-720. doi: 10.1007/s00247-012-2345-y
2. Damasio MB, Malattia C, Tanturri de Horatio L, Mattiuz C, Pistorio A, Bracaglia C, Barbuti D, Boavida P, Juhan KL, Ording LS, Rosendahl K, Martini A, Magnano G, Tomà P. MRI of the wrist in juvenile idiopathic arthritis: proposal of a paediatric synovitis score by a consensus of an international working group. Results of a multicentre reliability study. Pediatr Radiol 2012;42(9):1047-1055. doi: 10.1007/s00247-012-2392-4
3. Lambot K, Boavida P, Damasio MB, Tanturri de Horatio L, Desgranges M, Malattia C, Barbuti D, Bracaglia C, Müller LS, Elie C, Bader-Meunier B, Quartier P, Rosendahl K, Brunelle F. MRI assessment of tenosynovitis in children with juvenile idiopathic arthritis: inter- and intra-observer variability. Pediatr Radiol 2013;43(7):796-802. doi: 10.1007/s00247-012-2613-x
4. Boavida P, Lambot-Juhan K, Müller LS, Damasio B, de Horatio LT, Malattia C, Owens CM, Rosendahl K. Carpal erosions in children with juvenile idiopathic arthritis: repeatability of a newly devised MR-scoring system. Pediatr Radiol 2015;45(13):1972-1980. doi: 10.1007/s00247-015-3421-x
5. Shelmerdine SC, Di Paolo PL, Rieter JFMM, Malattia C, Tanturri de Horatio L, Rosendahl K. A novel radiographic scoring system for growth abnormalities and structural change in children with juvenile idiopathic arthritis of the hip. Pediatr Radiol 2018;48(8):1086-1095. doi: 10.1007/s00247-018-4136-6
6. Zadig P, von Brandis E, d'Angelo P, de Horatio LT, Ording-Müller LS, Rosendahl K, Avenarius D. Whole-body MRI in children aged 6-18 years. Reliability of identifying and grading high signal intensity changes within bone marrow. Pediatr Radiol 2022;52(7):1272-1282. doi: 10.1007/s00247-022-05312-y
7. Zadig PK, von Brandis E, Flatø B, Ording Müller LS, Nordal EB, de Horatio LT, Rosendahl K, Avenarius DFM. Whole body magnetic resonance imaging in healthy children and adolescents: Bone marrow appearances of the appendicular skeleton. Eur J Radiol 2022;153:110365. doi: 10.1016/j.ejrad.2022.110365
8. von Brandis E, Zadig PK, Avenarius DFM, Flatø B, Kristian Knudsen P, Lilleby V, Nguyen B, Rosendahl K, Ording Müller LS. Whole body magnetic resonance imaging in healthy children and adolescents. Bone marrow appearances of the axial skeleton. Eur J Radiol 2022;154:110425. doi: 10.1016/j.ejrad.2022.110425
9. Zadig P, von Brandis E, Ording Müller LS, Tanturri de Horatio L, Rosendahl K, Avenarius DFM. Pediatric whole-body magnetic resonance imaging: comparison of STIR and T2 Dixon sequences in the detection and grading of high signal bone marrow changes. Eur Radiol 2023. doi: 10.1007/s00330-023-09413-6
10. Thierry S, Fautrel B, Lemelle I, Guillemin F. Prevalence and incidence of juvenile idiopathic arthritis: a systematic review. Joint Bone Spine 2014;81(2):112-117. doi: 10.1016/j.jbspin.2013.09.003
11. Packham JC, Hall MA. Long-term follow-up of 246 adults with juvenile idiopathic arthritis: functional outcome. Rheumatology (Oxford) 2002;41(12):1428-1435. doi: 10.1093/rheumatology/41.12.1428
12. Gurcay E, Eksioglu E, Yuzer S, Bal A, Cakci A. Articular damage in adults with juvenile idiopathic arthritis. Rheumatol Int 2009;29(6):635-640. doi: 10.1007/s00296-008-0740-3

13. Zhao Y, Wallace C. Judicious use of biologicals in juvenile idiopathic arthritis. Curr Rheumatol Rep 2014;16(11):454. doi: 10.1007/s11926-014-0454-3
14. Ong MS, Ringold S, Kimura Y, Schanberg LE, Tomlinson GA, Natter MD, Investigators CR. Improved Disease Course Associated With Early Initiation of Biologics in Polyarticular Juvenile Idiopathic Arthritis: Trajectory Analysis of a Childhood Arthritis and Rheumatology Research Alliance Consensus Treatment Plans Study. Arthritis Rheumatol 2021;73(10):1910-1920. doi: 10.1002/art.41892
15. Schnabel A, Range U, Hahn G, Siepmann T, Berner R, Hedrich CM. Unexpectedly high incidences of chronic non-bacterial as compared to bacterial osteomyelitis in children. Rheumatol Int 2016;36(12):1737-1745. doi: 10.1007/s00296-016-3572-6
16. Fritz J, Tzaribatchev N, Claussen CD, Carrino JA, Horger MS. Chronic recurrent multifocal osteomyelitis: comparison of whole-body MR imaging with radiography and correlation with clinical and laboratory data. Radiology 2009;252(3):842-851. doi: 10.1148/radiol.2523081335
17. Falip C, Alison M, Boutry N, Job-Deslandre C, Cotten A, Azoulay R, Adamsbaum C. Chronic recurrent multifocal osteomyelitis (CRMO): a longitudinal case series review. Pediatr Radiol 2013;43(3):355-375. doi: 10.1007/s00247-012-2544-6
18. Arthurs OJ, van Rijn RR, Granata C, Porto L, Hirsch FW, Rosendahl K. European Society of Paediatric Radiology 2019 strategic research agenda: improving imaging for tomorrow's children. Pediatr Radiol 2019;49(8):983-989. doi: 10.1007/s00247-019-04406-4
19. Dixon WT. Simple proton spectroscopic imaging. Radiology 1984;153(1):189-194. doi: 10.1148/radiology.153.1.6089263
20. Ma J. Dixon techniques for water and fat imaging. J Magn Reson Imaging 2008;28(3):543-558. doi: 10.1002/jmri.21492
21. Bley TA, Wieben O, François CJ, Brittain JH, Reeder SB. Fat and water magnetic resonance imaging. J Magn Reson Imaging 2010;31(1):4-18. doi: 10.1002/jmri.21895
22. Omoumi P. The Dixon method in musculoskeletal MRI: from fat-sensitive to fat-specific imaging. Skeletal Radiol 2022;51(7):1365-1369. doi: 10.1007/s00256-021-03950-1
23. Guerini H, Omoumi P, Guichoux F, Vuillemin V, Morvan G, Zins M, Thevenin F, Drape JL. Fat Suppression with Dixon Techniques in Musculoskeletal Magnetic Resonance Imaging: A Pictorial Review. Semin Musculoskelet Radiol 2015;19(4):335-347. doi: 10.1055/s-0035-1565913
24. Lins CF, Salmon CEG, Nogueira-Barbosa MH. Applications of the Dixon technique in the evaluation of the musculoskeletal system. Radiol Bras 2021;54(1):33-42. doi: 10.1590/0100-3984.2019.0086
25. Maeder Y, Dunet V, Richard R, Becce F, Omoumi P. Bone Marrow Metastases: T2-weighted Dixon Spin-Echo Fat Images Can Replace T1-weighted Spin-Echo Images. Radiology 2018;286(3):948-959. doi: 10.1148/radiol.2017170325
26. Yang S, Lassalle L, Mekki A, Appert G, Rannou F, Nguyen C, Lefèvre-Colau MM, Mutschler C, Drapé JL, Feydy A. Can T2-weighted Dixon fat-only images replace T1-weighted images in degenerative disc disease with Modic changes on lumbar spine MRI? Eur Radiol 2021;31(12):9380-9389. doi: 10.1007/s00330-021-07946-2
27. Zanchi F, Richard R, Hussami M, Monier A, Knebel JF, Omoumi P. MRI of non-specific low back pain and/or lumbar radiculopathy: do we need T1 when using a sagittal T2-weighted Dixon sequence? Eur Radiol 2020;30(5):2583-2593. doi: 10.1007/s00330-019-06626-6
28. Nistala K, Babar J, Johnson K, Campbell-Stokes P, Foster K, Ryder C, McDonagh JE. Clinical assessment and core outcome variables are poor predictors of hip arthritis diagnosed by MRI in juvenile idiopathic arthritis. Rheumatology (Oxford) 2007;46(4):699-702. doi: 10.1093/rheumatology/kel401
29. Ostrowska M, Gietka P, Mańczak M, Michalski E, Sudoł-Szopińska I. MRI Findings in Hip in Juvenile Idiopathic Arthritis. J Clin Med 2021;10(22). doi: 10.3390/jcm10225252
30. Buchmann RF, Jaramillo D. Imaging of articular disorders in children. Radiol Clin North Am 2004;42(1):151-168, vii. doi: 10.1016/S0033-8389(03)00159-3

31. Smith MD. The normal synovium. Open Rheumatol J 2011;5:100-106. doi: 10.2174/1874312901105010100
32. Hemke R, Tzaribachev N, Barendregt AM, Merlijn van den Berg J, Doria AS, Maas M. Imaging of the knee in juvenile idiopathic arthritis. Pediatr Radiol 2018;48(6):818-827. doi: 10.1007/s00247-017-4015-6
33. Barendregt AM, van Gulik EC, Groot PFC, Dolman KM, van den Berg JM, Nassar-Sheikh Rashid A, Schonenberg-Meinema D, Lavini C, Rosendahl K, Hemke R, Kuijpers TW, Maas M, Nusman CM. Prolonged time between intravenous contrast administration and image acquisition results in increased synovial thickness at magnetic resonance imaging in patients with juvenile idiopathic arthritis. Pediatr Radiol 2019;49(5):638-645. doi: 10.1007/s00247-018-04332-x
34. Thoenen J, MacKay JW, Sandford HJC, Gold GE, Kogan F. Imaging of Synovial Inflammation in Osteoarthritis, From the. AJR Am J Roentgenol 2022;218(3):405-417. doi: 10.2214/AJR.21.26170
35. Lassere M, McQueen F, Østergaard M, Conaghan P, Shnier R, Peterfy C, Klarlund M, Bird P, O'Connor P, Stewart N, Emery P, Genant H, Edmonds J. OMERACT Rheumatoid Arthritis Magnetic Resonance Imaging Studies. Exercise 3: an international multicenter reliability study using the RA-MRI Score. J Rheumatol 2003;30(6):1366-1375.
36. Bird P, Joshua F, Lassere M, Shnier R, Edmonds J. Training and calibration improve inter-reader reliability of joint damage assessment using magnetic resonance image scoring and computerized erosion volume measurement. J Rheumatol 2005;32(8):1452-1458.
37. Haavardsholm EA, Ostergaard M, Ejbjerg BJ, Kvan NP, Uhlig TA, Lilleås FG, Kvien TK. Reliability and sensitivity to change of the OMERACT rheumatoid arthritis magnetic resonance imaging score in a multireader, longitudinal setting. Arthritis Rheum 2005;52(12):3860-3867. doi: 10.1002/art.21493
38. Eley KA, Watt-Smith SR, Sheerin F, Golding SJ. "Black Bone" MRI: a potential alternative to CT with three-dimensional reconstruction of the craniofacial skeleton in the diagnosis of craniosynostosis. Eur Radiol 2014;24(10):2417-2426. doi: 10.1007/s00330-014-3286-7
39. Eley KA, Watt-Smith SR, Golding SJ. "Black Bone" MRI: a novel imaging technique for 3D printing. Dentomaxillofac Radiol 2017;46(3):20160407. doi: 10.1259/dmfr.20160407
40. Low XZ, Lim MC, Nga V, Sundar G, Tan AP. Clinical application of "black bone" imaging in paediatric craniofacial disorders. Br J Radiol 2021;94(1124):20200061. doi: 10.1259/bjr.20200061
41. Paunipagar BK, Rasalkar D. Imaging of articular cartilage. Indian J Radiol Imaging 2014;24(3):237-248. doi: 10.4103/0971-3026.137028
42. Gold GE, Chen CA, Koo S, Hargreaves BA, Bangerter NK. Recent advances in MRI of articular cartilage. AJR Am J Roentgenol 2009;193(3):628-638. doi: 10.2214/AJR.09.3042
43. Avenarius DF, Ording Müller LS, Rosendahl K. Erosion or normal variant? 4-year MRI follow-up of the wrists in healthy children. Pediatr Radiol 2016;46(3):322-330. doi: 10.1007/s00247-015-3494-6
44. Augusto ACL, Goes PCK, Flores DV, Costa MAF, Takahashi MS, Rodrigues ACO, Padula LC, Gasparetto TD, Nogueira-Barbosa MH, Aihara AY. Imaging Review of Normal and Abnormal Skeletal Maturation. Radiographics 2022;42(3):861-879. doi: 10.1148/rg.210088
45. Burdiles A, Babyn PS. Pediatric bone marrow MR imaging. Magn Reson Imaging Clin N Am 2009;17(3):391-409, v. doi: 10.1016/j.mric.2009.03.001
46. Laor T, Jaramillo D. MR imaging insights into skeletal maturation: what is normal? Radiology 2009;250(1):28-38. doi: 10.1148/radiol.2501071322
47. Avenarius DFM, Ording Müller LS, Rosendahl K. Joint Fluid, Bone Marrow Edemalike Changes, and Ganglion Cysts in the Pediatric Wrist: Features That May Mimic Pathologic Abnormalities-Follow-Up of a Healthy Cohort. AJR Am J Roentgenol 2017;208(6):1352-1357. doi: 10.2214/AJR.16.17263
48. Shabshin N, Schweitzer ME, Morrison WB, Carrino JA, Keller MS, Grissom LE. High-signal T2 changes of the bone marrow of the foot and ankle in children: red marrow or traumatic changes? Pediatr Radiol 2006;36(7):670-676. doi: 10.1007/s00247-006-0129-y

49. Ording Müller LS, Avenarius D, Olsen OE. High signal in bone marrow at diffusion-weighted imaging with body background suppression (DWIBS) in healthy children. Pediatr Radiol 2011;41(2):221-226. doi: 10.1007/s00247-010-1774-8
50. Lauenstein TC, Freudenberg LS, Goehde SC, Ruehm SG, Goyen M, Bosk S, Debatin JF, Barkhausen J. Whole-body MRI using a rolling table platform for the detection of bone metastases. Eur Radiol 2002;12(8):2091-2099. doi: 10.1007/s00330-002-1344-z
51. Lecouvet FE. Whole-Body MR Imaging: Musculoskeletal Applications. Radiology 2016;279(2):345-365. doi: 10.1148/radiol.2016142084
52. Nievelstein RA, Littooij AS. Whole-body MRI in paediatric oncology. Radiol Med 2016;121(5):442-453. doi: 10.1007/s11547-015-0600-7
53. Schäfer JF, Granata C, von Kalle T, Kyncl M, Littooij AS, Di Paolo PL, Sefic Pasic I, Nievelstein RAJ, ESPR OTFot. Whole-body magnetic resonance imaging in pediatric oncology - recommendations by the Oncology Task Force of the ESPR. Pediatr Radiol 2020;50(8):1162-1174. doi: 10.1007/s00247-020-04683-4
54. Gaunt T, Humphries PD. Whole-body MRI in children: state of the art. BJR Open 2022;4(1):20210087. doi: 10.1259/bjro.20210087
55. Damasio MB, Magnaguagno F, Stagnaro G. Whole-body MRI: non-oncological applications in paediatrics. Radiol Med 2016;121(5):454-461. doi: 10.1007/s11547-015-0619-9
56. Deplano L, Piga M, Porcu M, Stecco A, Suri JS, Mannelli L, Cauli A, Carriero A, Saba L. Whole-Body MRI in Rheumatology: Major Advances and Future Perspectives. Diagnostics (Basel) 2021;11(10). doi: 10.3390/diagnostics11101770
57. Vilanova JC, García-Figueiras R, Luna A, Baleato-González S, Tomás X, Narváez JA. Update on Whole-body MRI in Musculoskeletal Applications. Semin Musculoskelet Radiol 2019;23(3):312-323. doi: 10.1055/s-0039-1685540
58. Huang Y, Zhang X, Guo H, Chen H, Guo D, Huang F, Xu Q, Qu X. Phase-constrained reconstruction of high-resolution multi-shot diffusion weighted image. J Magn Reson 2020;312:106690. doi: 10.1016/j.jmr.2020.106690
59. Summers P, Saia G, Colombo A, Pricolo P, Zugni F, Alessi S, Marvaso G, Jereczek-Fossa BA, Bellomi M, Petralia G. Whole-body magnetic resonance imaging: technique, guidelines and key applications. Ecancermedicalscience 2021;15:1164. doi: 10.3332/ecancer.2021.1164
60. Zadig P, von Brandis E, Lein RK, Rosendahl K, Avenarius D, Ording Müller LS. Whole-body magnetic resonance imaging in children - how and why? A systematic review. Pediatr Radiol 2021;51(1):14-24. doi: 10.1007/s00247-020-04735-9
61. Darge K, Jaramillo D, Siegel MJ. Whole-body MRI in children: current status and future applications. Eur J Radiol 2008;68(2):289-298. doi: 10.1016/j.ejrad.2008.05.018
62. Saunders R, Davis JA, Kranke P, Weissbrod R, Whitaker DK, Lightdale JR. Clinical and economic burden of procedural sedation-related adverse events and their outcomes: analysis from five countries. Ther Clin Risk Manag 2018;14:393-401. doi: 10.2147/TCRM.S154720
63. Artunduaga M, Liu CA, Morin CE, Serai SD, Udayasankar U, Greer MC, Gee MS. Safety challenges related to the use of sedation and general anesthesia in pediatric patients undergoing magnetic resonance imaging examinations. Pediatr Radiol 2021;51(5):724-735. doi: 10.1007/s00247-021-05044-5
64. Giedion A, Holthusen W, Masel LF, Vischer D. [Subacute and chronic "symmetrical" osteomyelitis]. Ann Radiol (Paris) 1972;15(3):329-342.
65. Zhao DY, McCann L, Hahn G, Hedrich CM. Chronic nonbacterial osteomyelitis (CNO) and chronic recurrent multifocal osteomyelitis (CRMO). J Transl Autoimmun 2021;4:100095. doi: 10.1016/j.jtauto.2021.100095
66. Grote V, Silier CC, Voit AM, Jansson AF. Bacterial Osteomyelitis or Nonbacterial Osteitis in Children: A Study Involving the German Surveillance Unit for Rare Diseases in Childhood. Pediatr Infect Dis J 2017;36(5):451-456. doi: 10.1097/INF.0000000000001469

67. Silier CCG, Greschik J, Gesell S, Grote V, Jansson AF. Chronic non-bacterial osteitis from the patient perspective: a health services research through data collected from patient conferences. BMJ Open 2017;7(12):e017599. doi: 10.1136/bmjopen-2017-017599
68. Girschick H, Finetti M, Orlando F, Schalm S, Insalaco A, Ganser G, Nielsen S, Herlin T, Koné-Paut I, Martino S, Cattalini M, Anton J, Mohammed Al-Mayouf S, Hofer M, Quartier P, Boros C, Kuemmerle-Deschner J, Pires Marafon D, Alessio M, Schwarz T, Ruperto N, Martini A, Jansson A, Gattorno M, registry PRITOPatE. The multifaceted presentation of chronic recurrent multifocal osteomyelitis: a series of 486 cases from the Eurofever international registry. Rheumatology (Oxford) 2018;57(8):1504. doi: 10.1093/rheumatology/key143
69. Costa-Reis P, Sullivan KE. Chronic recurrent multifocal osteomyelitis. J Clin Immunol 2013;33(6):1043-1056. doi: 10.1007/s10875-013-9902-5
70. Hofmann SR, Schnabel A, Rösen-Wolff A, Morbach H, Girschick HJ, Hedrich CM. Chronic Nonbacterial Osteomyelitis: Pathophysiological Concepts and Current Treatment Strategies. J Rheumatol 2016;43(11):1956-1964. doi: 10.3899/jrheum.160256
71. Taddio A, Zennaro F, Pastore S, Cimaz R. An Update on the Pathogenesis and Treatment of Chronic Recurrent Multifocal Osteomyelitis in Children. Paediatr Drugs 2017;19(3):165-172. doi: 10.1007/s40272-017-0226-4
72. Berkowitz YJ, Greenwood SJ, Cribb G, Davies K, Cassar-Pullicino VN. Complete resolution and remodeling of chronic recurrent multifocal osteomyelitis on MRI and radiographs. Skeletal Radiol 2018;47(4):563-568. doi: 10.1007/s00256-017-2812-5
73. Kishimoto M, Taniguchi Y, Tsuji S, Ishihara Y, Deshpande GA, Maeda K, Okada M, Komagata Y, Kobayashi S, Okubo Y, Tomita T, Kaname S. SAPHO syndrome and pustulotic arthro-osteitis. Mod Rheumatol 2022;32(4):665-674. doi: 10.1093/mr/roab103
74. Bader-Meunier B, Van Nieuwenhove E, Breton S, Wouters C. Bone involvement in monogenic autoinflammatory syndromes. Rheumatology (Oxford) 2018;57(4):606-618. doi: 10.1093/rheumatology/kex306
75. Roderick MR, Shah R, Rogers V, Finn A, Ramanan AV. Chronic recurrent multifocal osteomyelitis (CRMO) - advancing the diagnosis. Pediatr Rheumatol Online J 2016;14(1):47. doi: 10.1186/s12969-016-0109-1
76. Hofmann SR, Kubasch AS, Range U, Laass MW, Morbach H, Girschick HJ, Hedrich CM. Serum biomarkers for the diagnosis and monitoring of chronic recurrent multifocal osteomyelitis (CRMO). Rheumatol Int 2016;36(6):769-779. doi: 10.1007/s00296-016-3466-7
77. Hofmann SR, Schwarz T, Möller JC, Morbach H, Schnabel A, Rösen-Wolff A, Girschick HJ, Hedrich CM. Chronic non-bacterial osteomyelitis is associated with impaired Sp1 signaling, reduced IL10 promoter phosphorylation, and reduced myeloid IL-10 expression. Clin Immunol 2011;141(3):317-327. doi: 10.1016/j.clim.2011.08.012
78. Zhao Y, Wu EY, Oliver MS, Cooper AM, Basiaga ML, Vora SS, Lee TC, Fox E, Amarilyo G, Stern SM, Dvergsten JA, Haines KA, Rouster-Stevens KA, Onel KB, Cherian J, Hausmann JS, Miettunen P, Cellucci T, Nuruzzaman F, Taneja A, Barron KS, Hollander MC, Lapidus SK, Li SC, Ozen S, Girschick H, Laxer RM, Dedeoglu F, Hedrich CM, Ferguson PJ, Chronic Nonbacterial Osteomyelitis/Chronic Recurrent Multifocal Osteomyelitis Study Group and the Childhood Arthritis and Rheumatology Research Alliance Scleroderma V, A.toinflammatory and Rare Diseases Subcommittee. Consensus Treatment Plans for Chronic Nonbacterial Osteomyelitis Refractory to Nonsteroidal Antiinflammatory Drugs and/or With Active Spinal Lesions. Arthritis Care Res (Hoboken) 2018;70(8):1228-1237. doi: 10.1002/acr.23462
79. Nico MAC, Araújo FF, Guimarães JB, da Cruz IAN, Silva FD, Carneiro BC, Filho AGO. Chronic nonbacterial osteomyelitis: the role of whole-body MRI. Insights Imaging 2022;13(1):149. doi: 10.1186/s13244-022-01288-3
80. Leclair N, Thörmer G, Sorge I, Ritter L, Schuster V, Hirsch FW. Whole-Body Diffusion-Weighted Imaging in Chronic Recurrent Multifocal Osteomyelitis in Children. PLoS One 2016;11(1):e0147523. doi: 10.1371/journal.pone.0147523

81. Andronikou S, Mendes da Costa T, Hussien M, Ramanan AV. Radiological diagnosis of chronic recurrent multifocal osteomyelitis using whole-body MRI-based lesion distribution patterns. Clin Radiol 2019;74(9):737.e733-737.e715. doi: 10.1016/j.crad.2019.02.021
82. Andronikou S, Kraft JK, Offiah AC, Jones J, Douis H, Thyagarajan M, Barrera CA, Zouvani A, Ramanan AV. Whole-body MRI in the diagnosis of paediatric CNO/CRMO. Rheumatology (Oxford) 2020;59(10):2671-2680. doi: 10.1093/rheumatology/keaa303
83. Arnoldi AP, Schlett CL, Douis H, Geyer LL, Voit AM, Bleisteiner F, Jansson AF, Weckbach S. Whole-body MRI in patients with Non-bacterial Osteitis: Radiological findings and correlation with clinical data. Eur Radiol 2017;27(6):2391-2399. doi: 10.1007/s00330-016-4586-x
84. Sato TS, Watal P, Ferguson PJ. Imaging mimics of chronic recurrent multifocal osteomyelitis: avoiding pitfalls in a diagnosis of exclusion. Pediatr Radiol 2020;50(1):124-136. doi: 10.1007/s00247-019-04510-5
85. Wipff J, Costantino F, Lemelle I, Pajot C, Duquesne A, Lorrot M, Faye A, Bader-Meunier B, Brochard K, Despert V, Jean S, Grall-Lerosey M, Marot Y, Nouar D, Pagnier A, Quartier P, Job-Deslandre C. A large national cohort of French patients with chronic recurrent multifocal osteitis. Arthritis Rheumatol 2015;67(4):1128-1137. doi: 10.1002/art.39013
86. Ravelli A, Martini A. Juvenile idiopathic arthritis. Lancet 2007;369(9563):767-778. doi: 10.1016/S0140-6736(07)60363-8
87. Petty RE, Southwood TR, Manners P, Baum J, Glass DN, Goldenberg J, He X, Maldonado-Cocco J, Orozco-Alcala J, Prieur AM, Suarez-Almazor ME, Woo P, Rheumatology ILoAf. International League of Associations for Rheumatology classification of juvenile idiopathic arthritis: second revision, Edmonton, 2001. J Rheumatol 2004;31(2):390-392.
88. Martini A. It is time to rethink juvenile idiopathic arthritis classification and nomenclature. Ann Rheum Dis 2012;71(9):1437-1439. doi: 10.1136/annrheumdis-2012-201388
89. Martini A, Ravelli A, Avcin T, Beresford MW, Burgos-Vargas R, Cuttica R, Ilowite NT, Khubchandani R, Laxer RM, Lovell DJ, Petty RE, Wallace CA, Wulffraat NM, Pistorio A, Ruperto N, (PRINTO) PRITO. Toward New Classification Criteria for Juvenile Idiopathic Arthritis: First Steps, Pediatric Rheumatology International Trials Organization International Consensus. J Rheumatol 2019;46(2):190-197. doi: 10.3899/jrheum.180168
90. Chen K, Zeng H, Togizbayev G, Martini A. New classification criteria for juvenile idiopathic arthritis. Int J Rheum Dis 2023;26(10):1889-1892. doi: 10.1111/1756-185X.14813
91. Ravelli A, Consolaro A, Horneff G, Laxer RM, Lovell DJ, Wulffraat NM, Akikusa JD, Al-Mayouf SM, Antón J, Avcin T, Berard RA, Beresford MW, Burgos-Vargas R, Cimaz R, De Benedetti F, Demirkaya E, Foell D, Itoh Y, Lahdenne P, Morgan EM, Quartier P, Ruperto N, Russo R, Saad-Magalhães C, Sawhney S, Scott C, Shenoi S, Swart JF, Uziel Y, Vastert SJ, Smolen JS. Treating juvenile idiopathic arthritis to target: recommendations of an international task force. Ann Rheum Dis 2018;77(6):819-828. doi: 10.1136/annrheumdis-2018-213030
92. Wallace CA, Giannini EH, Spalding SJ, Hashkes PJ, O'Neil KM, Zeft AS, Szer IS, Ringold S, Brunner HI, Schanberg LE, Sundel RP, Milojevic D, Punaro MG, Chira P, Gottlieb BS, Higgins GC, Ilowite NT, Kimura Y, Hamilton S, Johnson A, Huang B, Lovell DJ, Alliance CAaRR. Trial of early aggressive therapy in polyarticular juvenile idiopathic arthritis. Arthritis Rheum 2012;64(6):2012-2021. doi: 10.1002/art.34343
93. Ključevšek D, Emeršič N, Toplak N, Avčin T. Clinical and MRI outcome of cervical spine lesions in children with juvenile idiopathic arthritis treated with anti-TNFα drugs early in disease course. Pediatr Rheumatol Online J 2017;15(1):38. doi: 10.1186/s12969-017-0173-1
94. Swart JF, de Roock S, Wulffraat NM. What are the immunological consequences of long-term use of biological therapies for juvenile idiopathic arthritis? Arthritis Res Ther 2013;15(3):213. doi: 10.1186/ar4213
95. Rostom S, Amine B, Bensabbah R, Abouqal R, Hajjaj-Hassouni N. Hip involvement in juvenile idiopathic arthritis. Clin Rheumatol 2008;27(6):791-794. doi: 10.1007/s10067-008-0853-9

96. Fantini F, Corradi A, Gerloni V, Failoni S, Gattinara M, Aprile L, Ferraris W, Arnoldi C. The natural history of hip involvement in juvenile rheumatoid arthritis: a radiological and magnetic resonance imaging follow-up study. Rev Rhum Engl Ed 1997;64(10 Suppl):173S-178S.
97. Lamer S, Sebag GH. MRI and ultrasound in children with juvenile chronic arthritis. Eur J Radiol 2000;33(2):85-93. doi: 10.1016/s0720-048x(99)00158-8
98. Sudoł-Szopińska I, Jurik AG, Eshed I, Lennart J, Grainger A, Østergaard M, Klauser A, Cotten A, Wick MC, Maas M, Miese F, Egund N, Boutry N, Rupreht M, Reijnierse M, Oei EH, Meier R, O'Connor P, Feydy A, Mascarenhas V, Plagou A, Simoni P, Platzgummer H, Rennie WJ, Mester A, Teh J, Robinson P, Guglielmi G, Åström G, Schueller-Weiderkamm C. Recommendations of the ESSR Arthritis Subcommittee for the Use of Magnetic Resonance Imaging in Musculoskeletal Rheumatic Diseases. Semin Musculoskelet Radiol 2015;19(4):396-411. doi: 10.1055/s-0035-1564696
99. Hemke R, Herregods N, Jaremko JL, Åström G, Avenarius D, Becce F, Bielecki DK, Boesen M, Dalili D, Giraudo C, Hermann KG, Humphries P, Isaac A, Jurik AG, Klauser AS, Kvist O, Laloo F, Maas M, Mester A, Oei E, Offiah AC, Omoumi P, Papakonstantinou O, Plagou A, Shelmerdine S, Simoni P, Sudoł-Szopińska I, Tanturri de Horatio L, Teh J, Jans L, Rosendahl K. Imaging assessment of children presenting with suspected or known juvenile idiopathic arthritis: ESSR-ESPR points to consider. Eur Radiol 2020;30(10):5237-5249. doi: 10.1007/s00330-020-06807-8
100. Mazzoni M, Pistorio A, Magnaguagno F, Viola S, Urru A, Magnano GM, Ravelli A, Malattia C. Predictive Value of Magnetic Resonance Imaging in Patients With Juvenile Idiopathic Arthritis in Clinical Remission. Arthritis Care Res (Hoboken) 2023;75(1):198-205. doi: 10.1002/acr.24757
101. Baildam E. A commentary on TREAT: the trial of early aggressive drug therapy in juvenile idiopathic arthritis. BMC Med 2012;10:59. doi: 10.1186/1741-7015-10-59
102. Hemke R, van Rossum MA, van Veenendaal M, Terra MP, Deurloo EE, de Jonge MC, van den Berg JM, Dolman KM, Kuijpers TW, Maas M. Reliability and responsiveness of the Juvenile Arthritis MRI Scoring (JAMRIS) system for the knee. Eur Radiol 2013;23(4):1075-1083. doi: 10.1007/s00330-012-2684-y
103. Østergaard M, Peterfy C, Conaghan P, McQueen F, Bird P, Ejbjerg B, Shnier R, O'Connor P, Klarlund M, Emery P, Genant H, Lassere M, Edmonds J. OMERACT Rheumatoid Arthritis Magnetic Resonance Imaging Studies. Core set of MRI acquisitions, joint pathology definitions, and the OMERACT RA-MRI scoring system. J Rheumatol 2003;30(6):1385-1386.
104. Malattia C, Damasio MB, Pistorio A, Ioseliani M, Vilca I, Valle M, Ruperto N, Viola S, Buoncompagni A, Magnano GM, Ravelli A, Tomà P, Martini A. Development and preliminary validation of a paediatric-targeted MRI scoring system for the assessment of disease activity and damage in juvenile idiopathic arthritis. Ann Rheum Dis 2011;70(3):440-446. doi: 10.1136/ard.2009.126862
105. Angenete OW, Augdal TA, Rygg M, Rosendahl K. MRI in the Assessment of TMJ-Arthritis in Children with JIA; Repeatability of a Newly Devised Scoring System. Acad Radiol 2022;29(9):1362-1377. doi: 10.1016/j.acra.2021.09.024
106. Jaremko JL, Lambert RGW, Pedersen SJ, Weber U, Lindsay D, Al-Ani Z, Steer K, Pianta M, Wichuk S, Maksymowych WP. OMERACT Hip Inflammation Magnetic Resonance Imaging Scoring System (HIMRISS) Assessment in Longitudinal Study. J Rheumatol 2019;46(9):1239-1242. doi: 10.3899/jrheum.181043
107. Maksymowych WP, Cibere J, Loeuille D, Weber U, Zubler V, Roemer FW, Jaremko JL, Sayre EC, Lambert RG. Preliminary validation of 2 magnetic resonance image scoring systems for osteoarthritis of the hip according to the OMERACT filter. J Rheumatol 2014;41(2):370-378. doi: 10.3899/jrheum.131083
108. Argyropoulou MI, Fanis SL, Xenakis T, Efremidis SC, Siamopoulou A. The role of MRI in the evaluation of hip joint disease in clinical subtypes of juvenile idiopathic arthritis. Br J Radiol 2002;75(891):229-233. doi: 10.1259/bjr.75.891.750229

109. Porter-Young FM, Offiah AC, Broadley P, Lang I, McMahon AM, Howsley P, Hawley DP. Inter- and intra-observer reliability of contrast-enhanced magnetic resonance imaging parameters in children with suspected juvenile idiopathic arthritis of the hip. Pediatr Radiol 2018;48(13):1891-1900. doi: 10.1007/s00247-018-4216-7
110. Kirkhus E, Flatø B, Riise O, Reiseter T, Smith HJ. Differences in MRI findings between subgroups of recent-onset childhood arthritis. Pediatr Radiol 2011;41(4):432-440. doi: 10.1007/s00247-010-1897-y
111. Abd El-Azeem MI, Taha HA, El-Sherif AM. Role of MRI in evaluation of hip joint involvement in juvenile idiopathic arthritis. The Egyptian Rheumatologist 2012;34(2):75-82. doi: https://doi.org/10.1016/j.ejr.2012.03.001
112. Panwar J, Tolend M, Redd B, Srinivasalu H, Colbert RA, Akikusa J, Appenzeller S, Carrino JA, Herregods N, Jans L, Highmore K, von Kalle T, Kirkhus E, Rumsey DG, Jaremko JL, Clemente IEJ, van Rossum MA, Stimec J, Tse SM, Twilt M, Tzaribachev N, Sudol-Szopinska I, Meyers AB, Doria AS. Consensus-driven conceptual development of a standardized whole body-MRI scoring system for assessment of disease activity in juvenile idiopathic arthritis: MRI in JIA OMERACT working group. Semin Arthritis Rheum 2021;51(6):1350-1359. doi: 10.1016/j.semarthrit.2021.07.017
113. Hedrich CM, Hofmann SR, Pablik J, Morbach H, Girschick HJ. Autoinflammatory bone disorders with special focus on chronic recurrent multifocal osteomyelitis (CRMO). Pediatr Rheumatol Online J 2013;11(1):47. doi: 10.1186/1546-0096-11-47
114. Landis JR, Koch GG. The measurement of observer agreement for categorical data. Biometrics 1977;33(1):159-174.
115. Bland JM, Altman DG. Statistical methods for assessing agreement between two methods of clinical measurement. Lancet 1986;1(8476):307-310.
116. Hemke R, Tzaribachev N, Nusman CM, van Rossum MAJ, Maas M, Doria AS. Magnetic Resonance Imaging (MRI) of the Knee as an Outcome Measure in Juvenile Idiopathic Arthritis: An OMERACT Reliability Study on MRI Scales. J Rheumatol 2017;44(8):1224-1230. doi: 10.3899/jrheum.160821
117. Østergaard M, Klarlund M. Importance of timing of post-contrast MRI in rheumatoid arthritis: what happens during the first 60 minutes after IV gadolinium-DTPA? Ann Rheum Dis 2001;60(11):1050-1054. doi: 10.1136/ard.60.11.1050
118. Yamato M, Tamai K, Yamaguchi T, Ohno W. MRI of the knee in rheumatoid arthritis: Gd-DTPA perfusion dynamics. J Comput Assist Tomogr 1993;17(5):781-785. doi: 10.1097/00004728-199309000-00022
119. Cohen J. Weighted kappa: nominal scale agreement with provision for scaled disagreement or partial credit. Psychol Bull 1968;70(4):213-220. doi: 10.1037/h0026256
120. Feinstein AR, Cicchetti DV. High agreement but low kappa: I. The problems of two paradoxes. J Clin Epidemiol 1990;43(6):543-549. doi: 10.1016/0895-4356(90)90158-l
121. Gwet KL. Computing inter-rater reliability and its variance in the presence of high agreement. Br J Math Stat Psychol 2008;61(Pt 1):29-48. doi: 10.1348/000711006X126600
122. Bland JM, Altman DG. A note on the use of the intraclass correlation coefficient in the evaluation of agreement between two methods of measurement. Comput Biol Med 1990;20(5):337-340. doi: 10.1016/0010-4825(90)90013-f
123. Bankier AA, Levine D, Halpern EF, Kressel HY. Consensus interpretation in imaging research: is there a better way? Radiology 2010;257(1):14-17. doi: 10.1148/radiol.10100252
124. Espeland A, Vetti N, Kråkenes J. Are two readers more reliable than one? A study of upper neck ligament scoring on magnetic resonance images. BMC Med Imaging 2013;13:4. doi: 10.1186/1471-2342-13-4
125. Huang X, O'Connor M, Ke LS, Lee S. Ethical and methodological issues in qualitative health research involving children: A systematic review. Nurs Ethics 2016;23(3):339-356. doi: 10.1177/0969733014564102

126. Helseth S, Slettebø A. Research involving children: some ethical issues. Nurs Ethics 2004;11(3):298-308. doi: 10.1191/0969733004ne697oa
127. Cattalini M, Soliani M, Caparello MC, Cimaz R. Sex Differences in Pediatric Rheumatology. Clin Rev Allergy Immunol 2019;56(3):293-307. doi: 10.1007/s12016-017-8642-3
128. von Kalle T, Heim N, Hospach T, Langendörfer M, Winkler P, Stuber T. Typical patterns of bone involvement in whole-body MRI of patients with chronic recurrent multifocal osteomyelitis (CRMO). Rofo 2013;185(7):655-661. doi: 10.1055/s-0033-1335283
129. Papakonstantinou O, Prountzos S, Karavasilis E, Atsali E, Bizimi V, Alexopoulou E, Fotis L. Whole-body magnetic resonance imaging findings and patterns of chronic nonbacterial osteomyelitis in a series of Greek pediatric patients. Acta Radiol Open 2022;11(6):20584601221106701. doi: 10.1177/20584601221106701
130. Iyer RS, Thapa MM, Chew FS. Chronic recurrent multifocal osteomyelitis: review. AJR Am J Roentgenol 2011;196(6 Suppl):S87-91. doi: 10.2214/AJR.09.7212
131. Byrdy-Daca M, Duczkowski M, Sudoł-Szopińska I, Żelewska M, Piłat K, Daca F, Nieciecki M, Sztwiertnia P, Walecki J, Cieszanowski A, Świątkowski J, Bereźniak M, Sułkowska K, Czubak J, Gołębiowski M, Palczewski P. Spinal Involvement in Patients with Chronic Non-Bacterial Osteomyelitis (CNO): An Analysis of Distinctive Imaging Features. J Clin Med 2023;12(23). doi: 10.3390/jcm12237419
132. Hospach T, Langendoerfer M, von Kalle T, Maier J, Dannecker GE. Spinal involvement in chronic recurrent multifocal osteomyelitis (CRMO) in childhood and effect of pamidronate. Eur J Pediatr 2010;169(9):1105-1111. doi: 10.1007/s00431-010-1188-5
133. Schnabel A, Range U, Hahn G, Berner R, Hedrich CM. Treatment Response and Longterm Outcomes in Children with Chronic Nonbacterial Osteomyelitis. J Rheumatol 2017;44(7):1058-1065. doi: 10.3899/jrheum.161255
134. Kostik MM, Kopchak OL, Maletin AS, Mushkin AY. The peculiarities and treatment outcomes of the spinal form of chronic non-bacterial osteomyelitis in children: a retrospective cohort study. Rheumatol Int 2020;40(1):97-105. doi: 10.1007/s00296-019-04479-2
135. Khanna G, Sato TS, Ferguson P. Imaging of chronic recurrent multifocal osteomyelitis. Radiographics 2009;29(4):1159-1177. doi: 10.1148/rg.294085244
136. Bhat CS, Anderson C, Harbinson A, McCann LJ, Roderick M, Finn A, Davidson JE, Ramanan AV. Chronic non bacterial osteitis- a multicentre study. Pediatr Rheumatol Online J 2018;16(1):74. doi: 10.1186/s12969-018-0290-5
137. Shi X, Hou X, Hua H, Dong X, Liu X, Cao F, Li C. Case report: Child chronic nonbacterial osteomyelitis with rapid progressive scoliosis-an association with disease? Front Pediatr 2023;11:1076443. doi: 10.3389/fped.2023.1076443
138. Kaiser D, Bolt I, Hofer M, Relly C, Berthet G, Bolz D, Saurenmann T. Chronic nonbacterial osteomyelitis in children: a retrospective multicenter study. Pediatr Rheumatol Online J 2015;13:25. doi: 10.1186/s12969-015-0023-y
139. Vittecoq O, Said LA, Michot C, Mejjad O, Thomine JM, Mitrofanoff P, Lechevallier J, Ledosseur P, Gayet A, Lauret P, le Loët X. Evolution of chronic recurrent multifocal osteitis toward spondylarthropathy over the long term. Arthritis Rheum 2000;43(1):109-119. doi: 10.1002/1529-0131(200001)43:1<109::AID-ANR14>3.0.CO;2-3
140. Sudoł-Szopińska I, Herregods N, Doria AS, Taljanovic MS, Gietka P, Tzaribachev N, Klauser AS. Advances in Musculoskeletal Imaging in Juvenile Idiopathic Arthritis. Biomedicines 2022;10(10). doi: 10.3390/biomedicines10102417
141. Rieter JF, de Horatio LT, Nusman CM, Müller LS, Hemke R, Avenarius DF, van Rossum MA, Malattia C, Maas M, Rosendahl K. The many shades of enhancement: timing of post-gadolinium images strongly influences the scoring of juvenile idiopathic arthritis wrist involvement on MRI. Pediatr Radiol 2016;46(11):1562-1567. doi: 10.1007/s00247-016-3657-0

142. van Vucht N, Santiago R, Lottmann B, Pressney I, Harder D, Sheikh A, Saifuddin A. The Dixon technique for MRI of the bone marrow. Skeletal Radiol 2019;48(12):1861-1874. doi: 10.1007/s00256-019-03271-4
143. Athira R, Cannane S, Thushara R, Poyyamoli S, Nedunchelian M. Diagnostic Accuracy of Standalone T2 Dixon Sequence Compared with Conventional MRI in Sacroiliitis. Indian J Radiol Imaging 2022;32(3):314-323. doi: 10.1055/s-0042-1753467
144. Özgen A. The Value of the T2-Weighted Multipoint Dixon Sequence in MRI of Sacroiliac Joints for the Diagnosis of Active and Chronic Sacroiliitis. AJR Am J Roentgenol 2017;208(3):603-608. doi: 10.2214/AJR.16.16774

Paper 1

d'Angelo, P., Tanturri de Horatio, L., Toma, P., Ording Müller, L.S., Avenarius, D., von Brandis, E., ... Rosendahl, K. (2021).

Chronic nonbacterial osteomyelitis - clinical and magnetic resonance imaging features

Pediatric Radiology, 51, 282–288.

Pediatric Radiology (2021) 51:282–288
https://doi.org/10.1007/s00247-020-04827-6

ORIGINAL ARTICLE

Chronic nonbacterial osteomyelitis — clinical and magnetic resonance imaging features

Paola d'Angelo[1] · Laura Tanturri de Horatio[1] · Paolo Toma[1] · Lil-Sofie Ording Müller[2] · Derk Avenarius[3] · Elisabeth von Brandis[2] · Pia Zadig[3] · Ines Casazza[1] · Manuela Pardeo[4] · Denise Pires-Marafon[4] · Martina Capponi[4] · Antonella Insalaco[4] · Benedetti Fabrizio[4] · Karen Rosendahl[3,5]

Received: 8 April 2020 / Revised: 25 June 2020 / Accepted: 23 August 2020 / Published online: 9 October 2020

Abstract

Background Chronic nonbacterial osteomyelitis (CNO) is a rare autoinflammatory bone disorder. Little information exists on the use of imaging techniques in CNO.

Materials and methods We retrospectively reviewed clinical and MRI findings in children diagnosed with CNO between 2012 and 2018. Criteria for CNO included unifocal or multifocal inflammatory bone lesions, symptom duration >6 weeks and exclusion of infections and malignancy. All children had an MRI (1.5 tesla) performed at the time of diagnosis; 68 of these examinations were whole-body MRIs including coronal short tau inversion recovery sequences, with additional sequences in equivocal cases.

Results We included 75 children (26 boys, or 34.7%), with mean age 10.5 years (range 0–17 years) at diagnosis. Median time from disease onset to diagnosis was 4 months (range 1.5–72.0 months). Fifty-nine of the 75 (78.7%) children presented with pain, with or without swelling or fever, and 17 (22.7%) presented with back pain alone. Inflammatory markers were raised in 46/75 (61.3%) children. Fifty-four of 75 (72%) had a bone biopsy. Whole-body MRI revealed a median number of 6 involved sites (range 1–27). Five children (6.7%) had unifocal disease. The most commonly affected bones were femur in 46 (61.3%) children, tibia in 48 (64.0%), pelvis in 29 (38.7%) and spine in 20 (26.7%). Except for involvement of the fibula and spine, no statistically significant differences were seen according to gender.

Conclusion Nearly one-fourth of the children presented with isolated back pain, particularly girls. The most common sites of disease were the femur, tibia and pelvic bones. Increased inflammatory markers seem to predict the number of MRI sites involved.

Keywords Bones · Children · Chronic nonbacterial osteomyelitis (CNO) · Inflammation · Magnetic resonance imaging · Scoring system · Whole body

Introduction

Chronic nonbacterial osteomyelitis (CNO) is an inflammatory, non-infectious disorder of the musculoskeletal system covering a wide clinical spectrum, with asymptomatic involvement of a single site at the one end and episodes of chronic recurrent multifocal osteomyelitis (CRMO) at the other end [1–4]. It is characterized by localized pain — often at night — and swelling, and primarily affects the metaphyses of long bones, although lesions can occur in any part of the skeleton [5–7]. Affection of tissues other than bone, such as skin, eyes, gastrointestinal tract and lungs, has been described [8]. CNO has a protracted course with numerous exacerbations and relapses at new and old sites. It primarily occurs in children and adolescents, with a peak of onset at 7–12 years and a reported incidence of 0.4–10.0/100,000 [1, 9, 10]. The true incidence is, however, thought to be higher because the findings are nonspecific. Although children with CNO

✉ Karen Rosendahl
Karen.rosendahl@unn.no

[1] Department of Radiology, Ospedale Pediatrico Bambino Gesu, Rome, Italy

[2] Section of Pediatric Radiology, Oslo University Hospital, Oslo, Norway

[3] Section of Pediatric Radiology, University Hospital of North Norway, 9019 Tromsø, Norway

[4] Department of Rheumatology, Ospedale Pediatrico Bambino Gesu, Rome, Italy

[5] Department of Clinical Medicine, UiT the Arctic University of Norway, Tromsø, Norway

frequently have mild to moderately increased levels of inflammatory markers, no findings — be they biochemical or imaging-based — are diagnostic for the disease. Currently, CNO is a diagnosis of exclusion, based on imaging or through histological examination of bone biopsies, which reveal acute and chronic inflammatory as well as reparative bone features like hyperostosis, without an infectious agent [11, 12].

Treatment strategies for children with CNO vary widely [13, 14]. Nonsteroidal anti-inflammatory drugs (NSAIDs) are commonly used as a first-line treatment, while second-line therapies include glucocorticoids, methotrexate, sulfasalazine, tumor necrosis factor (TNF)-α inhibitors and bisphosphonates [1, 7]. Although MRI, including whole-body examination, is widely used to diagnose and monitor CNO, little information exists on the use of imaging techniques, and standardized and validated assessment systems are lacking. Moreover, normal population-based standards for the MR appearances of the pediatric skeleton across age groups are nearly non-existent. Therefore, we combined clinical, laboratory (including histology when available) and imaging data from a large number of children with CNO to examine the patient characteristics, clinical presentation and pattern of involvement, with a special focus on MRI findings.

Materials and methods

This multicenter retrospective study included children residing in Rome or Bergen with a diagnosis of CNO. We obtained data on age, gender, age of symptom onset, age at diagnosis, duration, clinical symptoms, laboratory and radiologic findings at diagnosis and follow-up of patients ages 0–18 years from the clinical journal systems and the radiology information system (RIS) and picture archiving and communication system (PACS) at Ospedale Pediatrico Bambino Gesu Hospital (OPBG), Rome, and Haukeland University Hospital (HUS), Bergen, respectively. The institutional board at OPBG approved the study.

Patients

We included all children with mono- or multifocal inflammatory lesions diagnosed as CNO at the two participating pediatric centers during the period 2012–2018. The criteria for CNO were mono- or multifocal inflammatory bone lesions, duration of symptoms >6 weeks, and exclusion of infections and malignancy [7]. Demographic, clinical and laboratory data and histological findings, when available, were collected from the medical records. Normal ranges used for laboratory data were as follows: C-reactive protein (CRP)<0.5 mg/dL, erythrocyte sedimentation rate (ESR)<15 mm/h. In addition, we grouped inflammation (based on blood markers, ESR and CRP) as mild when at least one marker was raised but not >100, or moderate when at least one marker was >100.

Imaging

All MRIs performed at the time of diagnosis were re-analyzed by three of the authors (P.d'A., L.T.d.H. and K.R., with 3, 12 and 30 years of experience in paediatric radiology, respectively) (Fig. 1). We scored the following features: the bone(s) involved (noting epiphyseal, metaphyseal or diaphyseal location in the long bones), periosteal reaction, growth plate involvement, vertebral compression and the presence of soft-tissue inflammation (Figs. 2, 3, 4, 5, 6 and 7). Bone marrow edema and soft-tissue inflammation were defined as increased signal intensity (as compared to the remainder of the bone, or to the contralateral side) on water-sensitive sequences. All MRIs were performed on a 1.5-tesla (T) Siemens MRI system — at OPBG an Aera and at HUS an Avanto machine was used (Siemens, Erlangen, Germany). The whole-body MRI included a coronal short tau inversion recovery (STIR) sequence (repetition time/echo time/inversion time [TR/TE/TI] 5,000/58/160 ms and flip angle 147°; and a sagittal STIR sequence of the spine and feet, with additional T1-weighted images (TR/TE 400/7 ms) in equivocal cases. Typical duration of examination for the whole-body MRI was 35–45 min.

Statistical analysis

Descriptive statistics were reported as mean (with standard deviations) and percentages or median (ranges). Differences between genders, as have been reported by others, were examined using *t*-

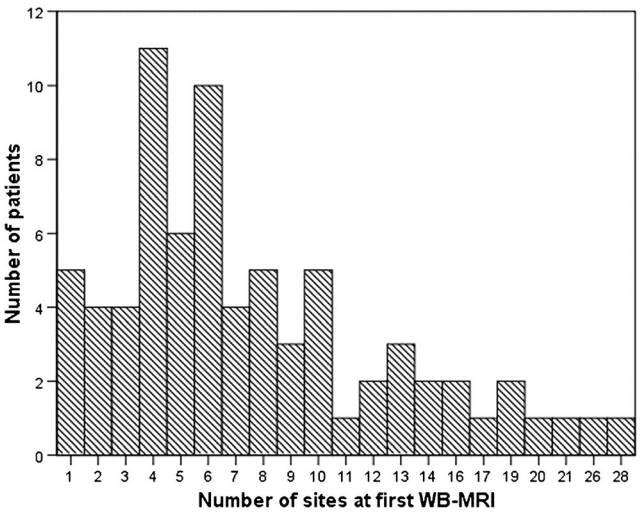

Fig. 1 Graph shows number of sites based on the initial whole-body MRI (WB-MRI) examination in 67 of the 75 children with chronic nonbacterial osteomyelitis

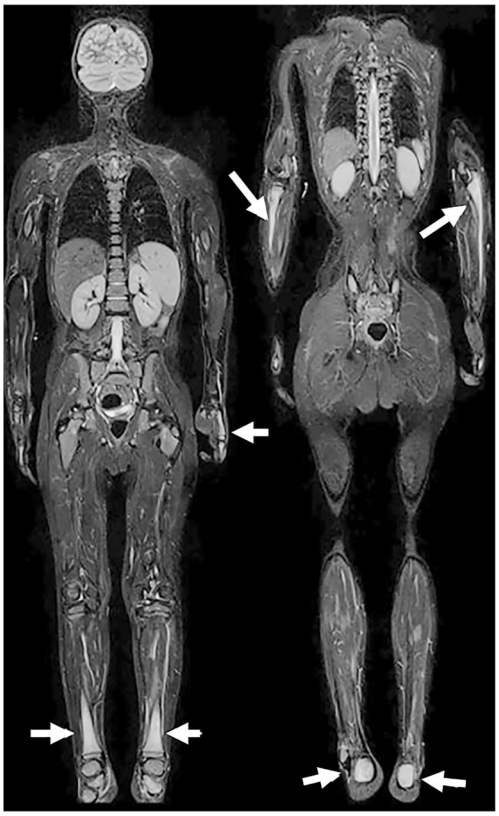

Fig. 2 Chronic nonbacterial osteomyelitis in a 14-year-old boy. Whole-body coronal T2-W short tau inversion recovery images (left to right: anterior to posterior, repetition time/echo time = 5,000/58 ms) show high signal of both proximal ulnae, left hand, both lower legs and calcanei (*arrows*). Note normal signal from the proximal femurs

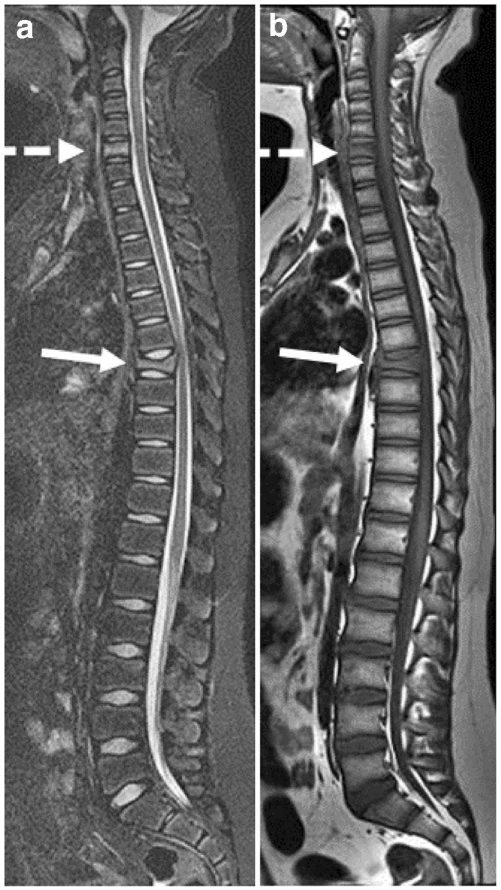

Fig. 3 Chronic nonbacterial osteomyelitis in a 13-year-old boy. **a, b** Sagittal T2-W short tau inversion recovery MR image (repetition time/echo time [TR/TE] 5,000/58 ms) (**a**) and T1-W MR image (TR/TE 400/7 ms) (**b**) of the spine show signal change and vertebral compression of the 7th thoracic vertebrae (*solid arrow*) and signal changes of the 6th cervical vertebrae (*dashed arrow*)

tests or Fisher exact/chi-square tests as appropriate. Multiple linear regression analysis was used to test whether rise in inflammatory markers (ESR/CRP), time to diagnosis, age or gender significantly predicted the total number of bony sites involved at diagnosis. Statistical analyses were performed using SPSS version 25 (IBM, Armonk, NY). All tests were two-sided and statistical significance was set to $P<0.05$.

Results

We included 75 children (26 boys, 34.7%) with a mean age of 10.5 years (standard deviation [SD] 3.2 years, range 0–17 years) at diagnosis. One child was younger than 2 years at time of diagnosis. The median time of symptom onset to diagnosis was 4 months (range 1.5 to 72.0 months). Fifty-nine of the 75 children (78.7%) presented with pain, with or without swelling or fever (Table 1). Seventeen children (22.7%) presented with isolated low back pain (spine or sacroiliac joints). Arthritis was seen in one child, who had ankle involvement. Cutaneous involvement, such as psoriasis, lupus erythematosus, papular lesions or pustulosis, was seen in 8 children (10.7%). Inflammatory markers were increased in 46/75 (61.3%) (Table 1). A biopsy of the most prominent bone lesion on imaging was performed in 54/75 children (72.0%); biopsies showed features consistent with subacute/chronic osteomyelitis in 27 and nonspecific changes in 17, and were inconclusive in the remaining 10. Five children (6.7%) presented with single-site involvement (two lower bones, one humerus, one spine and one mandible); all except one underwent bone biopsy.

Magnetic resonance imaging was performed at baseline in all children; 68 had a whole-body MRI, revealing a median number of 6 sites (range 1–27) (Fig. 1). The long bones in the lower limbs were affected in 58/75 (77.3%) of the cases, the pelvis in 29/75 (38.7%), the spine in 20/75 (26.7%) and the long bones of the upper limbs in 20/75 (26.7%). Except for the fibula and spine, no

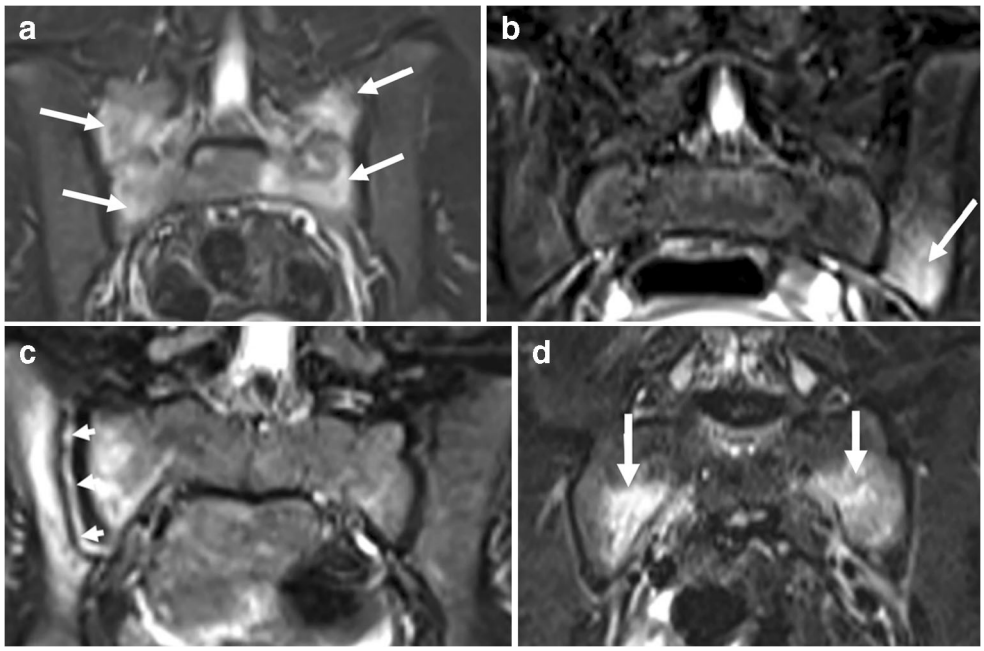

Fig. 4 Chronic nonbacterial osteomyelitis with sacroiliac joint involvement in four children aged 10–15 years. Coronal T2-W short tau inversion recovery MR images (repetition time/echo time = 5,000/58 ms). **a** Bone marrow edema at the sacral side, bilaterally (*arrows*) in an 11-year-old girl. **b** Bone marrow edema at the left iliac side (*arrow*) in a 9-year-old girl. **c** High signal in the right joint space *arrows*, with surrounding bone marrow edema at the iliac and sacral sides in an 8-year-old girl. **d** Bone marrow edema at the sacral sides, bilaterally in a 15-year-old girl (*arrows*)

statistically significant differences in involvement were seen according to gender (Table 2). A periosteal reaction was seen in four children, all of whom presented with focal pain, while soft-tissue involvement was seen in eight children.

Among the 68 children who had whole-body MRI, 82 epiphyseal, 80 metaphyseal and 5 physeal lesions were found in the long tubular bones. All physeal lesions were associated with metaphyseal or epiphyseal involvement. Twenty-seven children had diaphyseal lesions, all of which were located in the long bones of the lower extremities. Three of these 27 children had additional periosteal and soft-tissue reaction. Involvement of the epiphysis, metaphysis and diaphysis of the long tubular bones, by gender, is presented in Table 3.

We used multiple linear regression analysis to test whether rise in inflammatory markers (ESR/CRP), time to diagnosis, age or gender significantly predicted the total number of bony sites involved at diagnosis. Preliminary analysis did not reveal any violation of the assumptions of normality, linearity, multicolinearity or homoscedasticity. The results of the

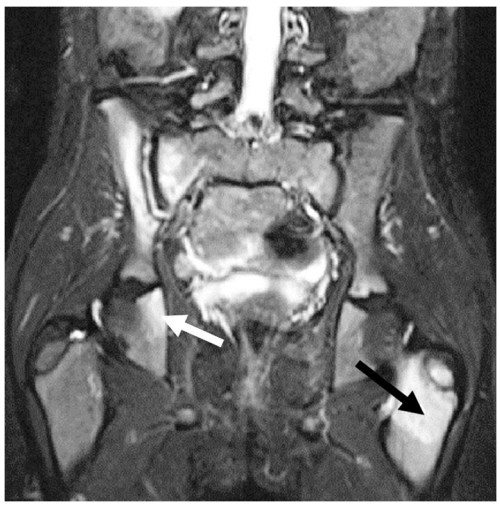

Fig. 5 Chronic nonbacterial osteomyelitis in a 7-year-old girl. Coronal T2-W short tau inversion recovery MR image (repetition time/echo time = 5,000/58 ms) shows involvement of the right sacroiliac joint (high signal in the joint space with surrounding bone marrow edema), the right ischial bone (*white arrow*) and the left femoral metaphysis/apophysis (*black arrow*). Note the subtle high signal of the right femoral metaphysis, within normal variation

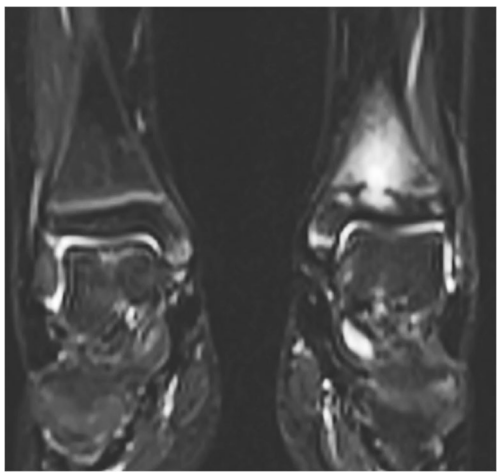

Fig. 6 Chronic nonbacterial osteomyelitis in a 9-year-old girl. Coronal T2-W short tau inversion recovery MR image (repetition time/echo time = 5,000/58 ms) of both ankles shows involvement of the left metaphysis, growth plate and epiphysis. The right side is normal

Fig. 7 Chronic nonbacterial osteomyelitis in an 8-year-old boy. Coronal T2-W short tau inversion recovery MR image (repetition time/echo time = 5,000/58 ms) of the knees/legs shows involvement of the right tibial metaphysis and diaphysis, and the right epiphysis (*arrow*). The findings were confirmed on T1-weighted images

regression indicated that the four predictors explained only 11.2% of the variance (R^2=0.11, F (1.692), *P*=0.14). Elevation of inflammatory markers significantly predicted the number of sites (β=0.250, *P*=0.045). Neither age (β=0.186, *P*=0.132) nor gender (β=0.103, *P*=0.387) nor disease duration (β=0.025, *P*=0.841) predicted the number of involved bone sites significantly.

Discussion

We have shown, in a large two-center cohort of children and adolescents diagnosed with CNO, that bony pain, with or without swelling, was the most common presenting symptom, that two-thirds were girls and that the femur, tibia and pelvis were most often involved. On whole-body MRI, epiphyses and metaphyses appeared to be equally involved. In contrast to previous reports, median time from time of onset to diagnosis was relatively low, with a median of 4 months, reflecting an increased awareness of the diagnosis during the last few years [7, 15]. Nearly one-fourth of the children presented with low back pain, particularly girls, with MR features exhibiting those of vertebral bone marrow edema. Age at presentation and gender distribution confirmed previous reports [7, 15].

The number of sites, both with and without symptoms at presentation, as demonstrated on the initial whole-body MRI varied between 1 and 27, with a median of 6. Whether the asymptomatic sites are true so-called silent lesions or subclinical disease, as suggested by others [1, 15], or merely reflect

Table 1 Age and symptoms for 75 children (26 boys) diagnosed to have chronic nonbacterial osteomyelitis (CNO) based on history and clinical, laboratory and imaging findings, with an additional biopsy in 54 children (72%)

	Boys (*n*=26)	Girls (*n*=49)	*P*-value[a]	Total (*n*=75)[b]
Age at diagnosis, year, mean (SD)	10.4 (3.3)	10.5 (3.1)	0.832	10.5 (3.2)
Age at onset, years, mean (SD)	9.5 (3.4)	10.0 (3.0)	0.534	9.8 (3.1)
Symptoms at presentation, number (%)				
Body pain	19	40	0.393	59 (78.7)
Localized pain[c]	9	10		19 (25.3)
Low back pain	3	14		17 (22.7)
Multifocal pain	5	5		10 (13.3)
Localized pain and swelling	1	11		12 (16.0)
Localized pain and fever (>38°C)	1	0		1 (1.3)
Fever only	2	2		4 (5.3)
Swelling only	1	2		3 (4.0)
Limp	3	5		8 (10.7)
Elevated inflammatory blood makers[d], number (%)	13	33	0.209	46 (61.3)
Mild	10	20		30 (40.0)
Moderate	3	13		16 (21.3)
Increased white blood count (WBC)	0	1		1 (1.3)

[a] Differences between genders were examined using *t*-tests or chi-square tests as appropriate; 2-sided *P*-values are given; *P*<0.05 is significant

[b] One boy age 4 months presented with agitation, crying

[c] Other than low back pain

[d] Erythrocyte sedimentation rate and C-reactive protein

SD standard deviation

Table 2 Number of children with bone changes at different sites consistent with inflammatory change as diagnosed on whole-body MRI at presentation (7 of the 75 children did not have a complete whole-body MRI)

	Boys (*n*=26)	Girls (*n*=49)	*P*-value[a]	Total (%) (*n*=75)
Lower limbs				
Femur	19	27	0.128	46 (61.3)
Tibia	18	30	0.492	48 (64.0)
Fibula	12	9	**0.011**	21 (28.0)
Feet	13	16	0.142	29 (38.7)
Upper limbs				
Humerus	4	11	0.467	15 (20.0)
Radius	3	6	0.929	9 (12.0)
Ulna	2	3	0.795	5 (6.7)
Hands	0	4	0.134	4 (5.3)
Spine	3	17	**0.031**	20 (26.7)
Sacrum	6	12	0.892	18 (24.0)
Sacroiliac joints	1	7	0.163	8 (10.7)
Pelvis	8	21	0.306	29 (38.7)
Ileum	4	15	0.149	19 (25.3)
Sternum	4	10	0.595	14 (18.7)
Scapula	2	6	0.543	8 (10.7)
Clavicle	3	11	0.248	14 (18.7)
Mandible	3	5	0.859	8 (10.7)
Ribs	3	1	0.081	4 (5.3)

[a] Differences between genders were examined using chi-square tests; 2-sided *P*-values are given; $P<0.05$ is significant (bold values)

signal changes during normal bone growth remains unclear. From previous work we know that more than half of healthy children ages 5–16 years have bone-marrow-edema-like changes in the hand skeleton [16, 17]. Others have shown similar findings to the feet [18] and pelvis [19]. Further studies with a meticulous focus on the association between MRI findings and clinical symptoms are warranted to clarify the significance of asymptomatic MRI findings.

Table 3 Number of children with epiphyseal, metaphyseal or diaphyseal involvement of at least one of the long bones, in 75 children with chronic nonbacterial osteomyelitis (7 of the 75 children did not have a complete whole-body MRI)

	Males (*n*=26)	Females (*n*=49)	*P*-value[a]	Total (%) (*n*=75)
Distal epiphysis	11	15	0.189	26 (34.7)
Proximal epiphysis	12	7	**0.027**	19 (25.3)
Diaphysis	12	15	0.131	27 (36.0)
Distal metaphysis	13	24	0.938	37 (49.3)
Proximal metaphysis	16	27	0.799	43 (57.3)

[a] Differences between genders were examined using chi-square tests; 2-sided *P*-values are given; $P<0.05$ is significant (bold values)

In a large registry study from 2018 including 486 children with CRMO from 19 countries, mean age 9.9 years, MRI revealed 4.1 sites per patient, as compared to 6 in our case series [7]. The relatively low number of whole-body MRI in their study, i.e. <30% of the patients, might explain part of the difference because whole-body MRI most likely introduces false-positive findings, or lesions. Population differences might also have played a role. Another study, by Andronikou et al. [20], which included 37 people with CRMO, reported on 8.6 lesions per patient based on whole-body MRI, with 89% of patients having multifocal disease. They noticed two patterns, namely a multifocal predominantly tibial involvement and paucifocal clavicular and spinal disease. In our series we were not able to identify specific patterns in distribution.

The number of radiologic lesions has been used as a marker of disease activity in the context of the Pediatric CNO (PedCNO) score [21]. In addition to the number of radiologic lesions, the PedCNO includes ESR, severity of disease as judged by the physician, severity of the disease estimated by child or parent, and the Childhood Health Assessment Questionnaire (CHAQ) score. Zhao and colleagues [22] further described the characteristics of CNO lesions based on MRI findings using a grading system to score the severity of bone edema and soft-tissue inflammation as well as the presence of periosteal reaction, hyperostosis, growth plate damage and vertebral compression. Applying this scoring tool to a retrospective cohort of 18 people with CNO, the authors reported a significant decrease in the number of non-vertebral lesions and the maximum severity of bone edema in the group receiving aggressive treatment [14, 22]. They noted, however, that it remains unclear which MRI characteristics can be reliably assessed and to which degree they are sensitive to change. Moreover, it is not known how the MRI findings relate to other clinical assessment tools. In our large case series of 75 children with CNO, only 4 had a periosteal reaction, 3 related to diaphyseal involvement and 1 in a rib. Thus, periosteal reaction is probably too rare to be used as prognostic support, as are soft-tissue and physeal involvement. As for the extent and intensity of bone marrow edema, we did not score this in particular. However, being a key finding in CNO, it is reasonable to believe that the extent/degree of bone edema might be of value, assuming that we will be able to distinguish between true inflammatory change and changes caused by normal growth. Currently, there is no agreement on a standardized evaluation tool [14].

In our series, elevation of the inflammatory markers significantly predicted the number of MRI sites, suggesting that the number of MRI sites represents a marker for disease activity.

There are several limitations to our study, including its retrospective design and the lack of whole-body MRI in seven of the patients. Moreover, image quality is suboptimal for assessing physeal lesions and periosteal reaction, thus these features might be underestimated. The possibility of artifacts, particularly for borderline structures such as the sternum and ribs, is also a potential bias. The strengths of the study were the large number of children with whole-body MRI and the meticulous image analysis.

Conclusion

Nearly one-fourth of children with CNO, particularly girls, presented with isolated back pain only. The most common sites of disease were the femur, tibia and pelvic bones. Elevation of inflammatory markers seems to predict the number of MRI sites of disease.

Acknowledgments Open Access funding provided by UiT The Arctic University of Norway.

Compliance with ethical standards

Conflicts of interest None

References

1. Hofmann SR, Schnabel A, Rosen-Wolff A et al (2016) Chronic nonbacterial osteomyelitis: pathophysiological concepts and current treatment strategies. J Rheumatol 43:1956–1964
2. Girschick HJ, Raab P, Surbaum S et al (2005) Chronic nonbacterial osteomyelitis in children. Ann Rheum Dis 64:279–285
3. Falip C, Alison M, Boutry N et al (2013) Chronic recurrent multifocal osteomyelitis (CRMO): a longitudinal case series review. Pediatr Radiol 43:355–375
4. Iyer RS, Thapa MM, Chew FS (2011) Chronic recurrent multifocal osteomyelitis: review. AJR Am J Roentgenol 196:S87–S91
5. Grote V, Silier CC, Voit AM, Jansson AF (2017) Bacterial osteomyelitis or nonbacterial osteitis in children: a study involving the German Surveillance Unit for Rare Diseases in Childhood. Pediatr Infect Dis J 36:451–456
6. Silier CCG, Greschik J, Gesell S et al (2017) Chronic non-bacterial osteitis from the patient perspective: a health services research through data collected from patient conferences. BMJ Open 7: e017599
7. Girschick H, Finetti M, Orlando F et al (2018) The multifaceted presentation of chronic recurrent multifocal osteomyelitis: a series of 486 cases from the Eurofever international registry. Rheumatology 57:1203–1211
8. Costa-Reis P, Sullivan KE (2013) Chronic recurrent multifocal osteomyelitis. J Clin Immunol 33:1043–1056
9. Taddio A, Zennaro F, Pastore S, Cimaz R (2017) An update on the pathogenesis and treatment of chronic recurrent multifocal osteomyelitis in children. Paediatr Drugs 19:165–172
10. Berkowitz YJ, Greenwood SJ, Cribb G et al (2018) Complete resolution and remodeling of chronic recurrent multifocal osteomyelitis on MRI and radiographs. Skelet Radiol 47:563–568
11. Jurik AG, Moller BN (1986) Inflammatory hyperostosis and sclerosis of the clavicle. Skelet Radiol 15:284–290
12. Carr AJ, Cole WG, Roberton DM, Chow CW (1993) Chronic multifocal osteomyelitis. J Bone Joint Surg Br 75:582–591
13. Ramanan AV, Hampson LV, Lythgoe H et al (2019) Defining consensus opinion to develop randomised controlled trials in rare diseases using Bayesian design: an example of a proposed trial of adalimumab versus pamidronate for children with CNO/CRMO. PLoS One 14:e0215739
14. Zhao Y, Wu EY, Oliver MS et al (2018) Consensus treatment plans for chronic nonbacterial osteomyelitis refractory to nonsteroidal antiinflammatory drugs and/or with active spinal lesions. Arthritis Care Res 70:1228–1237
15. Roderick MR, Shah R, Rogers V et al (2016) Chronic recurrent multifocal osteomyelitis (CRMO) — advancing the diagnosis. Pediatr Rheumatol Online J 14:47
16. Ording Müller L-S (2012) Establishment of normative MRI standards for the paediatric skeleton to better outline pathology. Focused on juvenile idiopathic arthritis. Doctoral dissertation. University of Tromsø, Tromsø
17. Avenarius DFM, Ording Muller LS, Rosendahl K (2017) Joint fluid, bone marrow edemalike changes, and ganglion cysts in the pediatric wrist: features that may mimic pathologic abnormalities — follow-up of a healthy cohort. AJR Am J Roentgenol 208:1352–1357
18. Shabshin N, Schweitzer ME, Morrison WB et al (2006) High-signal T2 changes of the bone marrow of the foot and ankle in children: red marrow or traumatic changes? Pediatr Radiol 36:670–676
19. Ording Muller LS, Avenarius D, Olsen OE (2011) High signal in bone marrow at diffusion-weighted imaging with body background suppression (DWIBS) in healthy children. Pediatr Radiol 41:221–226
20. Andronikou S, Mendes da Costa T, Hussien M, Ramanan AV (2019) Radiological diagnosis of chronic recurrent multifocal osteomyelitis using whole-body MRI-based lesion distribution patterns. Clin Radiol 74:737
21. Beck C, Morbach H, Beer M et al (2010) Chronic nonbacterial osteomyelitis in childhood: prospective follow-up during the first year of anti-inflammatory treatment. Arthritis Res Ther 12:R74
22. Zhao Y, Chauvin NA, Jaramillo D, Burnham JM (2015) Aggressive therapy reduces disease activity without skeletal damage progression in chronic nonbacterial osteomyelitis. J Rheumatol 42:1245–1251

Paper 2

Tanturri de Horatio, L., Shelmerdine, S.C., d'Angelo, P., Di Paolo, P.L., Magni-Manzoni, S., Malattia, C., … Rosendahl, K. (2023).

A novel magnetic resonance imaging scoring system for active and chronic changes in children and adolescents with juvenile idiopathic arthritis of the hip

Pediatric Radiology, 53, 426–437.

Pediatric Radiology (2023) 53:426–437
https://doi.org/10.1007/s00247-022-05502-8

ORIGINAL ARTICLE

A novel magnetic resonance imaging scoring system for active and chronic changes in children and adolescents with juvenile idiopathic arthritis of the hip

Laura Tanturri de Horatio[1,2] · Susan C. Shelmerdine[3,4,5,6] · Paola d'Angelo[1] · Pier Luigi Di Paolo[1] · Silvia Magni-Manzoni[7] · Clara Malattia[8,9] · Maria Beatrice Damasio[10] · Paolo Tomà[1] · Derk Avenarius[2,11] · Karen Rosendahl[2,11]

Received: 27 April 2022 / Revised: 10 August 2022 / Accepted: 1 September 2022 / Published online: 23 September 2022

Abstract

Background Hip involvement predicts severe disease in juvenile idiopathic arthritis (JIA) and is accurately assessed by MRI. However, a child-specific hip MRI scoring system has not been validated.

Objective To test the intra- and interobserver agreement of several MRI markers for active and chronic hip changes in children and young adults with JIA and to examine the precision of measurements commonly used for the assessment of growth abnormalities.

Materials and methods Hip MRIs from 60 consecutive children, adolescents and young adults with JIA were scored independently by two sets of radiologists. One set scored the same MRIs twice. Features of active and chronic changes, growth abnormalities and secondary post-inflammatory changes were scored. We used kappa statistics to analyze inter- and intraobserver agreement for categorical variables and a Bland–Altman approach to test the precision of continuous variables.

Results Among active changes, there was good intra- and interobserver agreement for grading overall inflammation (kappa 0.6–0.7). Synovial enhancement showed a good intraobserver agreement (kappa 0.7–0.8), while the interobserver agreement was moderate (kappa 0.4–0.5).

Regarding acetabular erosions on a 0–3 scale, the intraobserver agreement was 0.6 for the right hip and 0.7 for the left hip, while the interobserver agreement was 0.6 for both hips. Measurements of joint space width, caput–collum–diaphyseal angle, femoral neck–head length, femoral width and trochanteric distance were imprecise.

Conclusion We identified a set of MRI markers for active and chronic changes in JIA and suggest that the more robust markers be included in future studies addressing clinical validity and long-term patient outcomes.

Keywords Adolescents · Children · Hip · Inflammation · Joint damage · Juvenile idiopathic arthritis · Magnetic resonance imaging · Scoring system · Young adults

✉ Laura Tanturri de Horatio
laura.tanturri@opbg.net; lho100@uit.no

[1] Department of Imaging,
IRCCS Bambino Gesù Children's Hospital,
Piazza Di Sant'Onofrio 4, 00165 Rome, Italy

[2] Department of Clinical Medicine,
the Artic University of Norway,
Tromsø, Norway

[3] Department of Clinical Radiology,
Great Ormond Street Hospital for Children NHS Foundation Trust,
Great Ormond Street, London, UK

[4] Great Ormond Street Hospital for Children,
UCL Great Ormond Street Institute of Child Health,
London, UK

[5] NIHR Great Ormond Street Hospital Biomedical Research Centre,
Bloomsbury, London, UK

[6] Department of Radiology, St. George's Hospital,
London, UK

[7] Rheumatology Division, IRCCS,
Bambino Gesù Children's Hospital,
Rome, Italy

[8] Clinica Pediatrica E Reumatologia,
IRCCS Istituto Giannina Gaslini,
Genoa, Italy

[9] Department of Neurosciences, Rehabilitation, Ophthalmology,
Genetic and Maternal Infantile Sciences (DINOGMI),
University of Genoa,
Genoa, Italy

[10] Divisione Radiologia, IRCCS Istituto Giannina Gaslini,
Genoa, Italy

[11] Department of Radiology,
University Hospital of North Norway,
Tromsø, Norway

Introduction

Juvenile idiopathic arthritis (JIA) is the most common chronic rheumatologic disease in children [1]. It comprises a group of clinically heterogeneous arthritides of unknown origin that develop before the age of 16 years and persist for at least 6 weeks. The disease is characterized by a chronic inflammatory process of the synovium and periarticular tissue that can lead to structural damage and growth abnormalities. The incidence of JIA varies from 1.6 to 23 in 100,000, with a prevalence of 3.8–400 in 100,000 [2].

Hip involvement is common in children with JIA, occurring in approximately 20–50% of cases [3] and is considered a predictor of severe disease, carrying a high risk of disability. Typically, both hips are affected, but unilateral involvement is occasionally seen. The majority of children with active hip disease develop irreversible changes within 5 years of diagnosis [4] and approximately 26–44% require a total hip replacement within the first 10 years of disease onset [5].

Early detection and targeted treatment of active disease is essential to improve long-term outcomes [6]. Although most children with JIA have ongoing disease into adulthood, it has been suggested that there is a "window of opportunity" during the early, subclinical stage, where prompt instigation of treatment might delay progression and induce remission [7, 8]. Unfortunately, clinical assessment of the hips, even when performed by experienced rheumatologists, is difficult because the hip joint is deeplying and not easy to palpate. There is thus a need for accurate diagnostic tools to depict both active and chronic JIA-related joint changes, as has been highlighted in several studies [6, 9].

For adults with rheumatoid arthritis, several validated scoring systems for hip involvement exist, including the Hip Inflammation Magnetic Resonance Imaging Scoring System (HIMRISS) and Hip Osteoarthritis MRI Scoring System (HOAMS) [10, 11]. For children, however, although several scoring systems have been proposed [12–16], no child- and hip-specific scoring system including both inflammatory and permanent changes has been validated [17]. In one study including 79 children with hip involvement, of whom 22 had confirmed JIA, the inter- and intraobserver agreement of several selected parameters were addressed using a simplified MR-based scoring system on a 0–1 scale [14]. The most reliable features were the presence of joint effusion, bone marrow edema and the subjective assessment of synovium [14]. The study reported significant differences across parameters in the intraobserver reliability and a poor–moderate interobserver reliability for most parameters [14]. However, the study was limited to the active inflammatory domain. Moreover, as underlined by the authors, most children with JIA did not have a confirmed inflammatory disease, further weakening the robustness of the study [14]. Other authors have compared MRI and clinical or laboratory findings in small datasets, thus without testing the precision of the MRI markers applied [12, 13, 15, 16].

More recently, two papers addressing non-enhanced MRI in the diagnosis of hip changes in JIA were published — one retrospective observational study including 97 children with clinically suspected hip JIA [18] and one study on whole-body MRI for the quantification of a total inflammatory joint score [19]. However, again, repeatability studies of the suggested scores were not performed.

Our study is a first step toward establishing a robust MRI-based scoring system for active and chronic JIA changes of the hip to be used for monitoring treatment effect in daily practice as well as measuring outcomes in clinical trials. We tested the intra- and interobserver agreement of a set of MRI markers for active and chronic hip changes and examined the precision of measurements commonly used for assessing growth abnormalities.

Materials and methods

This study is part of a large longitudinal multicenter project (Health-e-Child) aimed to establish imaging-based scoring systems for children and adolescents with JIA with wrist or hip involvement. Leading pediatric musculoskeletal radiologists and clinical rheumatologists at four centers — Bambino Gesù Children's Hospital (OPBG), Rome; Giannina Gaslini Institute (IGG), Genoa; Hopital Necker Enfant Malades (HNEM), Paris; and Great Ormond Street Hospital (GOSH), London — were involved in devising an MRI-based scoring system for JIA. The present project was approved by the institutional research ethics committee at OPBG and IGG. Written informed consent was obtained from all the patients or their caregivers. For the purpose of this particular study, we included 60 consecutive children, adolescents and young adults over a 2-year interval with a diagnosis of JIA and confirmed or suspected hip involvement (37 studied at OPBG and 23 at IGG) according to the International League of Associations for Rheumatology (ILAR) classification [20]. Children and adolescents of any disease severity and activity level were included, irrespective of current or previous medical treatments. All patients underwent MRI without sedation.

Magnetic resonance imaging protocol

All MRI examinations were performed on a 1.5-tesla (T) MRI system (Achieva Intera; Philips Medical Systems,

Best, The Netherlands), using a body coil. The field-of-view included the whole pelvis to allow visualization of both hips. The children were imaged supine with the legs straight and the feet in a neutral position.

The following sequences were acquired:

- Three-dimensional (3-D) T1-weighted turbo spin-echo (TSE) sequence with repetition time/echo time (TR/TE) 600/10 ms, acquired and reconstructed voxel size of $1 \times 1 \times 1$ mm, number of signal averages 2, acquisition time about 5 min;
- T2-weighted TSE fat-saturated (FS) sequence with TR/TE 4,400/70 ms, voxel size $0.55 \times 0.69 \times 3$ mm, base resolution 218, section thickness/gap 3/0.3 mm, number of signal averages 1, acquisition time about 4 min;
- 3-D spoiled gradient echo (GRE) FS sequence with TR/TE 40/7 ms, flip angle (FA) 25°, voxel size $1 \times 1 \times 1$ mm, acquisition time about 4 min, acquired immediately ("early") and approximately 5 min ("late") after manual injection of 0.2 mL/kg of gadoteric acid 0.5 mmol/m (Dotarem; Guerbet, Roissy, France) through a 21-gauge (G) cannula inserted into an arm vein, followed by a flush of 10 mL saline.

All sequences were acquired in the coronal plane. The mean imaging time, including the time for positioning and injection, was approximately 25 min.

Scoring

Prior to scoring, we conducted three calibration sessions lasting 2 days each, using 30 MRI cases not included for analysis in this study to ensure standard terminologies and definitions could be agreed upon. We used an imaging atlas with relevant examples of each variable and grade as a reference to help maintain a consistent standard of scoring across all readers (see Online Supplementary Material 1 for the scoring system and Online Supplementary Material 2 for imaging atlas).

All hip MRIs were scored by two sets of radiologists. The first set scored the same MR images twice (the second time after a wash-out period of 3 weeks). In this set, the scoring was performed in consensus by one pediatric radiologist (L.T.dH., with 14 years of experience) and one of two additional pediatric radiologists (P.L.D.P., with 9 years of experience, or P.dA., with 5 years of experience) at OPBG. The second set included one pediatric radiologist (S.C.S., with 7 years of experience) at GOSH, who scored all the MRI images once independently. All radiologists were blinded to disease duration, clinical symptoms and findings, JIA subtype and prior imaging.

Inflammatory changes

Based on the pre- and late post-contrast 3-D GRE and the coronal T2-W FS images, we scored:

1. Synovial enhancement intensity (using different scoring scales, Fig. 1) and synovial thickening (measured both subjectively and objectively);
2. Presence of effusion;
3. Degree of overall synovial inflammation including thickening and enhancement intensity;
4. Degree of overall inflammation (Fig. 2), adding effusion to the degree of overall synovial inflammation;
5. Bone marrow edema, which was defined as an area of high signal intensity on T2-W FS images with corresponding

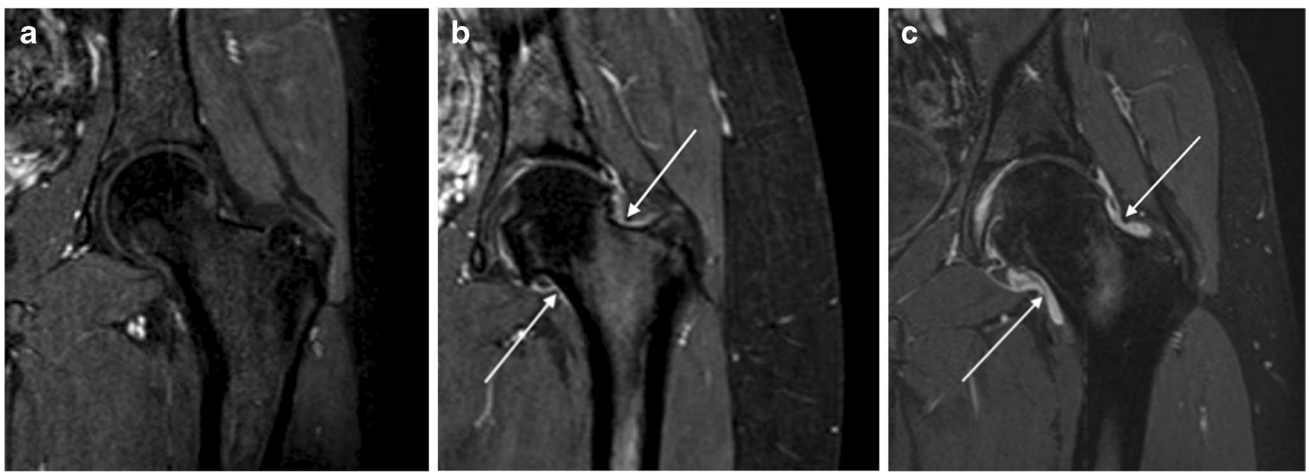

Fig. 1 Degree of post-contrast synovial enhancement of the left-hip MRIs in three children with juvenile idiopathic arthritis (JIA), demonstrated on coronal three-dimensional (3-D) gradient echo MRI sequences with fat saturation. **a** No visible synovial enhancement (score 0) in a 17-year-old boy. **b** Mildly increased enhancement (*arrows*) (score 1) in a 16-year-old girl. **c** Severely increased enhancement (*arrows*) (score 2) in a 15-year-old boy

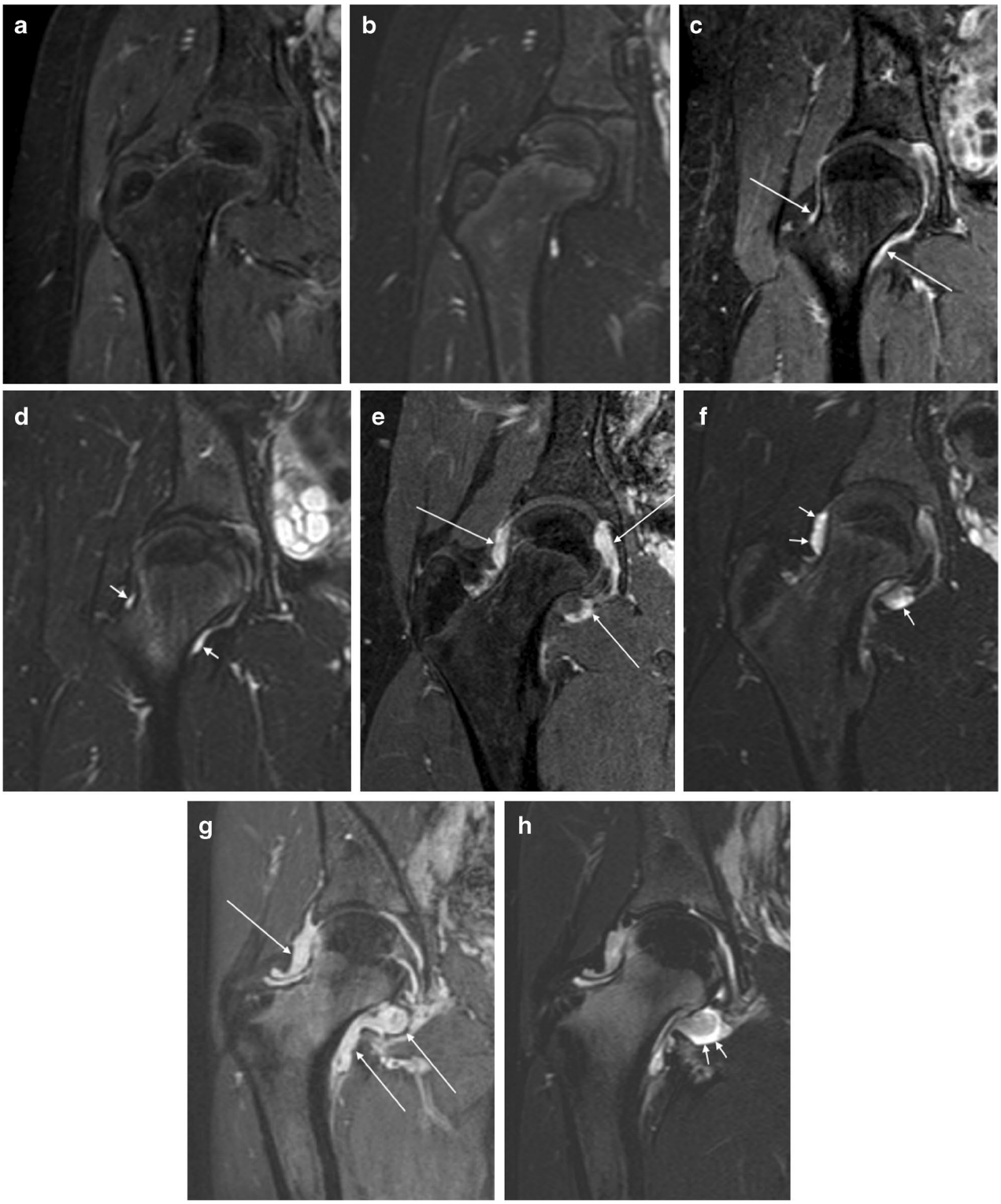

Fig. 2 Overall degree of inflammation in right-hip MRIs in four pairs of images from four children with juvenile idiopathic arthritis (JIA) across different levels of severity. All images are demonstrated using coronal post-contrast three-dimensional (3-D) gradient echo with fat saturation (**a, c, e, g**) and coronal fat-saturated T2-weighted turbo spin-echo (**b, d, f, h**) MRI sequences. **a, b** No inflammation (score 0) in a 12-year-old boy. **c, d** Mild synovial thickening with moderate increase in post-contrast enhancement (*long arrows*) and sliver of effusion (*short arrows*) (score 1) in a 16-year-old girl. **e, f** Moderate synovial thickening with moderately increased post-contrast enhancement (*long arrows*) and mild effusion (*short arrows*) (score 2) in a 15-year-old boy. **g, h** Severe synovial thickening and increased post-contrast enhancement, more evident at the medial aspect of the joint (*long arrows*), with mild/moderate effusion (*short arrows*) (score 3) in a 17-year-old girl

low signal intensity on T1-W images and was assessed in the femoral head based on the proportion of bone involved (volume) (Fig. 3), in the acetabulum (measured subjectively) and in the femoral neck as absent or present (0/1).

Structural joint damage

Structural joint damage was evaluated on the 3-D TSE T1-W images, using fluid-sensitive and post-contrast images when appropriate. The following features were evaluated and scored:

1. Erosion (defined as a bony depression seen on at least two planes) in the femoral head based on the proportion of head volume involved, in the femoral neck as absent or present (0/1) and in the acetabulum (Fig. 4). Active erosions (defined as an erosion filled with enhancing pannus) were scored in the femoral head (Fig. 5).
2. Flattening of the femoral head was assessed in the coronal plane (mid-section) compared to what is expected for age, first subjectively and thereafter using a Mose circle. Bone cysts were described as sharply delineated, enhancing lesions with high signal on fluid-sensitive sequences and were scored as absent/present in three locations (femoral head, neck and acetabulum).

Cartilage damage

Based on 3-D GRE T1-W sequences, we assessed the joint cartilage width superiorly (mid-weight-bearing area), first judging it subjectively to be normal, mildly, moderately or severely narrowed and then taking measurements in millimeters. We also evaluated and scored cartilage in terms of signal abnormalities and morphological changes, as well as symmetry (right versus left joint space width). Based on the coronal T1-W sequences, we measured femoral neck width (in mm), femoral head/neck length (in mm), caput–collum–diaphyseal (CCD) angle and trochanteric femoral head distance (in mm). We also evaluated whether the physis was patent; the presence of coxa magna, coxa brevis or protrusio acetabuli; and the presence of fovea enlargement. Finally, we evaluated the presence of osteophytes and sclerosis on both coronal T1-W and fluid-sensitive FS sequences.

Statistical analysis

Continuous data are presented as means (±standard deviation [SD]), ordinal data as medians (ranges) and dichotomous data as proportions. We analyzed intra- and interobserver agreement using a simple or a weighted (linear) Cohen kappa coefficient with 95% confidence interval. A kappa score of <0.2 was considered poor, 0.21–0.40 fair, 0.41–0.60 moderate, 0.61–0.80 good and 0.81–1.00 very good [21]. We analyzed differences in measurements using 95% limits of agreement (termed repeatability coefficient, when used for repeat measurements) as per Bland–Altman. Bland–Altman plots are generally interpreted informally and a clinically acceptable agreement was set at 15% [22]. A significance level of 0.05 was decided a priori and all the reported *P*-values are two-tailed. Statistical analyses were performed using SPSS Statistics, version 27 (IBM, Armonk, NY).

Results

We included 60 MRIs from 60 children and young adults with JIA (35 female) and confirmed or suspected hip involvement, with a mean age 14.9 years (range 5.5–20 years). Of these, 23 had oligoarticular JIA (18 oligoarticular-extended and 5 oligoarticular-persistent), 17 had the polyarticular JIA subtype, 8 had enthesitis-related arthritis, 10 systemic JIA, 1 psoriatic JIA and 1 undifferentiated JIA. The mean disease duration at the time of the MRI was 8.6 years (range 0.2–18 years). The distribution of changes seen for the right hip is shown in Fig. 6.

Table 1 shows the agreement within and between readers for the assessment and grading of inflammatory and structural JIA changes as examined on MRI for right and left hips, separately.

Inflammatory domain

There was a good intra- and interobserver agreement (with a kappa value of 0.7 and 0.6, respectively) for grading overall impression of inflammation on a 0–3 scale (effusion included). Similarly, grading overall impression of inflammation, omitting effusion, performed well, with an intraobserver kappa of 0.7–0.8 and an interobserver kappa of 0.4 (Table 1).

Grading synovial enhancement performed best on a 0–2 scale, with a good intraobserver and a moderate interobserver agreement (kappa of 0.7–0.8 and 0.4–0.5, respectively). The intraobserver agreement for subjective evaluation of synovial thickening was good to very good (kappa of 0.8–0.9) while the interobserver agreement was moderate (0.4–0.5) (Table 1).

There was good intraobserver agreement for grading effusion with kappas of 0.6–0.7, while the interobserver agreement for the same variable was fair (kappa 0.3–0.4). Regarding bone marrow edema, the intraobserver agreement

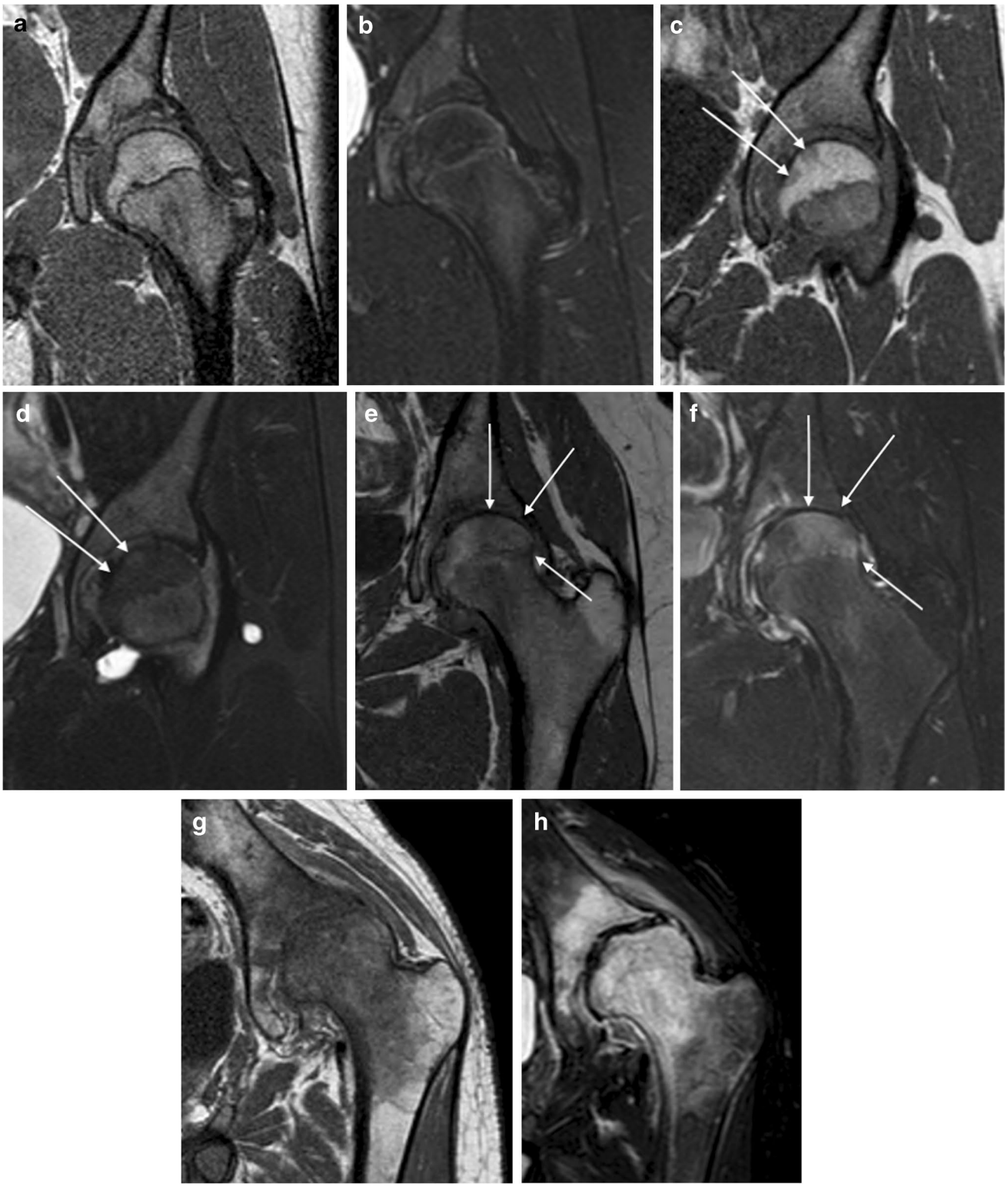

Fig. 3 Femoral head bone marrow edema demonstrated on MRI of the left hip in four pairs of images from four children with juvenile idiopathic arthritis (JIA) across different severity levels. Bone marrow edema was defined as hypointense areas on T1-W sequences with corresponding hyperintense areas on fat-saturated T2-W sequences in the bone marrow. All images are demonstrated using coronal three-dimensional (3-D) T1-weighted turbo spin-echo (**a, c, e, g**) and fat-saturated T2-weighted turbo spin echo (**b, d, f, h**) MRI sequences. **a, b** No visible bone marrow edema (score 0) in a 13-year-old boy. **c, d** Two focal areas of bone marrow edema (less than 33% of the bone volume, *arrows*) (score 1) in a 11-year-old girl. **e, g** Large area of bone marrow edema (between 33 and 66% of the bone volume, *arrows*) (score 2) in a 14-year-old girl. **g, h** Widespread bone marrow edema (almost 100% of the bone volume) (score 3) in a 15-year-old boy

Fig. 4 Erosions demonstrated on MRI at the left acetabulum as shown on coronal three-dimensional (3-D) T1-weighted turbo spin-echo sequences in patients with juvenile idiopathic arthritis (JIA). **a** No visible acetabular erosions (score 0) in a 20-year-old woman. **b** Some erosions on the superior aspect of the acetabulum (< 33% of the surface, *arrows*) (score 1) in a 18-year-old man. **c** Multiple acetabular erosions (between 34% and 66% of the surface, *arrows*) (score 2) in a 13-year-old boy. **d** Erosive changes of the whole acetabular surface (*arrows*) (score 3) in a 19-year-old woman with complete destruction of the femoral head (*arrows*)

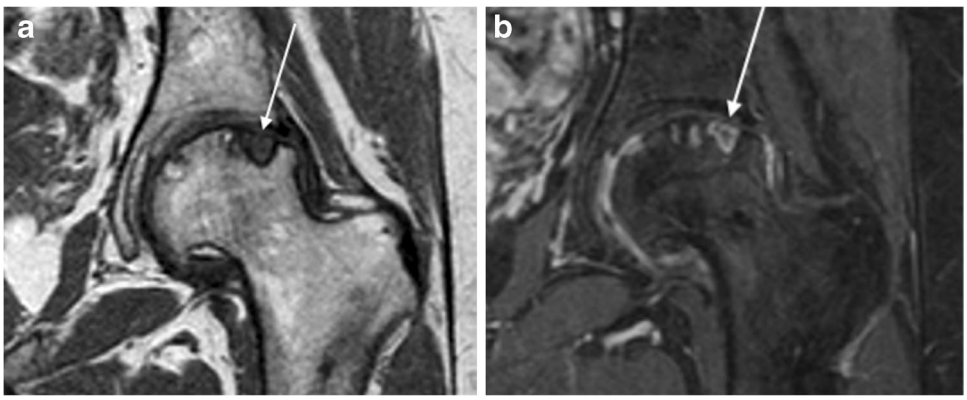

Fig. 5 Left-hip MRI of active erosion in an 18-year-old woman with juvenile idiopathic arthritis (JIA). **a, b** Coronal three-dimensional (3-D) T1-weighted turbo spin-echo (**a**) and post-contrast 3-D gradient echo with fat saturation (**b**). These images show an active erosion (erosion filled with enhancing pannus) (*arrows*)

was good, with a kappa value 0.7 for all locations bilaterally (femoral epiphysis, acetabulum and femoral neck); however, the interobserver kappa values were poor, ranging between 0.2 and 0.4 (Table 1).

Structural damage domain

There was a good intra- and interobserver agreement for grading erosions in the acetabulum on a 0–3 scale, with kappa values of 0.6–0.7 and 0.6, respectively. Regarding the grading

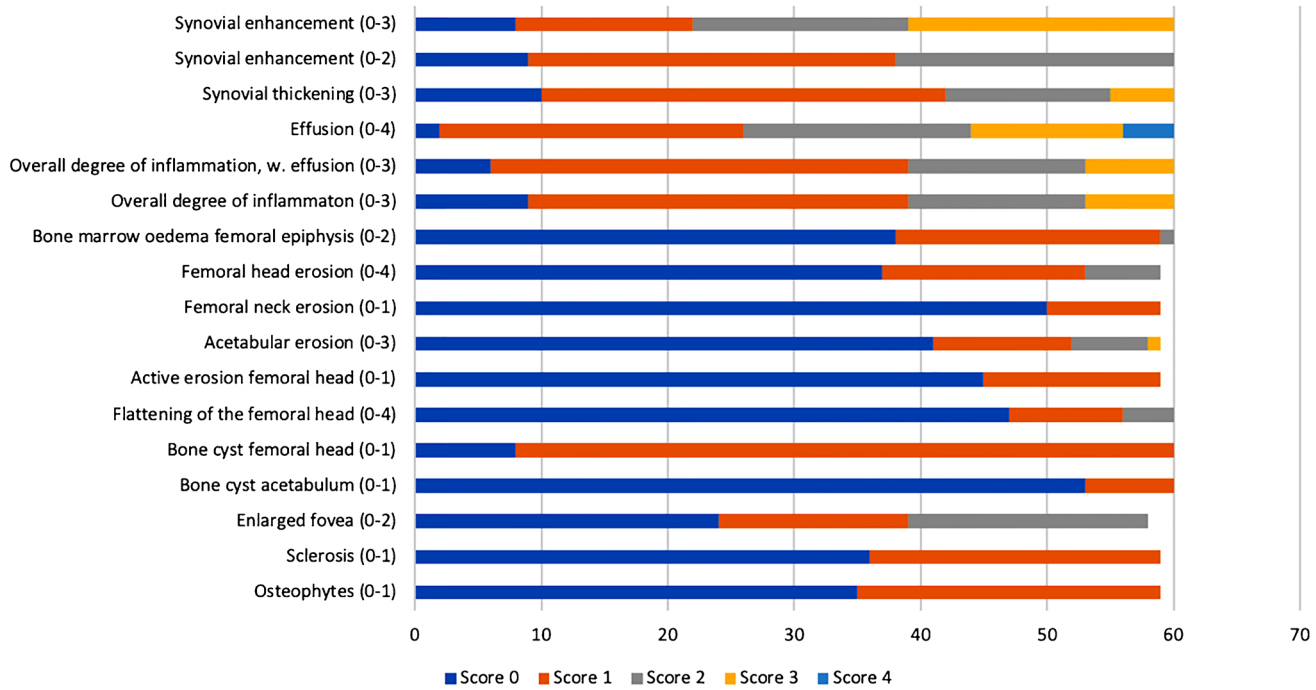

Fig. 6 Distribution of MRI scores for the various features assessed in 60 children through young adults with juvenile idiopathic arthritis (JIA) in this study (right hip, observer 1, second reading). The x-axis shows the number of examined hips

of femoral head erosions, the intraobserver agreement was highly satisfactory (kappa values of 0.7–0.8), while the interobserver agreememt was moderate (kappa 0.4–0.5) (Table 1).

There was an excellent intraobserver agreement for grading active erosions of the femoral head, with kappa values of 0.9 and the interobserver agreement was good with a kappa of 0.6. The kappa values for the femoral head flattening with or without the use of a Mose circle performed well for the same observer (kappa value of 0.7 for the right hip and 0.6 for the left hip), while agreement was significantly lower between observers (0.3–0.4).

There was only one cyst in the femoral neck, thus we could not estimate a kappa value.

The agreement for bone cyst on the femoral head and acetabulum, enlarged fovea, sclerosis and osteophytes is listed in Table 1.

Measurement of joint space width evaluated in millimeters performed poorly, with wide 95% limits of agreement (LOA) ranging from –1.6 to 2.0 mm for the intraobserver and from –2.7 to 3.3 mm for the interobserver values, corresponding to 129% and 214% of the mean value, respectively (Table 2). Kappa values for the subjective assessment of joint cartilage width on a 0–3 scale were good, ranging from 0.6 to 0.7 for the same observer, while the interobserver agreement was poor, with a kappa value of 0.2. The agreement for signal abnormalities/morphological changes on a 0–4 scale was fair (kappa values of 0.3–0.4) (Table 1).

Markers for the assessment of growth

Measurements of the CCD, femoral head–neck length, femoral neck width and trochanteric femoral head distance were imprecise, with a wide 95% LOA (Table 2).

Discussion

This study is part of a larger project to establish MRI markers for active and chronic disease in children, adolescents and young adults with JIA with hip involvement. In this substudy we tested numerous markers (isolated and in combination) to identify those that are sufficiently robust to be included in a future MRI scoring system. The study is novel in that it provides the precision of various MR imaging biomarkers for both inflammatory and chronic changes in children and adolescents with JIA-related hip involvement. One previous paper addressed the accuracy of a simplified MR score for assessing active changes, reporting a variable intraobserver agreement across both observers and parameters, ranging from poor to excellent, while the interobserver

Table 1 Test–retest analysis of features used to describe inflammatory and chronic changes on MRI in 60 children through young adults (35 females) ages 6–20 years with juvenile idiopathic arthritis and hip involvement

Type of damage	Right hip		Left hip	
	Intra-reader kappa (95% CI)	Inter-reader kappa (95% CI)	Intra-reader kappa (95% CI)	Inter-reader kappa (95% CI)
Inflammatory domain				
Synovial enhancement (0–3)	0.7 (0.6–0.9)	0.3 (0.2–0.4)	0.7 (0.5–0.8)	0.4 (0.2–0.5)
Synovial enhancement (0–2)	0.8 (0.6–0.9)	0.4 (0.2–0.6)	0.7 (0.5–0.8)	0.5 (0.3–0.7)
Synovial enhancement (0–1)	0.7 (0.4–1.0)	0.2 (–0.1–0.5)	0.5 (0.0–0.9)	0.1 (–0.2–0.5)
Synovial thickening subjective (0–3)	0.9 (0.8–1.0)	0.5 (0.3– 0.7)	0.8 (0.6– 0.9)	0.4 (0.2–0.6)
Effusion (0–4)	0.6 (0.4–0.8)	0.4 (0.2–0.6)	0.7 (0.5–0.8)	0.3 (0.2–0.4)
Overall synovial inflammation (0–3)	0.8 (0.6–1.0)	0.4 (0.2–0.6)	0.7 (0.5–0.9)	0.4 (0.3–0.6)
Overall degree of inflammation, including effusion (0–3)	0.7 (0.5–0.9)	0.6 (0.4–0.7)	0.7 (0.5–0.9)	0.6 (0.4–0.7)
Bone marrow edema				
Femoral epiphysis (0–2)	0.7 (0.5–0.9)	0.4 (0.1–0.6)	0.7 (0.5–0.9)	0.3 (0.1–0.6)
Acetabulum (0–1)	0.7 (0.6–0.9)	0.2 (0.0–0.4)	0.7 (0.5–0.9)	0.3 (0.1–0.4)
Femoral neck (0–1)	0.7 (0.5–0.9)	0.3 (0.0–0.5)	0.7 (0.6–0.9)	0.3 (0.0–0.5)
Structural bone damage domain				
Erosion				
Femoral head (0–3)	0.7 (0.5–0.9)	0.4 (0.2–0.6)	0.8 (0.6–0.9)	0.5 (0.3–0.7)
Femoral neck (0–1)	0.8 (0.5–1.0)	0.2 (0.1–0.6)	0.7 (0.5–0.9)	0.1 (0.1–0.4)
Acetabulum (0–3)	0.6 (0.4–0.8)	0.6 (0.4–0.8)	0.7 (0.5–0.8)	0.6 (0.4–0.8)
Acetabulum (0–2)	0.6 (0.4–1.0)	0.3 (0.1–0.5)	0.7 (0.5–0.8)	0.4 (0.2–0.6)
Active erosion femoral head (0–1)	0.9 (0.8–1.0)	0.6 (0.3–0.9)	0.9 (0.7–1.0)	0.6 (0.4–0.9)
Flattening of the femoral head[a] (0–4)	0.7 (0.5–0.9)	0.4 (0.2–0.6)	0.6 (0.4–0.8)	0.3 (0.1–0.5)
Flattening femoral head Mose[b] (0–4)	0.7 (0.5–0.9)	0.3 (0.1–0.5)	0.6 (0.4–0.8)	0.3 (0.1–0.5)
Bone cyst (0–1)				
Femoral head	0.9 (0.6–1.0)	0.7 (0.4–1.0)	0.8 (0.6–1.0)	0.7 (0.5–1.0)
Acetabulum	0.8 (0.5–1.0)	0.3 (0.0–0.7)	0.8 (0.5–1.0)	0.6 (0.3–0.9)
Enlarged fovea (0–2)	0.7 (0.6–0.9)	–0.1 (0.2–0.1)	0.8 (0.6–0.9)	0.1 (0.1–0.2)
Sclerosis (0–1)	0.8 (0.6–0.9)	0.1 (0.1–0.2)	0.8 (0.7–1.0)	0.1 (0.0–0.2)
Osteophytes (0–1)	0.9 (0.8–1.0)	0.0 (0.0–0.2)	0.9 (0.8–1.0)	0.2 (0.0–0.4)
Joint space width (0–3)	0.7 (0.6–0.9)	0.2 (0.0–0.4)	0.6 (0.5–0.8)	0.2 (0.1–0.4)
Cartilage changes (0–4)	0.4 (0.3–0.6)	0.3 (0.1–0.4)	0.4 (0.2–0.6)	0.3 (0.1–0.4)

CI confidence interval

[a]Flattening of femoral head as assessed subjectively

[b]Flattening of femoral head as assessed using a Mose circle

Table 2 Test–retest analysis of features used in evaluation of growth changes on MRI in 60 children with juvenile idiopathic arthritis and hip involvement (right hip)

Markers for assessment of growth	OBS 1		Intraobserver (OBS1) (1st vs. 2nd measurement)		OBS 2	Interobserver (OBS 1 vs. OBS 2)	
	1st mean (SD)	2nd mean (SD)	Mean diff. (SD)	95% LOA	Mean (SD)	Mean diff. (SD)	95% LOA
Femoral neck width, mm	29.0 (14.9)	25.0 (4.2)	4.4 (14.6)	–24.8 to 33.6	28.2 (8.4)	3.8 (7.5)	–11.2 to 18.8
Femoral head/neck length, mm	72.3 (19.6)	76.3 (13.6)	3.1 (14.4)	–25.7 to 31.9	26.4 (5.4)	3.8 (7.5)	–11.2 to 18.8
CCD angle, degrees	132.0 (7.5)	131.1 (8.6)	0.5 (6.8)	–13.1 to 14.1	132.9 (5.5)	1.5 (8.3)	–15.1 to 18.1
TFHD, mm	18.4 (5.8)	18.3 (5.9)	0.1 (2.8)	–5.5 to 5.7	22.6 (11.0)	0.1 (2.8)	–3.5 to 5.7
Joint space width, mm	2.8 (1.3)	3.0 (1.5)	0.2 (0.9)	–1.6 to 2.0	3.3 (1.3)	0.3 (1.5)	– 2.7 to 3.3

CCD caput–collum–diaphyseal angle, *diff.* difference, *LOA* limits of agreement, *OBS* observer, *SD* standard deviation, *TFHD* trochanteric–femoral head distance

agreement was consistently moderate for effusion and marrow edema and less satisfactory for other parameters [14].

We have identified a set of MRI markers for hip involvement in children and adolescents with JIA. The more precise inflammatory markers include overall degree of inflammation on a 0–3 scale, synovial enhancement on a 0–2 scale and active erosions on a 0–1 scale, while assessment of bone marrow edema performed well for the same-observer only. For structural bone damage, grading of femoral head and acetabular erosions performed well. Direct measurements were imprecise.

Surprisingly, our study showed that grading of synovial enhancement on a 0–1 scale performed poorer than grading based on 0–2 and 0–3 scales. This is most likely a result of the difficulties in setting a precise cut-off between physiological synovial enhancement and mildly increased enhancement suggestive of synovial inflammation. In contrast to the study by Porter-Young et al. [14], in our population very few cases were scored as non-enhancing, thus yielding a skewed dataset for the kappa analysis. Indeed, the lack of a precise cut-off is a diagnostic challenge in that it can lead to both overdiagnosis with unnecessary treatment, and underdiagnosis with an increased risk of structural damage and poorer long-term outcome. This underscores the need for prospective studies establishing reference standards across ages.

Another challenge in grading synovial enhancement is timing of the post-contrast images. Previous studies have shown that timing strongly influences the degree of synovial enhancement in the assessment of both wrists [23] and knees [24]. Despite the increasing use of MRI in arthritis, there is no consensus on the exact timing for post-contrast images, the suggested interval being within 5 min [25]. The rationale behind early post-contrast images is that, if acquisition is delayed too long, contrast washout from the synovium into the joint fluid obscures the borders between synovium and an effusion, as was demonstrated in two studies of patients with rheumatoid arthritis [26, 27]. Thus, a standardized protocol is crucial for follow-up of known pathology, and also for clinical trials across institutions. In the present study, we acquired post-contrast sequences approximately 5 min after the contrast injection.

Regarding bone marrow edema, despite good intraobserver agreement, the interobserver agreement was disappointing and not in line with a previous study on wrist MRI [28]. We speculate that the size and shape of the scored volumes might play a role because carpal bones are significantly smaller than hips, thus fewer slices are included for assessment.

We have possible explanations for the unsatisfactory interobserver agreement for some of the other features. Among the structural damage markers, we believe that the agreement for cartilage lesions was poor for two main reasons. First, the acetabular and femoral layer of articular cartilage is very thin in the hip joint and it is extremely difficult to reliably distinguish between partial- and full-thickness lesions. Second, in the growing child the cartilage becomes thinner with time, thus it is challenging to differentiate the physiological thickness reduction caused by growth from the presence of pathological erosions. Future studies comparing our data with the MRI data obtained from healthy children could help elucidate this matter. Moreover, osteophytes were present only in few patients, and this might have affected the suboptimal results.

Last, further calibrations could improve the inter-reader reliability. The poor results for direct measurements as the CCD, femoral neck–head length, femoral width and trochanteric distance were expected and in line with previous studies [29].

Of note is the excellent agreement for assessing active erosions, both within and between observers. Moreover, the assessment of acetabular erosions was precise, as was the assessment of femoral head and neck erosions for the same reader. Whether MRI might replace conventional radiographs, however, remains to be addressed.

Our study has some limitations. First, there is the subjective nature of any MRI scoring system, with differences in measurements and inherent biases caused by different radiologists' experience and understanding of the factors required to score, although we tried to alleviate this with calibration sessions and the use of an imaging atlas. Moreover, some of the features evaluated in our scoring system were extremely rare (i.e. cyst on femoral neck, coxa brevis), thus it was not possible to assess the agreement for those variables.

The strengths of the study are large sample size covering a wide spectrum of pathological changes, within both the inflammatory and the bone damage domains. Furthermore, we used state-of-the-art MRI protocols across two centers, both including intravenous contrast agent, and our scan parameters were selected to provide the best images within a reasonably short scan time. Last, we performed meticulous calibration sessions prior to the scoring sessions, preceded by a pilot study and an atlas, to ensure that readers could interpret imaging findings in a consistent manner.

In a next paper we plan to complete the validation process of the present MRI scoring system by testing its clinical validity and responsiveness to change, aiming to present a final MRI scoring system to be used as a primary outcome measure in clinical trials with the purpose of evaluating the efficacy of novel antirheumatic drugs for JIA similar to that already established for rheumatoid arthritis (RA) in adults [30–33]. Once obtained, this scoring system might be usefully employed in several settings in JIA patients. Particularly, it could be used prior to therapy to identify children who need more aggressive treatment and during the pharmacological treatment to monitor its efficacy and to assess more accurately their remission status. Moreover, it has been recently reported that persistent synovitis on hip MRI in children with JIA in clinical remission predicts disease flare

[34]. Therefore, our scoring system could be extremely helpful in children in clinical remission where the depiction of a silent synovitis on MRI might allow prompt treatment with a possible considerable improvement of disease progression.

Conclusion

This work is a first step toward establishing a valid MRI scoring system for JIA-related hip changes. Several of the MRI markers for both active and chronic changes showed a high reproducibility, the most interesting being the overall synovial inflammation and the evaluation of active erosions. We suggest that the more robust variables be used in future studies assessing clinical validity, responsiveness to change and long-term patient outcomes.

Supplementary Information The online version contains supplementary material available at https://doi.org/10.1007/s00247-022-05502-8.

Funding Open access funding provided by UiT The Arctic University of Norway (incl University Hospital of North Norway).

Declarations

Conflicts of interest None

References

1. Ravelli A, Martini A (2007) Juvenile idiopathic arthritis. Lancet 369:767–778
2. Thierry S, Fautrel B, Lemelle I, Guillemin F (2014) Prevalence and incidence of juvenile idiopathic arthritis: a systematic review. Joint Bone Spine 81:112–117
3. Rostom S, Amine B, Bensabbah R et al (2008) Hip involvement in juvenile idiopathic arthritis. Clin Rheumatol 27:791–794
4. Fantini F, Corradi A, Gerloni V et al (1997) The natural history of hip involvement in juvenile rheumatoid arthritis: a radiological and magnetic resonance imaging follow-up study. Rev Rhum Engl Ed 64:173S–178S
5. Packham JC, Hall MA (2002) Long-term follow-up of 246 adults with juvenile idiopathic arthritis: functional outcome. Rheumatology 41:1428–1435
6. Wallace CA, Giannini EH, Spalding SJ et al (2012) Trial of early aggressive therapy in polyarticular juvenile idiopathic arthritis. Arthritis Rheum 64:2012–2021
7. Zhao Y, Wallace C (2014) Judicious use of biologicals in juvenile idiopathic arthritis. Curr Rheumatol Rep 16:454
8. Ong MS, Ringold S, Kimura Y et al (2021) Improved disease course associated with early initiation of biologics in polyarticular juvenile idiopathic arthritis: trajectory analysis of a childhood arthritis and rheumatology Research Alliance Consensus Treatment Plans Study. Arthritis Rheumatol 73:1910–1920
9. Baildam E (2012) A commentary on TREAT: the trial of early aggressive drug therapy in juvenile idiopathic arthritis. BMC Med 10:59
10. Jaremko JL, Lambert RGW, Pedersen SJ et al (2019) OMERACT Hip Inflammation Magnetic Resonance Imaging Scoring System (HIMRISS) assessment in longitudinal study. J Rheumatol 46:1239–1242
11. Maksymowych WP, Cibere J, Loeuille D et al (2014) Preliminary validation of 2 magnetic resonance image scoring systems for osteoarthritis of the hip according to the OMERACT filter. J Rheumatol 41:370–378
12. Argyropoulou MI, Fanis SL, Xenakis T et al (2002) The role of MRI in the evaluation of hip joint disease in clinical subtypes of juvenile idiopathic arthritis. Br J Radiol 75:229–233
13. Nistala K, Babar J, Johnson K et al (2007) Clinical assessment and core outcome variables are poor predictors of hip arthritis diagnosed by MRI in juvenile idiopathic arthritis. Rheumatology 46:699–702
14. Porter-Young FM, Offiah AC, Broadley P et al (2018) Inter- and intra-observer reliability of contrast-enhanced magnetic resonance imaging parameters in children with suspected juvenile idiopathic arthritis of the hip. Pediatr Radiol 48:1891–1900
15. Kirkhus E, Flatø B, Riise O et al (2011) Differences in MRI findings between subgroups of recent-onset childhood arthritis. Pediatr Radiol 41:432–440
16. Abd El-Azeem MI, Taha HA, El-Sherif AM (2012) Role of MRI in evaluation of hip joint involvement in juvenile idiopathic arthritis. Egypt Rheumatol 34:75–82
17. Hemke R, Herregods N, Jaremko JL et al (2020) Imaging assessment of children presenting with suspected or known juvenile idiopathic arthritis: ESSR-ESPR points to consider. Eur Radiol 30:5237–5249
18. Ostrowska M, Gietka P, Mańczak M et al (2021) MRI findings in hip in juvenile idiopathic arthritis. J Clin Med 10:5252
19. Panwar J, Tolend M, Redd B et al (2021) Consensus-driven conceptual development of a standardized whole body-MRI scoring system for assessment of disease activity in juvenile idiopathic arthritis: MRI in JIA OMERACT Working Group. Semin Arthritis Rheum 51:1350–1359
20. Petty RE, Southwood TR, Manners P et al (2004) International League of Associations for Rheumatology classification of juvenile idiopathic arthritis: second revision, Edmonton, 2001. J Rheumatol 31:390–392
21. Landis JR, Koch GG (1977) The measurement of observer agreement for categorical data. Biometrics 33:159–174
22. Bland JM, Altman DG (1986) Statistical methods for assessing agreement between two methods of clinical measurement. Lancet 1:307–310
23. Rieter JF, de Horatio LT, Nusman CM et al (2016) The many shades of enhancement: timing of post-gadolinium images strongly influences the scoring of juvenile idiopathic arthritis wrist involvement on MRI. Pediatr Radiol 46:1562–1567
24. Barendregt AM, van Gulik EC, Groot PFC et al (2019) Prolonged time between intravenous contrast administration and image acquisition results in increased synovial thickness at magnetic

resonance imaging in patients with juvenile idiopathic arthritis. Pediatr Radiol 49:638–645
25. Hemke R, Tzaribachev N, Nusman CM et al (2017) Magnetic resonance imaging (MRI) of the knee as an outcome measure in juvenile idiopathic arthritis: an OMERACT reliability study on MRI scales. J Rheumatol 44:1224–1230
26. Østergaard M, Klarlund M (2001) Importance of timing of post-contrast MRI in rheumatoid arthritis: what happens during the first 60 minutes after IV gadolinium-DTPA? Ann Rheum Dis 60:1050–1054
27. Yamato M, Tamai K, Yamaguchi T, Ohno W (1993) MRI of the knee in rheumatoid arthritis: Gd-DTPA perfusion dynamics. J Comput Assist Tomogr 17:781–785
28. Tanturri de Horatio L, Damasio MB, Barbuti D et al (2012) MRI assessment of bone marrow in children with juvenile idiopathic arthritis: intra- and inter-observer variability. Pediatr Radiol 42:714–720
29. Shelmerdine SC, Di Paolo PL, Rieter JFMM et al (2018) A novel radiographic scoring system for growth abnormalities and structural change in children with juvenile idiopathic arthritis of the hip. Pediatr Radiol 48:1086–1095
30. Quinn MA, Conaghan PG, O'Connor PJ et al (2005) Very early treatment with infliximab in addition to methotrexate in early, poor-prognosis rheumatoid arthritis reduces magnetic resonance imaging evidence of synovitis and damage, with sustained benefit after infliximab withdrawal: results from a twelve-month randomized, double-blind, placebo-controlled trial. Arthritis Rheum 52:27–35
31. Østergaard M, Duer A, Nielsen H et al (2005) Magnetic resonance imaging for accelerated assessment of drug effect and prediction of subsequent radiographic progression in rheumatoid arthritis: a study of patients receiving combined anakinra and methotrexate treatment. Ann Rheum Dis 64:1503–1506
32. Wells G, Li T, Maxwell L et al (2008) Responsiveness of patient reported outcomes including fatigue, sleep quality, activity limitation, and quality of life following treatment with abatacept for rheumatoid arthritis. Ann Rheum Dis 67:260–265
33. Haavardsholm EA, Østergaard M, Hammer HB et al (2009) Monitoring anti-TNFalpha treatment in rheumatoid arthritis: responsiveness of magnetic resonance imaging and ultrasonography of the dominant wrist joint compared with conventional measures of disease activity and structural damage. Ann Rheum Dis 68:1572–1579
34. Mazzoni M, Pistorio A, Magnaguagno F et al (2021) Predictive value of MRI in patients with juvenile idiopathic arthritis in clinical remission. Arthritis Care Res. https://doi.org/10.1002/acr.24757

Paper 3

Tanturri de Horatio, L., Zadig, P.K., von Brandis, E., Ording Müller, L.S., Rosendahl, K. & Avenarius, D.F.M. (2023).

Whole-body MRI in children and adolescents: can T2-weighted Dixon fat-only images replace standard T1-weighted images in the assessment of bone marrow?

European Journal of Radiology, 166, 110968.

European Journal of Radiology 166 (2023) 110968

Contents lists available at ScienceDirect

European Journal of Radiology

journal homepage: www.elsevier.com/locate/ejrad

Whole-body MRI in children and adolescents: Can T2-weighted Dixon fat-only images replace standard T1-weighted images in the assessment of bone marrow?

Laura Tanturri de Horatio [a,b,*], Pia K. Zadig [a,c], Elisabeth von Brandis [d,e], Lil-Sofie Ording Müller [d], Karen Rosendahl [a,c], Derk F.M. Avenarius [a,c]

[a] Department of Clinical Medicine, UiT, The Arctic University of Norway, 9037, Tromsø, Norway
[b] Department of Pediatric Radiology, Ospedale Pediatrico Bambino Gesù, 00165 Rome, Italy
[c] Department of Radiology, University Hospital of North-Norway, 9038 Tromsø, Norway
[d] Division of Radiology and Nuclear Medicine, Oslo University Hospital, 0372 Oslo, Norway
[e] Faculty of Medicine, Institute of Clinical Medicine, University of Oslo, 0318 Oslo, Norway

ARTICLE INFO

Keywords:
Whole-body MRI
DIXON fat-only
Bone marrow
Children
Adolescents

ABSTRACT

Objective: When performing whole-body MRI for bone marrow assessment in children, optimizing scan time is crucial.
The aim was to compare T2 Dixon fat-only and TSE T1-weighted sequences in the assessment of bone marrow high signal areas seen on T2 Dixon water-only in healthy children and adolescents.
Materials and methods: Whole-body MRIs from 196 healthy children and adolescents aged 6 to 19 years (mean 12.0) were obtained including T2 TSE Dixon and T1 TSE-weighted images. Areas with increased signal on T2 Dixon water-only images were scored using a novel, validated scoring system and classified into "minor" or "major" findings according to size and intensity, where "major" referred to changes easily being misdiagnosed as pathology in a clinical setting. Areas were assessed for low signal on T2 Dixon fat-only images and, after at least three weeks to avoid recall bias, on the T1-weighted sequence by two experienced pediatric radiologists.
Results: 1250 high signal areas were evaluated on T2 Dixon water-only images. In 1159/1250 (92.7%) low signal was seen on both T2 Dixon fat-only and T1-weighted sequences while in 24 (1.9%) it was not present on either sequence, with an absolute agreement of 94.6%. Discordant findings were found in 67 areas, of which in 18 (1.5%) low signal was visible on T1-weighted images alone and in 49 (3.9%) on T2 Dixon fat-only alone. The overall kappa value between the two sequences was 0.39. The agreement was higher for major as compared to minor findings (kappa values of 0.69 and 0.29, respectively) and higher for the older age groups.
Conclusion: T2 Dixon fat-only can replace T1-weighted sequence on whole-body MRI for bone marrow assessment in children over the age of nine, thus reducing scan time.

1. Introduction

Whole-body MRI has become an important imaging method for the evaluation of bone marrow, enabling detection and in part characterization of a variety of both malignant and non-malignant diseases in adults as well as in children [1–5]. The examination is relatively time consuming, depending on the number and type of sequences performed, and by the anatomy included. Since some children, particularly the youngest, struggle to lie still for the entire exam duration, either because of their age or their medical condition or both, optimizing scan time is important to reduce anxiety in the child and achieve examination of good quality, less affected by motion artifacts. This is especially true for children who undergo frequent follow-ups to monitor the disease progression.

To date, standardized and validated whole-body MRI protocols in children and adolescents are lacking. In a recent systematic review, a significant variation as to body coverage, sequences and technical settings used was found [6]; among the fat-suppressed fluid-sensitive

Abbreviations: **STIR**, short inversion time inversion recovery; **CHESS**, chemical shift-selective fat saturation; **SNR**, signal-to-noise ratio; **TSE**, Turbo Spin Echo.

* Corresponding author at: Piazza S. Onofrio, 4, 00165 Rome, Italy.
E-mail address: laura.tanturri@opbg.net (L. Tanturri de Horatio).

https://doi.org/10.1016/j.ejrad.2023.110968
Received 12 May 2023; Received in revised form 26 June 2023; Accepted 7 July 2023
Available online 8 July 2023

sequences, the majority used a short time inversion recovery (STIR) often followed by a coronal T1-weighted sequence. Only one study [7] mentioned the T2-weighted Dixon. This sequence, as opposed to STIR, generates a set of four image reconstructions in a single acquisition: in-phase (equivalent to standard non-fat-suppressed images) and out-of-phase, fat-only (for fat quantification) and water-only (equivalent to fat-suppressed) (Fig. 1) [8].

In adult musculoskeletal imaging, Dixon T2-weighted water-only images are increasingly being used to provide fat-suppressed, fluid sensitive images [8–10]. The chemical shift based, water-fat separation is a robust fat suppression technique compared to alternative fat-suppression such as chemical shift-selective fat saturation (CHESS) and has a relatively higher signal-to-noise ratio (SNR) compared to STIR [11]. Further, the generation of fat-only images in the same acquisition has fueled an interest in the potential of T2 Dixon to replace T1-weighted Turbo Spin Echo (TSE) images for the assessment of bone marrow involvement in adults [12–16].

As for children and adolescents, to the best of our knowledge, no study exists comparing T2 Dixon fat-only and T1-weighted TSE images. The two sequences are fundamentally different. While T1-weighted TSE images are composed of signals from fat due to its low T1-value, the images also contain some signal from water-containing tissues. Conversely, fat-only Dixon images are reconstructed from the T2-weighted out-of-phase and in-phase images, without residual water signal. In theory, this might influence the appearance of water containing red bone marrow compared to yellow bone marrow across age groups.

In two previous studies we have demonstrated that healthy children have a wide range of signal intensity in the bone marrow on whole-body MRI [17,18]. In the present study we aimed to compare the signal on T2 Dixon fat-only and T1-weighted TSE sequences in areas where high signal was seen on T2 Dixon water-only in a cohort of healthy children and adolescents undergoing whole-body MRI. This will indicate if the use of T2 Dixon sequence can replace T1-weighted TSE images in a whole-body protocol, hence reduce scan time.

2. Methods

2.1. Study population

The present study is part of a prospective study performed during 2018–2020, including 196 healthy children and adolescents aged 6–19 years [17–20]. All had a whole-body 1.5 T MRI performed for research purposes only, at the Department of Radiology of Oslo University Hospital or University Hospital Northern-Norway. The participants were recruited via mail, announcements on social media or direct invitation, and included if there were no contraindications to MRI, a history of cancer, current infection, chronic or systemic disease, metabolic or musculoskeletal disorder, or a symptomatic trauma within the past four weeks. None of the participating individuals reported disease or symptoms from the musculoskeletal system when contacted within 18 months after the first examination.

For this sub-study we included baseline whole-body MRIs from all 196 individuals. The demographic details on the healthy pediatric cohort compared to the general population are reported in Table 1.

The study was approved by the Regional Ethics Committee (REK; no 2016/1696), and written informed consent was obtained from each participant and/or a caregiver according to national guidelines.

2.2. Whole-body MRI acquisition

The whole-body MRIs were performed during free breathing, using phased array surface coils and a 1.5 T MRI scanner (Philips medical systems, Best the Netherlands, Intera model release 2.3 (n = 118) or Magnetom Siemens Aera, software e11c (n = 78)). Coronal T2-weighted Dixon and T1-weighted sequences were acquired from the skull-base to toes in 3–5 steps. In 77/118 children and adolescents studied with the Philips scanner the STIR sequence was also performed. The scan parameters including scan time are shown in Table 2.

During the examination the child could either listen to music or watch a movie, and total scan time was approximately 30–45 min.

Table 1
Demographic details on the healthy pediatric cohort compared to the general population.

Variables	Study subjects, n = 196	Data from Statistics Norway*
Oslo University Hospital / University Hospital North Norway, n (%)	78 (39.8%) / 118 (60.2%)	–
Female, n (%)	101 (51.5%)	374,152 (48.8%)**
Age, years (range)Group 1 (n = 47)Group 2 (n = 52)Group 3 (n = 47)Group 4 (n = 50)	12.0 (6.0 – 18.9) **< 9** **9–11** **12–14** **15–19**	(6.0–15.0)
Median BMI, kg/m2 (range)	18 (13–30)	18 (-)
Sports-activity at least once a week, n (%)	167 (85%)	(84% – 89%)

* Statistics Norway, Helseforhold, levekårsundersøkelsen. Statistisk Sentralbyrå, statistikkbanken. https://www.ssb.no/statbank/table/06658. Accessed 24. May 2021.
** https://www.ssb.no/a/barnogunge/2020/tabeller/befolkning/bef0000.html. Age 6–17. Accessed 01. May 2022.

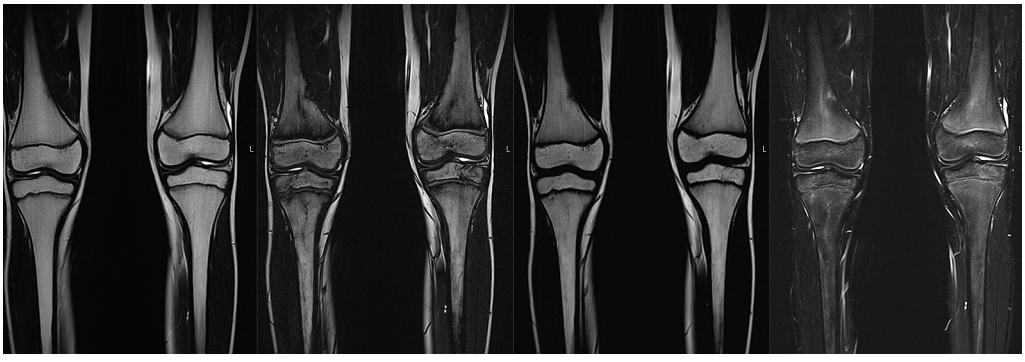

Fig. 1. Knee MRI of a healthy 12 year-old boy. T2 Dixon sequence with all four image reconstructions (a. in phase, b. out of phase, c. fat-only, d. water-only).

Table 2
Basic MRI parameters for the whole-body 1.5 T MRI. T2-weighted Dixon, T1-weighted TSE and STIR sequences (for Philips scanner in the upper table, for Siemens in the lower). TSE = Turbo Spin Echo, TR = Repetition Time, TE = Time to Echo, NSA = Number of Signal Averages.

Sequence	TR (ms)	TE (ms)	NSA	Slice thickness (mm)	Readout band width (Hz per pixel)	Acquired voxel size (mm)	Scan time (min)
Coronal T1-w TSE	450	5.1	1	3.5	391	0.9x0.9x3.5	1:48
Coronal T2-w Dixon fat-only	5156	100	1	3.5	293	0.9x0.9x3.5	3:16
STIR	3500	80	1	3.5	312	0.9x0.9x3.5	3:16
Sequence	TR (ms)	TE (ms)	NSA	Slice thickness (mm)	Readout band width (Hz per pixel)	Acquired voxel size (mm)	Scan time (min)
Coronal T1-w TSE	467	7.6	1	3.5	303	0.9x0.9x3.5	1:30–2:00
Coronal T2-w Dixon fat-only	5640	109	1	3.5	521	0.9x0.9x3.5	2:30–3:00

2.3. Image analysis

For the current study we employed a whole-body MRI child-specific scoring system for bone marrow assessment recently devised and validated using coronal T2 Dixon water-only images [20]. According to this scoring system, signal intensity was graded on a 0–2 scale, where 0 = absent, 1 = mildly increased, and 2 = moderate increased up to fluid-like signal and extension on a 1–4 scale, where 1 = very small lesion (<5%), 2 = involvement of up to 1/3 of the entire bone length, 3 = involvement of up to 2/3 of the entire bone length, 4 = involvement of up to the entire bone length. Based on intensity and extension, all the focal high signal intensity areas were scored and classified as "major" or "minor" findings, except for the hands, where only intensity was recorded (Table 3) [17,18]. High signal intensity areas with a speckled appearance (defined as two or more roundish/punctuated high signals, size 2–5 mm) in the epi-, meta-, or diaphysis of the long tubular bones were excluded from the analysis.

For the present study the whole body was arbitrarily divided into 117 anatomical areas.

Bone marrow high signal areas on T2 Dixon water-only were identified and scored in consensus by two radiologists with 20 and 6 years of experience in pediatric musculoskeletal imaging respectively, according to the abovementioned scoring system. In the event of discrepancies, the consensus was achieved by discussion.

The presence of corresponding low-signal was then assessed (absent/present) on T2 Dixon fat-only images and, in a blinded fashion after at least 3 weeks to avoid recall bias, on T1-weighted TSE images by the same radiologists. All readings were performed on a high-resolution Sectra viewing system (IDS7 PACS) and optimized room-light settings.

When high signal areas on T2-Dixon water-only images were not visible as low signal areas on either T1-weighted or T2 Dixon fat-only sequences, the images were also evaluated on T2 Dixon out-of-phase as visible or not for confirmation of T2-Dixon water-only signal as a true finding. Areas flawed by image artifacts or by too low SNR for image analysis were registered and excluded from further analysis.

2.4. Statistical analysis

Descriptive statistics were reported as numbers with percentages, means with standard deviations or medians with IQRs, where appropriate. To examine for differences according to age using Chi-Square tests, subjects were divided into four age groups (1 = < 9 years, 2 = 9–11 years, 3 = 12–14 years, 4 = 15–19). The agreement between T2 Dixon fat-only and T1 in the detection of low-signal areas was analyzed using kappa statistics (with 95% CI) and percentage absolute agreement. A kappa score of < 0.2 is considered poor, 0.21–0.40 fair, 0.41–0.60 moderate, 0.61–0.80 good and 0.81–1.00 very good [21]. All statistical analyses were performed using Predictive Analytics Software (SPSS) version 28 (IBM, Armonk, NY), and a p-value < 0.05 was considered statistically significant.

Table 3
Subclassification of MRI-findings into minor or major on T2 Dixon water-only images, based on signal intensity on a 0–2 scale and signal extension on a 0–4 scale.

Signal intensity on a 0–2 scale/extension on a 0–4 scale	
Major MRI findings	Signal intensity 1 and extension 3–4 or Signal intensity 2 and extension 2–4
Minor MRI findings	Signal intensity 1 and extension < 3 or Signal intensity 2 and extension < 2

3. Results

196 whole-body examinations from healthy children and adolescents (95 males) from 6 to 19 years of age with a mean of 12.0 years (SD 3.6 years) were included. Each group by age consisted of 47–52 individuals (Table 1). A total of 22.932 body-regions (117 anatomical areas for each patient) were evaluated on T2-Dixon water-only images. 1290 high signal areas were identified, of which 20 were excluded due to suboptimal T2 Dixon fat-only images and 20 due to suboptimal T1-w images, leaving a total of 1250 high signal areas (642 male, 608 female, p=<0.001, Fisher's exact) for the present study.

Among these 1250 high signal areas, 730 were of mildly increased signal intensity while 520 were moderately increased. The majority of high signal areas were seen in the lower limbs (n = 564), pelvis (n = 269) or upper limbs (n = 287). 48 areas were found in the mandibles/spine and 82 in the thoracic cage. The overall kappa value was 0.39 (0.28–0.51) (Table 4).

1191/1250 high signal areas could be classified according to intensity/extension as major or minor findings (355 and 836 respectively). 59 areas were located in the hands.

Of the 1250 high signal areas identified on T2-Dixon water-only, 1159 (92.7%) had corresponding low signal on both the T2 Dixon fat-only and T1 images (Figs. 2 and 3) while 24 (12 major) (1.9%) showed no low-signal on either of the sequences with an absolute agreement of 94.6% (Table 5).

All 24 high signal areas with no corresponding low signal on either of the sequences were visible on the out-of-phase images (Figs. 4 and 5). Their location is given in graphic e-only Table 6. The agreement between the two sequences differed between the age groups (p < 0.001) (Table 7). Excluding children under 9 years of age in the analysis gave a kappa value of 0.44 (0.31–0.56).

67 high signal areas (5.4%) showed no concordance between T1 weighted and T2 Dixon fat-only images. Of these, 49 returned low signal on T2 Dixon fat-only images alone, and 18 on T1-weighted images alone (3.9% and 1.5% of the total, respectively) (Table 5).

The agreement between T2 Dixon fat-only and T1-weighted images was better for "major" findings as compared to "minor" findings, with kappa values of 0.69 (0.51–0.87) and 0.29 (0.15–0.42), respectively. When evaluating intensity alone, the agreement between T2 Dixon fat-only and T1 was similar for both mildly and moderately increased signal intensity, with kappa values of 0.38 (0.25–0.51) and 0.39 (0.17–0.61), respectively.

As for locations, the agreement ranged between 0.51 (0.35–0.68) for lower limbs and −0.01 (-0.03–0.00) for the pelvis (Table 4). Discordance between the two sequences was frequently found in the humeri (12/67 cases, 18%) (Fig. 6) and in the ischiopubic/para-acetabular region (7/67

Table 4
The appearances of high signal areas in the bone marrow on whole-body MRI T2 Dixon fat-only and on T1-weighted TSE sequences, by localization.

		Visibility				Total	
		T1-w TSE only	T2 Dixon fat-only	Both	None		Kappa value (95%CI)
Localization							0.39
	-mandibles/spine	1	6	38	3	48	(0.04–0.74)
	-thoracic cage	1	1	79	1	82	0.49 (−0.12–1.0)
	-upper extremities	6	15	261	5	287	0.29 (0.06–0.51)
	-pelvis	2	9	258	0	269	−0.01 (-0.03–0.00)
	-lower extremities	8	18	523	15	564	0.51 (0.35–0.68)
Total		18	49	1159	24	1250	0.39 (0.28–0.51)

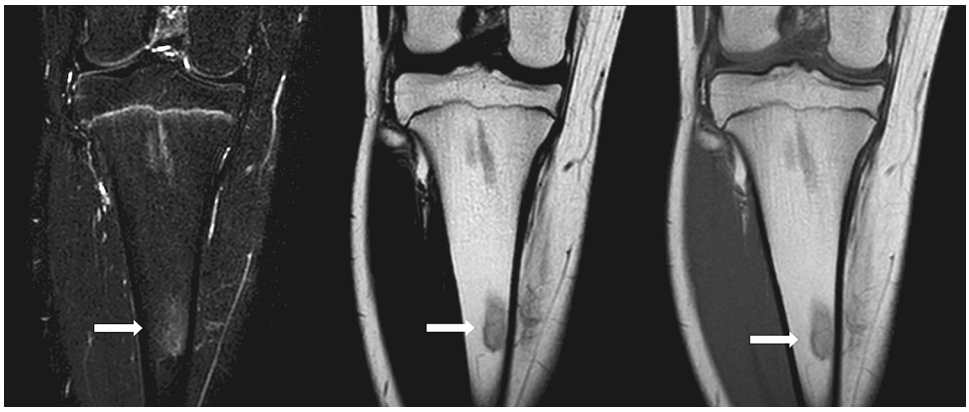

Fig. 2. 14-year-old girl with an oval, high intensity area in the tibia diaphysis as shown on a) T2 Dixon water-only image (arrow) b) T2 Dixon fat-only reconstruction, contrasted against yellow bone marrow (arrow) and c) T1-weighted image (arrow).

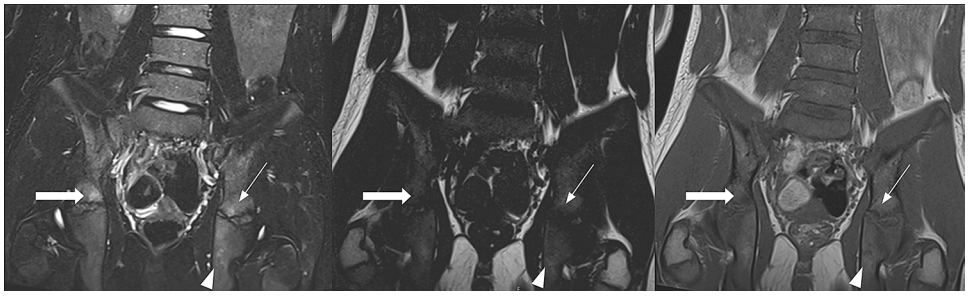

Fig. 3. Detail of the pelvis from a whole-body MRI in an 8-year-old girl, showing a) T2 Dixon water-only image with several high intensity areas in the right periacetabular region (arrow), and in the left periacetabular region (thin arrow, arrowhead). b) A T2 Dixon fat-only reconstruction illustrates the low signal intensity of red marrow in the axial skeleton, as compared to the appendicular skeleton. The high signal areas appear darker as well, albeit with little contrast to background (arrows and arrowhead). c) The axial skeleton on the corresponding T1-weighted image has more signal than the fat-only Dixon reconstruction; the detected areas have corresponding low signal (arrow and arrowhead), however the area in the left periacetabular region has only a slightly reduced signal (thin arrow).

Table 5
Agreement between T2 Dixon fat-only and T1-weighted TSE sequences in 1250 high signal areas previously identified on T2 Dixon water-only images from 196 healthy children and adolescents.

		T1-weighted TSE		
		No low signal	Low signal	Total
T2 Dixon fat-only	No signal	24 (1.9%)	18 (1.5%)	42 (3.4%)
	Low signal	49 (3.9%)	1159 (92.7%)	1208 (96.6%)
Total		73 (5.8 %)	1177 (94.2 %)	1250

areas, 10%).

4. Discussion

In this cohort of healthy children and adolescents, nearly 93% of the bone marrow areas with high signal identified on T2 Dixon water-only images returned low-signal on both T2 Dixon fat-only and T1-weighted images. <2% did not return low signal on either of the two sequences, with an absolute agreement of 94.6%. The kappa was fair to good with an average of 0.39. This value was not unexpected and does not affect the reliability of the results. In fact kappa value may be unsatisfactory when there is a considerable imbalance in the class distribution and in our study the marginal distribution is highly unbalanced since most areas were hypointense in T2-DSE FO and T1-w TSE and only a few were not.

Kappa value was higher in older children and for “major findings”, i.e. areas which in a clinical setting might have been mistaken for pathology. Conversely, the majority of the discordant findings were classified as “minor”. These are important observations supporting the use of T2 Dixon fat-only images as an alternative to T1-weighted images for assessment of bone marrow lesions on whole-body MRI in children over the age of nine.

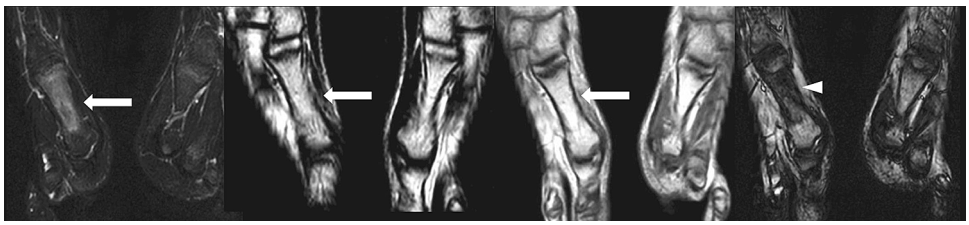

Fig. 4. MPR reconstructions of the right and left forefoot in a 13-year-old boy. a) Increased signal in the right first metatarsal on T2 Dixon water-only image (arrow). Neither T2 Dixon fat-only image (b) nor T1-weighted image (c) show corresponding low signal (arrows). d) The out-of-phase Dixon image depicts a reduction of signal in the right first metatarsal bone compared to the left side, confirming the increased water content (arrowhead).

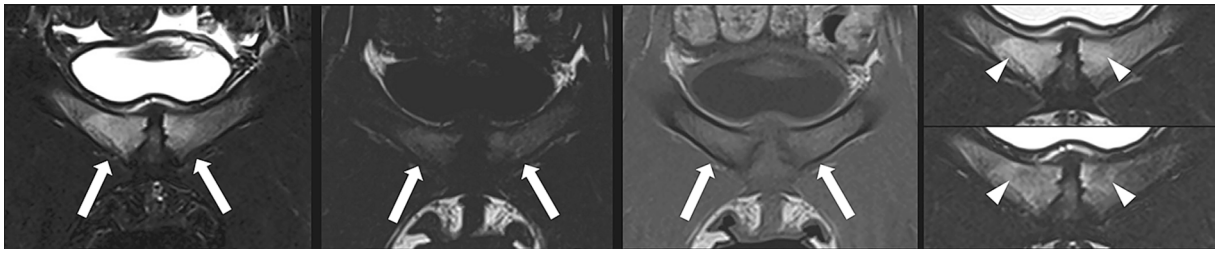

Fig. 5. Whole-body MRI in a 17-year-old adolescent. Details from the pubic bones, showing a) symmetrical high signal on T2 Dixon water-only images (arrows). b) On the T2 Dixon fat-only image the signal is difficult to evaluate and appears as not reduced (arrows). c) The pubic bones have homogeneous, not decreased signal on the T1 weighted image (arrows). d) On the in-phase (upper image) there is increased signal in the pubic bones (arrowheads), on the out-of-phase (lower image) there is patchy reduced signal in the same areas confirming the mixed water and fat content.

Table 6
Location of the 24 high signal areas on T2 Dixon water-only with no corresponding low signal on T2 Dixon fat-only and TSE T1.

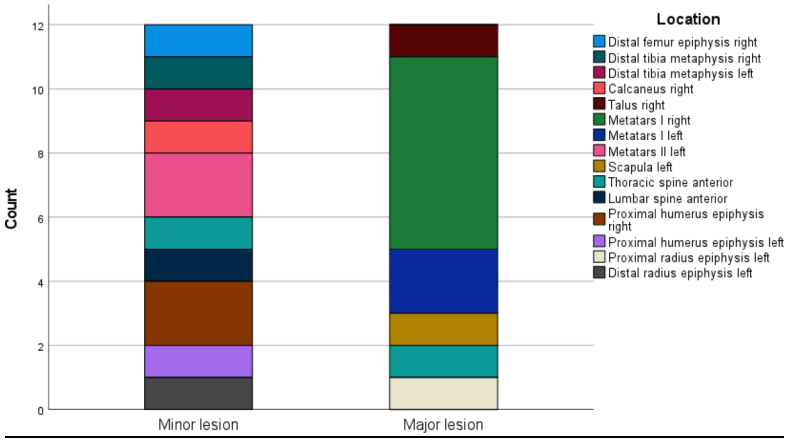

Table 7
Agreement between T1-weighted TSE and T2 Dixon fat-only sequence in areas with high signal on T2 Dixon water-only sequences according to different age groups.

		T1-weighted only	T2 Dixon fat-only	Both	None	Total	Kappa value (95%CI)
Age group, years	< 9	4	10	239	1	254	0.10 (-0.12–0.3)
	9–11	7	9	319	4	339	0.31 (0.06–0.56)
	12–14	2	20	295	13	330	0.51 (0.34–0.69)
	15–19	5	10	306	6	327	0.42 (0.18–0.66)
Total		18	49	1159	24	1250	0.39 (0.28–0.51)

When evaluating intensity alone, the agreement between the two sequences was quite similar for mild and moderately increased signal intensity, suggesting that the extension of a lesion is an important factor for the perception of findings.

In some of the cases showing low signal on both the T2 Dixon fat-only and the T1-weighted images, we experienced that the low signal was easier to recognize on the T2 Dixon fat-only images as compared to the T1-weighted images (Fig. 7). We speculate that this in part might be due to subtle movements of the child between T2 Dixon and T1-weighted scans, whilst water-only and fat-only images are acquired in the same sequence. Moreover, although fat-only images may occasionally lack the anatomical conspicuity of T1-weighted images, the poorer conspicuity might be overcome by the non-fat-suppressed in-phase images.

Regarding the 2% of high signal areas where low signal was absent

Fig. 6. Detail of the proximal humerus from a whole-body MRI in a 16 year-old girl. a) increased signal from the medial part of the proximal humerus diaphysis on the water-only Dixon reconstruction (arrow) b) low signal in the same location on the fat-only reconstruction (arrow) c) the T1 image does not show a decreased signal in the corresponding area (arrow).

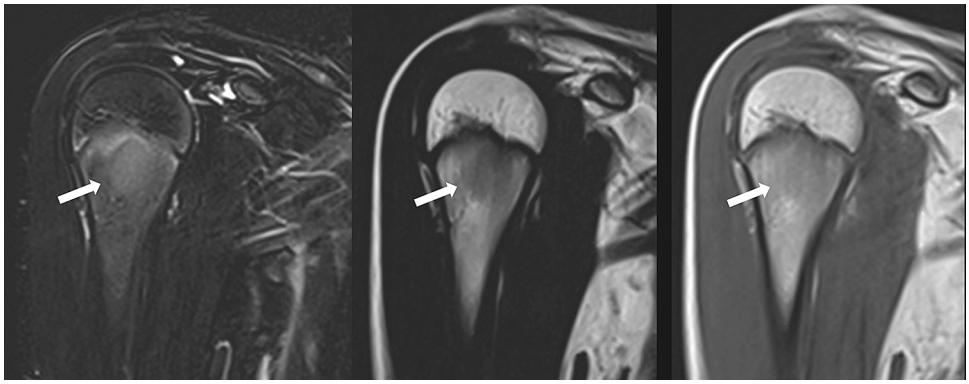

Fig. 7. Right proximal humerus in a 14-year-old boy, showing a) an area of increased signal on T2 Dixon water-only (arrow). b) T2 Dixon fat-only reconstruction shows a well delineated corresponding low signal area (arrow). c) The T1-weighted image displays a lower signal as well, but less well demarcated than the fat-only Dixon image (arrow).

on either of the two sequences, this might be due to residual amounts of fat signal in areas with increased water content as compared to the surrounding bone marrow. Interestingly, all these areas were visible on the out-of-phase images, confirming their true presence (Figs. 4 and 5). Out-of-phase images have proven helpful for the assessment of several musculoskeletal diseases, including neoplastic marrow lesions [22]. Two recent studies on patients with active and/or chronic sacroiliitis showed that the T2 Dixon out-of-phase images followed by the fat-only images were superior to the T1-weighted images in the detection of periarticular fat deposition [23,24].

As for locations, the best agreement between T2-Dixon fat-only and T1-weighted images was found for the lower extremities, which are most frequently affected in both inflammatory and infectious disorders in children and adolescents [25,26]. Discordance between the two sequences was most often seen in the proximal humeri and in the ischiopubic/para-acetabular regions. A possible explanation might be that the proximal humeri are more prone to movements from breathing, and are often further away from the coil, which can significantly degrade image quality. As for the pelvis, we hypothesize that areas close to the triradiate cartilage are challenging, as it can be difficult to define if the signal originates from the bone marrow or from the physiological cartilage. Both areas are known to contain a higher content of red bone marrow in the immature skeleton, resulting in lower signal on both sequences.

It must be remembered that the bone marrow is composed of a combination of hematopoietic red marrow and fatty yellow marrow, and that its composition changes throughout life in response to normal maturation (red to yellow conversion) and stress (yellow to red conversion) [4,27,28]. On T1-weighted imaging, increased signal reflects increased fat content and hence conversion from red marrow to yellow marrow. The overall T1 signal from red marrow is considerably lower as compared to fatty marrow, but typically higher than that from adjacent skeletal muscle [29]. Notably, in our cohort of healthy individuals we found several examples of areas with lower T1 signal compared to skeletal muscles (Fig. 8), a finding which has been previously reported to represent an infiltrative process in 35 out of 36 cases [30].

The agreement between the two sequences was higher amongst the older age groups as compared to children under 9 years of age. Amongst the cases with corresponding low signal on both sequences, we noticed that in several of our youngest children the signal intensity of the axial skeleton was in general lower on T2 Dixon fat-only than on T1 (Fig. 3). These findings are not unexpected as the amount of red marrow is higher in early childhood and marrow conversion in the appendicular skeleton occurs much more rapidly and to a greater degree than in the axial skeleton, challenging the interpretation of the T2 Dixon fat-only images in this age group.

In a previous paper we found a high agreement between STIR and T2 Dixon water-only sequences in the assessment of high signal marrow changes [19]. Based on this and present results, we would argue that STIR and anatomic T1-w sequences, often used for a whole-body MRI, might be both replaced by a single T2 Dixon sequence, reducing the total scan time, with a small caveat for those under the age of nine. The

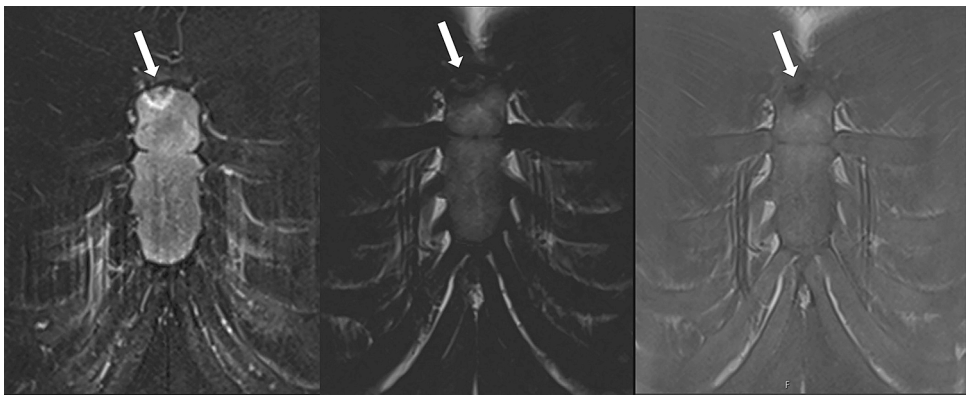

Fig. 8. 17-year-old adolescent with a) an area of irregularly increased signal on T2 Dixon water-only on the manubrium of the sternum (arrow) and corresponding low signal on both b) T2 Dixon fat-only (arrow) and c) T1-weighted image (arrow). The signal on the T1-weighted image is even lower than skeletal muscle.

effective time reduction could be of between 7 and 9 min depending on the number of stacks needed. This gain in time is not insignificant for a child since in paediatric patients the final minutes are less tolerated, thus the last sequences are those mostly affected by movement artefacts.

In recent years there has been a growing interest in the use of T2-Dixon fat-only in adult musculoskeletal imaging. Several studies have shown its potential to replace T1 images. In a retrospective study on 121 whole spine MRIs for suspected vertebral bone metastases, Maeder et al [12] concluded that T2-Dixon fat-only and water-only imaging provide diagnostic performance similar to that of the combination of morphologic sequences (T1 and T2 Dixon water-only). Evaluating the diagnostic performance of an MRI protocol including only sagittal T2-Dixon fat-only and water-only images as an alternative to a standard protocol in 114 adults with low back pain, Yang et al [13] reached the same conclusions. Thus, the authors suggest a shortened MRI protocol including a T2-Dixon sequence without an additional T1-weighted sequence, in this clinical setting. Also, Zanchi et al [14] retrospectively reviewing 50 lumbar spine MRI examinations, concluded that in subjects with non-specific low back pain and/or lumbar radiculopathy a simplified protocol of spine MRI in the sagittal plane with a T2-Dixon sequence provides the same information as a standard protocol including T1-weighted, T2-weighted, and fat-suppressed T2-weighted sequences.

To the best of our knowledge, this is the first paper examining the agreement between T2 Dixon fat-only and T1-weighted images as part of a whole-body MRI protocol in children and adolescents. The main strengths of our study are the high number of children and adolescents balanced by age, the high number of examined areas, the use of a validated scoring system for high signal areas, the wide range of signal intensity in the high signal lesions and the blinded design. The inclusion of two different centers using different vendors but similar MRI protocols and scan resolution strengthens the applicability of the results.

We acknowledge, however, some limitations. Firstly, the investigation was carried out on healthy children and adolescents only. However, the high proportion of "major findings" which, in a clinical setting could be mistaken for pathology, suggests that our results could be valid also for pathological processes. Secondly, the whole-body MRIs were performed on 1.5 T magnets. One might speculate that a 3 T magnet would provide higher agreement between the two sequences due to better image resolution. However, previous studies [13,14] have shown that the sequences perform equally well at 1.5 T and 3 T. Lastly, the results of this study are valid for the sequences used and could change if different resolutions or imaging parameters were applied.

In conclusion, the agreement between T2 Dixon fat-only and T1-weighted sequences in the assessment of bone marrow high signal areas in healthy children and adolescents indicates that a T1-weighted sequence can be replaced by T2 Dixon fat-only images in children older than 9 years. The scan time reduction resulting from the use of T2 Dixon sequence alone could have several advantages, in particular the reduction of exam-related stress in children and the achievement of good quality examinations, less affected by motion artefacts.

CRediT authorship contribution statement

Laura Tanturri de Horatio: Conceptualization, Data curation, Funding acquisition, Methodology, Validation, Writing – original draft. **Pia K. Zadig:** Resources, Investigation, Data curation. **Elisabeth von Brandis:** Resources, Investigation. **Lil-Sofie Ording Müller:** Resources, Writing – review & editing. **Karen Rosendahl:** Formal analysis, Methodology, Validation, Writing – review & editing. **Derk F.M. Avenarius:** Data curation, Methodology, Resources, Writing – review & editing.

Funding

This work was supported by the Northern Norway Regional Health Authority (Helse Nord, project number HNF1572-21).

Declaration of Competing Interest

The authors declare that they have no known competing financial interests or personal relationships that could have appeared to influence the work reported in this paper.

References

[1] A.M. Korchi, S. Hanquinet, M. Anooshiravani, L. Merlini, Whole-body magnetic resonance imaging: an essential tool for diagnosis and work up of non-oncological systemic diseases in children, Minerva Pediatr 66 (3) (2014) 169–176.
[2] S.R. Teixeira, J. Elias Junior, M.H. Nogueira-Barbosa, M.D. Guimarães, E. Marchiori, M.K. Santos, Whole-body magnetic resonance imaging in children: state of the art, Radiol Bras 48 (2) (2015) 111–120.
[3] M.B. Damasio, F. Magnaguagno, G. Stagnaro, Whole-body MRI: non-oncological applications in paediatrics, Radiol Med 121 (5) (2016) 454–461.
[4] J.P. Hynes, N. Hughes, P. Cunningham, E.C. Kavanagh, S.J. Eustace, Whole-body MRI of bone marrow: A review, J Magn Reson Imaging 50 (6) (2019) 1687–1701.
[5] J.M. Winfield, M.D. Blackledge, N. Tunariu, D.M. Koh, C. Messiou, Whole-body MRI: a practical guide for imaging patients with malignant bone disease, Clin Radiol 76 (10) (2021) 715–727.
[6] P. Zadig, E. von Brandis, R.K. Lein, K. Rosendahl, D. Avenarius, L.S. Ording Müller, Whole-body magnetic resonance imaging in children - how and why? A systematic review, Pediatr Radiol 51 (1) (2021) 14–24.
[7] M. Scheer, T. Dantonello, P. Brossart, D. Dilloo, L. Schweigerer, S. Feuchtgruber, M. Sparber-Sauer, C. Vokuhl, S.S. Bielack, T. Klingebiel, E. Koscielniak, T. von Kalle, C.w.s. (cws),, Importance of whole-body imaging with complete coverage of hands and feet in alveolar rhabdomyosarcoma staging, Pediatr Radiol 48 (5) (2018) 648–657.
[8] P. Omoumi, The Dixon method in musculoskeletal MRI: from fat-sensitive to fat-specific imaging, Skeletal Radiol 51 (7) (2022) 1365–1369.
[9] H. Guerini, P. Omoumi, F. Guichoux, V. Vuillemin, G. Morvan, M. Zins, F. Thevenin, J.L. Drape, Fat Suppression with Dixon Techniques in Musculoskeletal Magnetic Resonance Imaging: A Pictorial Review, Semin Musculoskelet Radiol 19 (4) (2015) 335–347.

[10] C.F. Lins, C.E.G. Salmon, M.H. Nogueira-Barbosa, Applications of the Dixon technique in the evaluation of the musculoskeletal system, Radiol Bras 54 (1) (2021) 33–42.
[11] F. Del Grande, F. Santini, D.A. Herzka, M.R. Aro, C.W. Dean, G.E. Gold, J. A. Carrino, Fat-suppression techniques for 3-T MR imaging of the musculoskeletal system, Radiographics 34 (1) (2014) 217–233.
[12] Y. Maeder, V. Dunet, R. Richard, F. Becce, P. Omoumi, Bone Marrow Metastases: T2-weighted Dixon Spin-Echo Fat Images Can Replace T1-weighted Spin-Echo Images, Radiology 286 (3) (2018) 948–959.
[13] S. Yang, L. Lassalle, A. Mekki, G. Appert, F. Rannou, C. Nguyen, M.M. Lefèvre-Colau, C. Mutschler, J.L. Drapé, A. Feydy, Can T2-weighted Dixon fat-only images replace T1-weighted images in degenerative disc disease with Modic changes on lumbar spine MRI? Eur Radiol 31 (12) (2021) 9380–9389.
[14] F. Zanchi, R. Richard, M. Hussami, A. Monier, J.F. Knebel, P. Omoumi, MRI of non-specific low back pain and/or lumbar radiculopathy: do we need T1 when using a sagittal T2-weighted Dixon sequence? Eur Radiol 30 (5) (2020) 2583–2593.
[15] N. Sollmann, S. Mönch, I. Riederer, C. Zimmer, T. Baum, J.S. Kirschke, Imaging of the degenerative spine using a sagittal T2-weighted DIXON turbo spin-echo sequence, Eur J Radiol 131 (2020), 109204.
[16] A. Saifuddin, R. Rajakulasingam, R. Santiago, M. Siddiqui, M. Khoo, I. Pressney, Comparison of lumbar degenerative disc disease using conventional fast spin echo, Br J Radiol 94 (1121) (2021) 20201438.
[17] P.K. Zadig, E. von Brandis, B. Flatø, L.S. Ording Müller, E.B. Nordal, L.T. de Horatio, K. Rosendahl, D.F.M. Avenarius, Whole body magnetic resonance imaging in healthy children and adolescents: Bone marrow appearances of the appendicular skeleton, Eur J Radiol 153 (2022), 110365.
[18] E. von Brandis, P.K. Zadig, D.F.M. Avenarius, B. Flatø, P. Kristian Knudsen, V. Lilleby, B. Nguyen, K. Rosendahl, L.S. Ording Müller, Whole body magnetic resonance imaging in healthy children and adolescents. Bone marrow appearances of the axial skeleton, Eur J Radiol 154 (2022), 110425.
[19] P. Zadig, E. von Brandis, L.S. Ording Müller, L. Tanturri de Horatio, K. Rosendahl, D.F.M. Avenarius, Pediatric whole-body magnetic resonance imaging: comparison of STIR and T2 Dixon sequences in the detection and grading of high signal bone marrow changes, Eur Radiol (2023).
[20] P. Zadig, E. von Brandis, P. d'Angelo, L.T. de Horatio, L.S. Ording-Müller, K. Rosendahl, D. Avenarius, Whole-body MRI in children aged 6–18 years, Reliability of identifying and grading high signal intensity changes within bone marrow, Pediatr Radiol 52 (7) (2022) 1272–1282.
[21] J.R. Landis, G.G. Koch, The measurement of observer agreement for categorical data, Biometrics 33 (1) (1977) 159–174.
[22] N. van Vucht, R. Santiago, B. Lottmann, I. Pressney, D. Harder, A. Sheikh, A. Saifuddin, The Dixon technique for MRI of the bone marrow, Skeletal Radiol 48 (12) (2019) 1861–1874.
[23] R. Athira, S. Cannane, R. Thushara, S. Poyyamoli, M. Nedunchelian, Diagnostic Accuracy of Standalone T2 Dixon Sequence Compared with Conventional MRI in Sacroiliitis, Indian J Radiol Imaging 32 (3) (2022) 314–323.
[24] A. Özgen, The Value of the T2-Weighted Multipoint Dixon Sequence in MRI of Sacroiliac Joints for the Diagnosis of Active and Chronic Sacroiliitis, AJR Am J Roentgenol 208 (3) (2017) 603–608.
[25] P. d'Angelo, L.T. de Horatio, P. Toma, L.S. Ording Müller, D. Avenarius, E. von Brandis, P. Zadig, I. Casazza, M. Pardeo, D. Pires-Marafon, M. Capponi, A. Insalaco, B. Fabrizio, K. Rosendahl, Chronic nonbacterial osteomyelitis - clinical and magnetic resonance imaging features, Pediatr Radiol 51 (2) (2021) 282–288.
[26] H. Peltola, M. Pääkkönen, Acute osteomyelitis in children, N Engl J Med 370 (4) (2014) 352–360.
[27] B.Y. Chan, K.G. Gill, S.L. Rebsamen, J.C. Nguyen, MR Imaging of Pediatric Bone Marrow, Radiographics 36 (6) (2016) 1911–1930.
[28] S.I. Shiran, L. Shabtai, L. Ben-Sira, D. Ovadia, S. Wientroub, T1-weighted MR imaging of bone marrow pattern in children with adolescent idiopathic scoliosis: a preliminary study, J Child Orthop 12 (2) (2018) 181–186.
[29] M.D. Patel, J. Brian, N.A. Chauvin, Pearls and Pitfalls in Imaging Bone Marrow in Pediatric Patients, Semin Ultrasound CT MR 41 (5) (2020) 472–487.
[30] K.W. Carroll, J.F. Feller, P.F. Tirman, Useful internal standards for distinguishing infiltrative marrow pathology from hematopoietic marrow at MRI, J Magn Reson Imaging 7 (2) (1997) 394–398.